Pharmacological blockade of voltage-gated calcium channels as a potential cardioprotective strategy

Charumathi Pushparaj

Dipòsit Legal: L.1703-2014
http://hdl.handle.net/10803/285047

Universitat de Lleida

IRB Lleida
Institut de Recerca Biomèdica

PHARMACOLOGICAL BLOCKADE OF VOLTAGE-GATED CALCIUM CHANNELS AS A POTENTIAL CARDIOPROTECTIVE STRATEGY

CHARUMATHI PUSHPARAJ
Doctoral Candidate

Directors
Dr. Carles Cantí Nicolás
Dr. Reinald Pamplona Gras

Lleida, 2014

Universitat de Lleida

IRB Lleida
Institut de Recerca Biomèdica

Dr. Carles Cantí Nicolás, Principal Investigator of Calcium signalling and neuronal differentiiation laboratory at the Institute for Biomedical Research, Lleida and **Dr. Reinald Pamplona Gras**, Principal Investigator of Metabolic Pathophysiology Laboratory at the Institute for Biomedical Research, Lleida, University of Lleida, as supervisors of the thesis,

Hereby state that,

Charumathi Pushparaj with a B.Sc. degree in Animal Science and Biotechnology from Bharathiar University, India and M.Sc. degree in Zoology from University of Madras, India has performed under our direction and supervision, and within the Laboratory of Calcium signalling and neuronal differentiation of the Department of experimental medicine, the experiment work entitled **"Pharmacological blockade of voltage-gated calcium channels as a potential cardioprotective strategy".**

The work accomplishes the adequate conditions in order to be defended in front of the corresponding Thesis Committee and, if it is case, to obtain the **Doctor Degree** from the *University of Lleida*.

Signed,

Dr. Carles Cantí Nicolás **Dr. Reinald Pamplona Gras**

Lleida, 2014

….To my parents, uncle and Ramesh

Acknowledgement

A four year challenging journey has come to a halt with this thesis in my hands. This journey has taught me a lot both professionally and personally and I am deeply indebted to each and everyone who joined hands with me in this journey, and to say "Thank you" would be an understatement of what I really feel to express.

My foremost expression of gratitude is to my supervisor Dr. Carles Canti, for having accepted me here in the lab, having accepted me for what I am, and for all the freedom and space he provided me to grow up in research. I am so grateful for his patience, motivation, enthusiasm, support and immense knowledge that have made me a PhD degree holder. Thanks a lot for standing by me at all the hardships I went through, and also for putting up with my utmost craziness and stupidity. I feel privileged to be your student.

I extend my gratitude to my co-supervisor, Dr. Reinald Pamplona for all his support and kind gesture throughout this work. His never say no attitude from the beginning has made this thesis possible.

There is no way that I can miss to thank the smartest lady in the lab, Dr. Judit Herreros. Judit, you have been an inspiration for me in every aspect of career and life. I hope that someday I could grow up as lively, energetic and enthusiastic and focussed as you are. Your advices and support have helped me a lot to come out of difficult situations and to handle them with an ease. Thanks a lot for your support and endurance.

I would like to thank AGAUR, University of Lleida and IRBLleida for the financial support to pursue my doctoral thesis.

I am very much grateful to Dr. Manel Portero, Dr. Monica David, Dr. Marta Llovera, Dr. Daniel Sanchez, Dr. Mario Encinas, Dr. Xavier Dolcet, Dr. Joaquim EGEA, Dr. Carme Espinet, Dr. Conxi Mora, Dr. Juan Verdaguer, Dr. Jacint Boix, Dr. Judit Ribas, Dr. Adriana Dusso and Dr. Jose Valdivielso for their kind help and encouragement during my stay here.

I greatly appreciate the timely help rendered by the technicians, which had made my work easy. Thanks to Anais.P, Marta.R, Cristina.G, Carme.G, Monica.D, Berta.D, Montse.F and Montse. O and also to the technicians from the animal house Jessica and Nuria.

Also, my thanks to Ana.V, Dolors, Azahar, Anna.S and Subirats from the Anatomia patologica group for their support. Thanks a lot to Milica, Noelia, Vikki and Petya for all the love and support. Milica, you have always been a source of inspiration for me. Every encounter with you has helped me wipe of my complaints and move on.

Thanks a lot to Estella, Ares, Gisel, Esmeralda and Berta for all the fun. You mean a lot to me. Ester and Ale thanks for all your love. You have always stood by me and supported a lot.

My heartfelt thanks to Maria, Nati, Marta.C, Junmei, Myriam, Marta.V, Laura, Andre, Nuria.E, Cris, Ma Alba, Paolo, Carlos and Isidre for all the love, care and fun during my stay here. Thanks a lot for tolerating all the hassle I sometimes used to create in the culture rooms (especially to Nuria.E) and for being very supportive.

A special word of appreciation to my very own labmates Nuria B, Arindam and Deepshikha for all that I learnt from them. I feel very happy to express my gratitude to Anna Macia, whose presence made the lab more vibrant and interactive. I have been saving the best for the last. The most wonderful person (I really mean it!!!) Mireia, I don't have any words to express my gratitude and love for her. I am glad that I shared the lab with her and working with her was all fun. I am so very grateful to her for her acceptance and care. She has stood by me all these four years, at the best and the worst moments. My Spanish and Catalan classes are incomplete without her. As I promised her, I partly dedicate my thesis for her (along with p62 ;)). Mireia I just don't want to say a "thanks" and finish it of here. You'll be in my thoughts forever.

My thanks also go to Ariadna and her parents, Valle and family, Alba and her family, for their unconditional love and care. Ariadna thanks a lot for all those adventure sessions.

Liliana and Carlos, if it's not you both, I wouldn't have dared to try many things in my life. Thanks for all those intense cross-feet, tabata and running sessions. Unfortunately, my laziness overcame all those experiments.

Ana, I just can't say thanks to all you have done to me. You were there for me every day to listen to me and to care for me. My day never ended without a warm hug from you. Thanks a lot for giving me a beautiful family. Mom, dad, Rosi and Rafa will always be in my thoughts.

My paranymphs, my girls- Disha and Upasana. I know that I don't have to thank you both. Whatever I may say here is not enough. Your genuine friendship, love and understanding are immense and can't be expressed. Love you both.

I am so grateful to all my friends in India for their understanding, love and support all these years. Arvind, Almas, Charu, Divi, Tharu, Shanthi, Deepa, Maha, Preethy, Revathi, KK, Hari, Chella, Poongs, Jey, Mani, Parthi anna, Santosh anna, my sangam, SMMS and all my friends. Wish I could mention each and everyone.

I take this opportunity to thank all my teachers and mentors who encouraged me in every step of my life and guided me until here. Mrs. Amutha, Mr. Prakasam, SMMS teachers, Vasuki

amma, Dr. Ezhili N, Dr. Harathi D, Dr. Ramu Manivannan are some who would always guide me throughout my life.

And of course my biggg family back in India, my uncles (my childhood heroes), ammachi and thatha, aunts, my mom-in-law and the whole family, thanks for all the love. Not to forget the little ones of the family, Abi, Karthik, Prabha and Durga who made sure that I enjoy every family occasion, though 5000 miles away from home.

A deep sense of gratitude to my mom and dad and also to my brother, whose immense support and love has made this possible. Thanks a lot to my mom and dad, for saying yes to whatever I did, for pushing me to stand on my own and letting me to be independent and for all the prayers. I hope I made your dreams come true and made you proud. Love you!!!

And finally Ramesh. You are amazing. If it's not you, this wouldn't have happened. Your unconditional love and support can't be expressed by words. And your sacrifice has given me immense strength to go through all hardships. Thanks a lot for standing by me side always. LOVE YOU.

Muchísima gracias!!!

-Charu

Index

Abbreviations

µM	Micromolar
AIF	Apoptosis-inducing factor
AMPK	AMP-activated protein kinase
ATF	Activating transcription factor
ATG	Autophagy related gene
AV	Autophagic Vacuole
BAX	BCL-2 associated X protein
Bcl-2	B-cell lymphoma 2
BiP	Binding immunoglobulin protein
Ca^{2+}	Calcium ion
CaMK	Calcium/Calmodulin-dependent protein kinase
cAMP	Cyclic adenosine monophosphate
Caspases	Cysteine-containing aspartate specific proteases
Ca_v	Voltage-gated calcium cannel
CDK	Cyclin dependent kinase
cDNA	Complementary deoxyribonucleic acid
CQ	Chloroquine
DHRP	Dihydropyridine receptor
DMSO	Dimethyl sulfoxide
DNA	Deoxyribonucleic acid
dNTP	Deoxyribonucleotide
dNTP	Deoxynucleotide triphosphate
ECC	Excitation contraction coupling
eIF2α	Eukaryotic initiation factor 2α
eIF3e	Eukaryotic translation initiation Factor 3, subunit e
ER	Endoplasmic reticulum

ERAD	ER-associated degradation
ERSE	ER stress response element
FBS	Foetal bovine serum
FURA2/AM	Fura-2-acetoxymethyl ester
GADD153	Growth Arrest And DNA Damage Inducible Gene 153
GAPDH	Glyceraldehyde 3-phosphate dehydrogenase
GRP 78	Glucose Regulated Protein 78
HF	Heart failure
HIF	Hypoxia-inducible factor
HRP	Horseradish peroxidase
IP_3	Inositol 1,4,5-trisphosphate
IRE1α	Inositol-requiring enzyme α
JNK	Jun N-terminal kinases
kbp	Kilobase pairs
kDa	Kilo Dalton
LC3	Light Chain 3
LR	Lysotracker red
MDC	Monodansylcadavarine
mRNA	Messenger RNA
NFAT	Nuclear factor of activated T cells
nM	Nano Molar
PBS	Phosphate buffer saline
PCD	Programmed Cell Death
PDGF	platelet-derived growth factor
PERK	protein kinase RNA-like endoplasmic reticulum kinase
PI	Propidium Iodide
PI3K	Phosphatidylinositol-3-kinase

PKC	protein kinase C
PTEN	Phosphatase And Tensin Homologue Deleted On Chromosome 10
PTP	permeability transition pore
q RT- PCR	Quantitative Real Time Polymerase Chain reaction
RNA	Ribonucleic acid
RT	Room temperature
RT-PCR	Reverse Transcriptase Polymerase Chain Reaction
RyR2	Ryanodine receptors
SDS	Sodium dodecyl sulphate
SDS-PAGE	Sodium dodecyl sulfate polyacrylamide gel electrophoresis
Sec.	Seconds
SERCA	Sarco- Endoplasmic reticulum Ca^{2+}-ATPase
shRNA	Short hairpin RNA
si RNA	Small interfering RNA
SOCC	Store operated calcium channel
SQSTM1	Sequestosome 1
TBST-buffer	Tris Buffer saline in Tween 20
Tg	Thapsigargin
TUNEL	Terminal deoxynucleotidyl transferase dUTP nick end labeling
Tween 20	Polyoxyethylene sorbitan monolaurate
UPR	Unfolded Protein Response
UPRE	UPR promoter element
UV	ultraviolet
VDAC	Voltage dependent anion channel
VEGF	Vascular endothelial growth factor
VGCC	Voltage-gated calcium cannel
VGP	Vertical growth phase

VOCC	Voltage operated Calcium channel
WB	Western Blot
XBP1	X Box Binding Protein1

Abstract

Abstract

Voltage-gated Ca^{2+} channels (VGCCs) are essential for initiating and regulating cardiac function. During the cardiac action potential, Ca^{2+} influx through L-type channels triggers the sarcoplasmic reticulum Ca^{2+} release that enables the EC coupling. Ca^{2+} can also enter cardiac myocytes through low-voltage-activated T-type channels, which are expressed throughout cardiac development until the end of the neonatal period, and can contribute to pacemaker activity as well as EC coupling to some extent. Importantly, T-type channels are re-expressed in ventricular myocytes under diverse pathological conditions such as ischemia or hypertrophy, suggesting that they play a role in cardiac disease.

In a first part of this study, we examined the effects of VGCC blockers on the homeostasis and viability of primary cultures of cardiac myocytes (CMs), because of the importance of apoptosis and necrosis in cardiac disease. In a second part, we analyzed the cell mechanisms unleashed by hypoxic and hypertrophic stimuli, the involvement of VGCCs and the putative cytoprotective effects of VGCC blockade. Our results show that L-type and T-type channel blockers induce a low-level and transient ER stress, albeit with a distinct conveyance into cell macroautophagy and viability: whereas L-type channel blockers trigger a macroautophagic process in CMs, ultimately promoting apoptosis, T-type channel blockers exert the opposite effect, by decreasing the autophagic flux and not affecting cell death. Furthermore, the blockade of T-type channels reduces Beclin1-dependent autophagy and protects CMs subject to hypoxia-reoxygenation (as an *in vitro* paradigm for ischemia-reperfusion). With respect to the effect of hypertrophic insults, the results attained draw a complex scenario in which the cardiomyocytes constitutive macroautophagy is inhibited, giving way to alternative forms of protein degradation.

In summary, we identify L-type and T-type channels as new targets for macroautophagy regulation of CMs, and provide new clues to the beneficial actions reported in clinical trials for T-type channel blockers, particularly against pathophysiological conditions involving a maladaptive autophagy.

Resumen

Los canales de calcio voltaje-dependientes (CCDV) son esenciales para iniciar y regular la función cardíaca.Durante el potencial de acción cardíaco, el influjo de Ca^{2+} a través de los canales de tipo L desencadena la liberación de Ca^{2+} del retículo sarcoplasmático necesaria para el excitación-contracción (EC). El Ca^{2+} también puede entrar en los miocitos a través de canales de Ca^{2+} de bajo umbral o tipo T, que se expresan a lo largo del desarrollo cardíaco hasta el final del período neonatal, y pueden contribuir a la actividad marcapasos así como al acoplamiento EC. De forma destacable, los canales de tipo T se re-expresan en cardiomiocitos ventriculares bajo diversas condiciones patológicas incluyendo la isquemia y la hipertrofia, sugiriendo que juegan un rol relevane en la enfermedad cardíaca.

En una primera parte de este estudio, examinamos los efectos de los bloqueantes de CCDV sobre la viabilidad y la homeostasis de cultivos primarios de cardiomiocitos (CMs), debido a la importancia de la apoptosis y la necrosis en la enfermedad cardíaca. En una segunda parte, analizamos los mecanismos celulares desencadenados por estímulos de hipoxia e hipertrofia, así como la implicación de los CCDV y los posibles efectos citoprotectores debidos al bloqueo de los CCDV. Nuestros resultados muestran que los bloqueantes de canales de tipo L y T inducen un estrés de retículo de bajo nivel y transitorio, aunque divergiendo en lo que respecta la viabilidad celular: mientras que los bloqueantes de canales de tipo L exacerban la macroautofagia, provocando la muerte celular, los bloqueantes de canales de tipo T reducen el flujo autofágico y no afectan negativamente a la viabilidad de los CMs. Adicionalmente, el bloqueo de los canales de tipo T reduce la autofagia dependiente de Beclin1 y protege a los CMs tratados con hipoxia-reoxigenación (un paradigma *in vitro* de la isquemia-reperfusión). Con respecto al efecto de la estimulación hipertrófica, los resultados conseguidos perfilan un escenario complejo en el que la macroautofagia constitutiva de los cardiomiocitos es inhibida, dando paso a formas alternativas de degradación proteica.

En conclusión, en este estudio hemos identificado a los canales de tipo L y T como nuevas dianas para la regulación de la autofagia en CMs, y obtenido datos novedosos sobre las acciones beneficiosas de los bloqueantes de canales de tipo T descritas en esayos clínicos, particularmente frente a condiciones patofisiológicas que implican una autofagia maladaptativa.

Resum

Els canals de calci dependents de voltatge (CCDV) són essencials per a iniciar i regular la funció cardíaca.Durant el potencial d'acció cardíac, l'influx de Ca^{2+} a través dels canals de tipus L desencadena l'alliberament de Ca^{2+} del reticle sarcoplasmàtic necessària per l'acoblament E-C. El Ca^{2+} també pot entrar en els miòcits a través de canals de Ca^{2+} de tipus T, que s'expréssen durant el desenvolupament cardíac fins el final del període neonatal, i poden contribuïr a l'activitat marcapassos així com a l'acoblament EC. De forma destacable, els canals de tipus T es re-expréssen als cardiomiòcits ventriculars en diverses condicions patològiques com la isquèmia i la hipertròfia, el què suggereix que juguen un rol relevant en l'enfermetat cardíaca.

En una primera part d'aquest estudi, vàrem examinar els efectes dels bloquejants de CCDV sobre l'homeostasi i la viabilitat de cultius primaris de cardiomiòcits (CMs), degut a la importància de l'apoptosi i la necrosi en l'enfermetat cardíaca. En una segona part, vàrem analitzar els mecanismes cel·lulars desencadenats per estímuls d'hipòxia i d'hipertròfia, així com l'implicació dels CCDV i els possibles efectes citoprotectors deguts al bloqueig dels CCDV. Els resultats obtinguts mostren que els bloquejants de canals de tipus L i T indueixen un estrés de reticle de baix nivell i transitori, però que divergeixem pel què fa al seu efecte sobre la viabilitat celular: mentre que els bloquejants de canals de tipus L exacerben la macroautofàgia, provocant la mort cel·lular, els bloquejants de canals de tipus T redueixen el flux autofàgic i no afecten negativament la viabilitat dels CMs. Addicionalment, el bloqueig dels canals de tipus T redueix l' autofàgia dependent de Beclin1 i protegeix els CMs tractats amb hipòxia-reoxigenació (un paradigma in vitro de l'isquèmia-reperfusió). Respecte l'efecte de l'estimulació hipertròfica, els resultats assolits perfilen un escenari complex en el que la macroautofàgia constitutiva dels cardiomiòcits és inhibida, donant pas a formes alternatives de degradació proteica.

En definitiva, en aquets estudi hem identificat els canals de tipus L i T com a noves dianes per la regulació de l'autofàgia en CMs, i obtingut dades novedoses sobre les accions beneficioses dels bloquejants de canals de tipus T descrites en assaigs clínics, particularment front patologies que impliquen una autofàgia maladaptativa.

Introduction

1. Introduction:

Over the past decade, cardiovascular diseases are among the leading causes of mortality globally. According to the World Health Organization, about 17.3 million people died in 2008 due to cardiac disease, representing 30% of global deaths [1]. The end result of many forms of cardiovascular disease is heart failure, a syndrome where the heart is unable to meet the metabolic demands of the body. Heart failure accompanied by cardiac remodelling induced by several factors such as cardiac hypertrophy, apoptosis, etc., lead to abnormalities of impulse conduction and arrhythmias. Heart failure can be described as a pathologic process characterized by a decrease of contractility and consequent decline of cardiac output, which involves a complex set of changes like inflammatory cytokines, endothelin, angiotensin II, and aldosterone which reprogram the cardiac muscle at the cellular and molecular levels [2].

Since the finding of Ringer in 1880s [3] proved that ionic calcium (Ca^{2+}) is essential for the contractility of the heart, it became apparent that Ca^{2+} homeostasis is certainly involved in the function of both normal and failing hearts. Much attention has been paid to the understanding of the role of Ca^{2+} regulation in heart failure [4]. Entry of Ca^{2+} in the cells is responsible for the excitation-contraction (E-C) coupling and, in addition, Ca^{2+} influx regulates the pacemaking activity and atrio-ventricular conduction of the hearts [5]. The influx of Ca^{2+} ions into the cells is facilitated by voltage gated Ca^{2+} channels (VGCC). Cytosolic Ca^{2+} binding proteins respond to the increased Ca^{2+} levels by altering the cell function and, after the signaling is over, Ca^{2+} is expelled from the cell through different active transporters placed in the plasma membrane, or actively internalized in intracellular stores. The endoplasmic reticulum (ER) is the most important Ca^{2+} storage site. Relevantly, the high luminal Ca^{2+} concentration in the ER is critical for determining the protein synthesis process within the ER. For this reason, any disturbance in the cellular Ca^{2+} homeostasis triggers the so called ER stress, which often leads to the activation of the Unfolded Protein Response (UPR). The UPR is an adaptive pool of molecular mechanisms designed to restore homeostasis. One of the possible outcomes of a sustained UPR is the induction of macroautophagy.

Although the role of ER stress and autophagy in cardiac remodeling and cardiomyopathies has been studied extensively, no link has been established between between VGCCs and UPR or autophagy. Would this link exist, VGCC pharmacological

modulators could be used as a potential therapeutic strategy in the treatment of cardiomyopathy. Thus it becomes necessary to understand the function of VGCCs in the calcium signaling (beyond E-C contraction) in the heart. This thesis provides a number of different approaches to study the role of VGCCs in regulating the homeostasis of cardiomyocytes (CMs), leading to cell death or survival, thereby intending to establish the basis for a new therapeutic approach for cardiovascular diseases by pharmacologic or genetic modification of VGCCs.

2. Heart:

2.1. Structure

The cardiovascular system is the first system to develop and function in an animal. The heart, located in the thoracic cavity between the lungs, is a hollow muscular organ, responsible for pumping blood through the blood vessels by repeated, rhythmic contractions. It is surrounded by a thick, membranous sac called Pericardium that protects and lubricates the heart. Pericardium is composed of striated involuntary muscles that produce electric impulses that cause the heart to contract, pumping the blood throughout the body (Figure 1)[6].

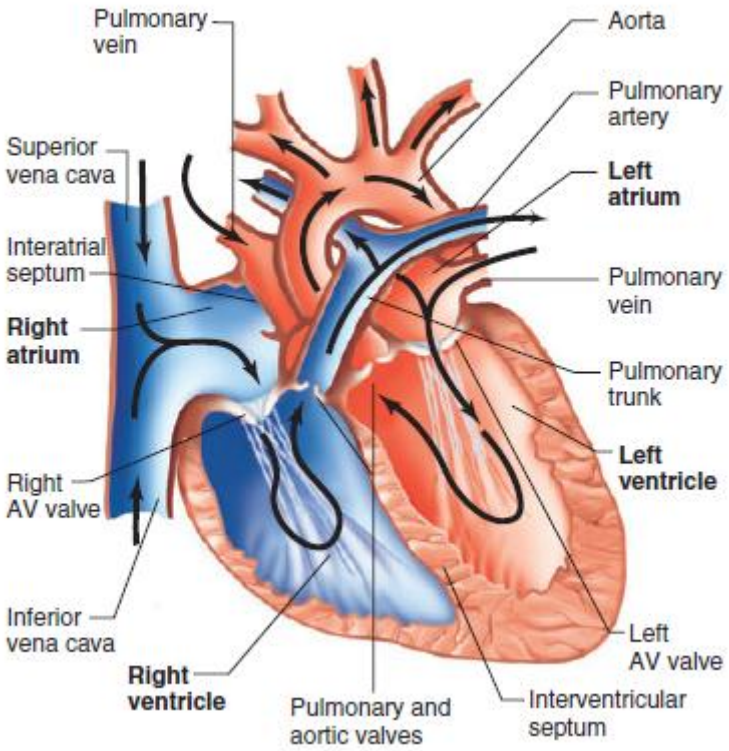

***Figure 1**: Diagrammatic section of the heart. The arrows indicate the direction of blood flow. (Adapted from Vander et al. Human Physiology 2003)*

The human heart has two chambers, the atria and the ventricles. There are two atria on either side of the heart. The right atrium receives de-oxygenated blood from the superior and inferior vena cava and the left atrium receives oxygenated blood from the left and right pulmonary veins. The ventricles collect blood from the atrium to be pumped out of the heart. The right ventricle pumps blood into the pulmonary circulation for the lungs and the left ventricle pumps blood into the systemic circulation for the rest of the body. The two ventricles are separated by a thick muscular wall called *septum*. Blood flows from the right atrium to the right ventricle through the tricuspid valve and is pumped out of the pulmonary semilunar valve to the lungs through the pulmonary artery. The oxygenated blood flows back to the left atrium via pulmonary veins. The blood from the left atrium flows to the left ventricle through the mitral valve, and again it is pumped through the aortic semilunar valve to the rest of the body through aorta. The deoxygenated blood returns to the heart through inferior and superior vena cavae and flows through the right atrium, where the process of oxygenation of blood begins again[6].

2.2. Physiology of heart:

The myocardium is the muscular tissue of the heart. The cardiac muscle cells are striated as the result of an arrangement of thick myosin and thin actin filaments similar to that of skeletal muscle. The individual cardiac muscle cells are separated by intercalated discs. The cardiac muscle is self-exciting and it has its own conduction system. This is in contrast with skeletal muscle, which requires either conscious or reflex nervous stimuli. The heart's rhythmic contractions occur spontaneously, although the frequency or the heart rate can be changed by nervous or hormonal influence such as exercise or the perception of danger.

The cardiac muscle is of three major types namely, atrial muscle, ventricular muscle and specialized excitatory and conductive muscle fibers. The atrial and ventricular cardiac muscles contract in the same way as skeletal muscle, except that the duration of contraction is much longer. Conversely, the specialized excitatory and conductive fibers contract feebly because of the presence of few contractile fibrils, instead, they exhibit

either automatic rhythmical electrical discharge in the form of action potentials or conduction of the action potentials through the heart, providing an excitatory system that controls the rhythmical beating of the heart.

2.3. Excitation-contraction coupling:

The term excitation-contraction coupling refers to the mechanism by which the action potential causes the myofibrils of muscle to contract. This mechanism is facilitated by an increase in the cell's cytosolic Ca^{2+} concentration. Like in skeletal muscle, the increase in cytosolic Ca^{2+} concentration in cardiac muscle is mainly due to the release of Ca^{2+} from the sarcoplasmic reticulum. The depolarization of the sarcolemma intiates the opening of the L-type Ca^{2+} channels (dihydropyridine receptors, DHRPs) located in the sarcolemma leading to the influx of Ca^{2+} ions through DHRPs. This Ca^{2+} combines with the regulator protein troponin and cross-bridge formation between actin and myosin is initiated.

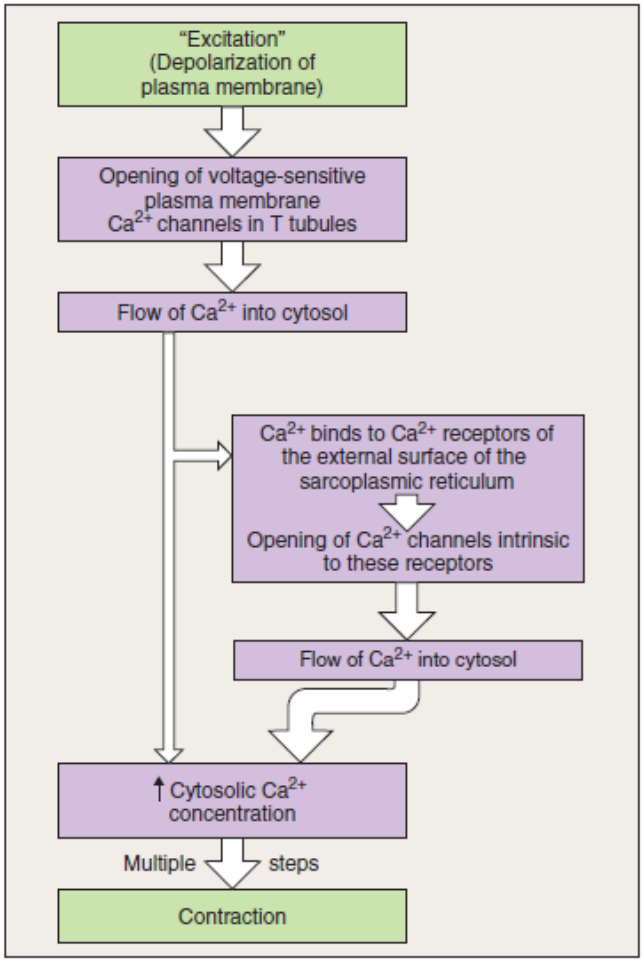

Figure 2: *Excitation-contraction coupling in cardiac muscle. Depolarization of the plasma membrane allows the flow of* Ca^{2+} *into the cytosol by opening the VGCC. This*

increase of Ca^{2+} in the cytosol triggers the contraction of the cell by mediating various processes. (Adapted from Vander et al. Human Physiology 2003)

In the cardiac muscle the action potential opens voltage-sensitive Ca^{2+} channels in the T-tubule membranes; then Ca^{2+} diffuses from the extracellular fluid through these channels into the cells, causing a small increase in the concentration of Ca^{2+} in the region immediately adjacent to the sarcoplasmic reticulum (SR) (Figure 2). This small increase in Ca^{2+} concentration facilitates Ca^{2+} binding to Ca^{2+} receptors on the external surface of the sarcoplasmic reticulum membranes (the ryanodine receptors). These Ca^{2+}-sensitive receptors contain intrinsic Ca^{2+} channels, and activation of the receptors opens the channels, allowing a large net diffusion of Ca^{2+} from the Ca^{2+}-rich interior of the sarcoplasmic reticulum into the cytosol (this is termed "Ca^{2+}-induced Ca^{2+} release"). It is mainly this Ca^{2+} that causes the contraction. Thus, even though most of the Ca^{2+} causing contraction comes from the sarcoplasmic reticulum, the process unlike that in skeletal muscle is dependent on the movement of *extracellular* Ca^{2+} into the muscle, the Ca^{2+} then acting as the signal for release of the sarcoplasmic reticulum Ca^{2+}. Contraction ends when the cytosolic Ca^{2+} concentration is restored to its original extremely low value by active transport of Ca^{2+} back into the sarcoplasmic reticulum. Also, an amount of Ca^{2+} equal to the small amount that had entered the cell from the extracellular fluid during excitation is transported out of the cell, so that the total cellular Ca^{2+} content remains constant. The transport into the sarcoplasmic reticulum is by primary active Ca^{2+}-ATPase pumps; the transport across the plasma membrane is also by Ca^{2+}-ATPase pumps plus Ca^{2+}/Na+ exchangers. The amount that cytosolic Ca^{2+} concentration increases during excitation is a major determinant of the strength of cardiac muscle contraction [7-10].

3. Voltage-Gated Calcium Channels (VGCC):

3.1. Introduction

VGCC channels play a crucial role in transducing changes in membrane potential into intracellular Ca^{2+} transients. These intracellular Ca^{2+} transients signal to initiate various physiological processes like neurotransmitter release, cell contraction, ion transport, cell proliferation and growth, in a diversity of cell types[7]. However, a signaling role for VGCCs (in addition to its role in EC-coupling) in muscle cells is largely unknown. Figure

3 schematically explains the initiation of various cellular processes upon Ca^{2+} entry via VGCC.

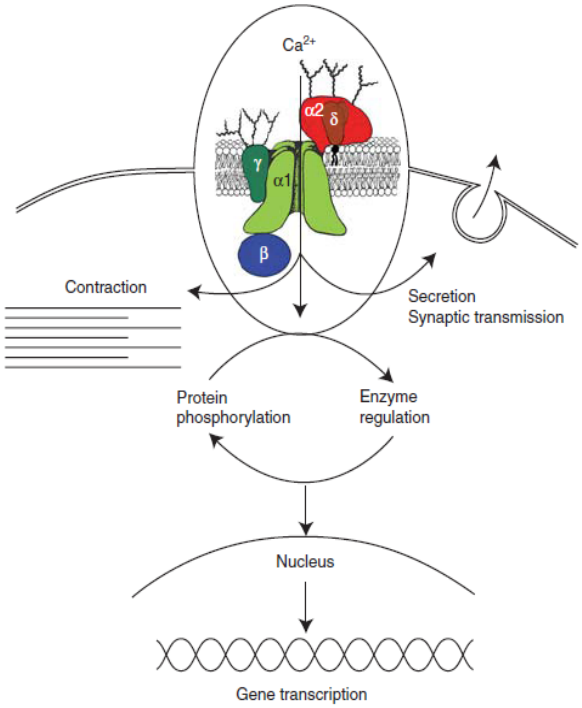

Figure 3: *Signal transduction by VGCC. Calcium influx through the voltage gated Ca^{2+} channels initiates various intracellular processes like contraction, protein phosporylation and dephosporylation, secretion, synaptic transmission and enzyme regulation. Inset in the plasma membrane shows the Subunit complex structure of VGCC. (Catterall W.A, 2011-Adapted from Takahashi et al. 1987)*

L-type VGCCs, as purified from skeletal muscle transverse tubules are complex structures formed of 5 subunits that are termed as α1, α2, β, γ and δ subunits. The α1 subunit or the pore-forming α subunit is a transmembrane structure with a length of 2000 amino acid residues and a molecular weight of 190 kDa. The α1 subunit is associated with α2δ dimer of 170 kDa through a disulfide linkage, an intracellular phosphorylated β subunit of 55 kDa and a transmembrane γ subunit of 33 kDa forming a large macromolecular complex. In the following subtopics, the structure and functions of each subunits of VGCC such α1, α_2/δ, β and γ, will be described in more detail.

3.2. Structure and functions of VGCC subunits:

3.2.1. α1 subunit:

The α1 subunit or the $Ca_v\alpha1$ is a 190-250 kDa protein formed of four homologous repeats (I-IV) connected through cytoplasmic loops. Each repeat contains six predicted transmembrane segments (S1-S6) and a pore-forming loop (P-loop) between S5 and S6. These four P-loops are essential for calcium conductance. The voltage-dependent movement of Ca^{2+} is facilitated by a voltage sensor that comprises S6 and S4 segments, which in turn facilitate the opening and closing of these channels. The α1 subunit appears to be capable of forming a functional calcium channel on its own and hence all the other subunits are sometimes referred to as auxillary or anxillary subunits, yet these channels affect largely the channel gating and expression. The expression of multiple forms of α1 subunit gives rise to diversity of calcium channels that are isolated by molecular cloning [8-14].

3.2.2. β subunit:

In their native state, all the high voltage activated calcium channels appear to contain β subunits. The β subunit bind to α- interaction domain, AID between the transmembrane domains I and II of the pore-forming α-1 subunit and affects the multiple channels properties such as voltage-dependent activation, inactivation rates, G-protein modulation, drug sensitivity and cell surface expression [15]. These β subunits are peripheral membrane proteins associated with the cytoplasmic aspect of the surface membrane with a molecular weight of ~ 55-60 kDa [16]. β subunits plays several important functions within the VGCC complex: a) they serve a key role in targeting the calcium channel subunits complex, b) they are regulated by protein kinases, c) they act as key modulators of the gating and pharmacological properties of α1 subunits.

Four isoforms of β subunit namely β1- β4 are known to exist in mammals [17]. Each of the β subunits appears able to partner with each of the α_1 subunits from high voltage-activated channels. The different β subunit isoform cause different shifts in voltage dependent gating; hence the association with different β subunit can result in the substantial change in the physiological functions of α_1 subunit.

3.2.3. α2/δ subunits:

The glycosylated proteins α_2 and δ are linked together by disulfide bonds to form a dimer of molecular weight 175 kDa. The structure of $\alpha_2\delta$ subunit was first determined using biochemical studies on purified dihydropyridine receptors from skeletal muscles. The cDNA sequence obtained made it clear that both α_2 and δ subunits are products of a single gene encoding the α_2/δ pre-protein, which is cleaved into α_2 and δ by post translational proteolytic process [18]. Four $\alpha_2\delta$ subunits have been cloned: $\alpha_2\delta$ -1, $\alpha_2\delta$ -2, $\alpha_2\delta$- 3 and $\alpha_2\delta$ - 4. The $\alpha_2\delta$ subunits are reported to be GPI-anchored, which has implications for their intracellular trafficking and endocytosis. Although little structural information is available for $\alpha_2\delta$ subunits, it is well established that the α2 domain is completely extracellular, whereas the δ domain contains a transmembrane sequence[18]. The $\alpha_2\delta$ subunits play an important role in enhancing the forward trafficking of the α_1 Ca^{2+} channel subunits for high voltage-activated channels, and decrease their turnover at the plasma membrane [19].

3.2.4. γ subunit:

A fifth subunit, known as γ (25-38 kDa), has 4 transmembrane domains. Purification of cardiac Ca^{2+} channels labelled by dihydropyridine Ca^{2+} antagonists revealed subunits of α_1, $\alpha_2\delta$, β and γ subunits of skeletal muscle Ca^{2+} channels, whereas immunoprecipitation of neuronal Ca^{2+} channels labeled again by dihydropyridine Ca^{2+} antagonists identified α1, $\alpha_2\delta$ and β subunits, but no γ subunits. Similarly, purification and immunoprecipitation of brain membrane preparations also revealed α_1, $\alpha_2\delta$ and β subunits, but no γ subunits. However, recent experiments have revealed the presence of a novel neuronal γ subunit, which serves to be a target of the stargazer mutation in mice. The stargazing-like γ subunits are also called as transmembrane AMPA receptor modulators, and are the primary modulators of glutamate receptors in the post synaptic membrane of brain neurons [7,20]. In spite of all these studies, detailed information on physiological and structural role of the γ subunits and their association with voltage gated Ca^{2+} channels is yet to be determined.

3.3. Classification of Ca^{2+} channels:

The first recordings of Ca^{2+} currents in CMs led way to the knowledge of multiple types of Ca^{2+} currents as defined by physiological and pharmacological criteria [21-22]. Ca^{2+} currents in cardiac smooth and skeletal muscles are distinguished by several factors such as single channel conductance, voltage-dependent activation and inactivation, marked upregulation by cAMP-dependent protein phosphorylation pathways and specific inhibition by Ca^{2+} channel antagonists including dihydropyridines, phenylalkylamines and benzothiazepines. The molecular cloning of VGCC subunits has paved way for an elaborate understanding of Ca^{2+} channel diversity. The considerable variation in the degree of depolarisation required to cause significant opening differentiates the voltage gated Ca^{2+} channels from one another. Based on this criterion, the voltage gated Ca^{2+} channels are grouped as low voltage-activated (LVA) and high voltage-activated (HVA) channels. HVAs are activated at depolarized membrane potentials (around -40 mV), whereas LVAs are activated at negative membrane potentials closer to the typical cell resting membrane potentials (-80 mV to -60 mV). Figure 4 shows the phylogenetic representation of the primary sequence of Ca^{2+} channels. Further studies on pharmacological and physiological properties led to a specific classification of native channels as T-, L-, N-, P/Q- and R- type [23-25] (T-, L-, N-, P/Q- and R- type are described in more details in the below subtopics). L-type, R-type, N-type and P/Q type Ca^{2+} channels are grouped under HVA Ca^{2+} channels and T-type Ca2+ channels are grouped under LVA Ca^{2+} channels

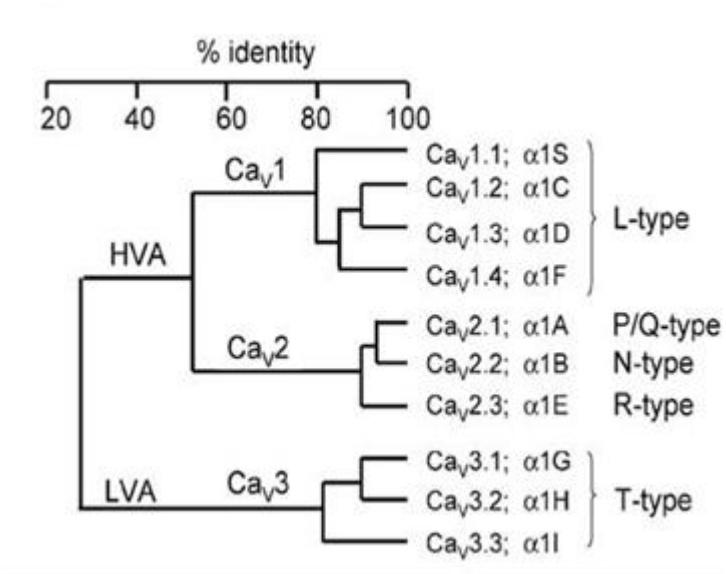

Figure 4: *Calcium channel dendrogram showing the percentage of identity between the different cloned calcium channels. (Modified from Catterall W.A, 2005)*

The pharmacology of the three subfamilies of Ca^{2+} channels is quite distinct. The L-type Ca^{2+} channels (Ca_v1 subfamily) are the molecular targets of the organic Ca^{2+} channel blockers used widely in the treatment of cardiovascular diseases. The L-type Ca^{2+} channel blockers include phenylalkylamines and dihydropyridines. The Ca_v2 subfamily of Ca^{2+} channels that include P/Q, N and R-type, is relatively insensitive to dihydropyridine Ca^{2+} channel blockers but they can be specifically blocked with high affinity by peptide toxins such as ω-Agatoxin and ω-Conotoxin [26].The T-type Ca2+ channels (Ca_v3) are insensitive to both dihydropyridines and known peptide toxins, except kurtoxin, a scorpion toxin known to inhibit $Ca_v3.1$ and $Ca_v3.2$ channel gating[27-28]. Mibefradil acts as a selective blocker for T-type as well as L-type Ca^{2+} currents [29]. Table 1 summarizes the localization, function and also the antagonists of the HVA and LVA Ca^{2+} channels.

Table 1:

Current	Channel	Localization	Specific antagonists	Cellular functions	Inherited diseases
L	$Ca_v1.1$ (α1S)	Skeletal muscles;	Dihydropyridines; phenylalkylamine	Excitation-contraction	**Hypokalemic periodic**

		transverse tubules	s, benzothiazepines	coupling	**paralysis**
	Ca_v 1.2 (α1C)	Cardiomyocytes; smooth muscle myocytes; endocrine cells; neuronal cell bodies; proximal dendrites	Dihydropyridines; phenylalkylamines, benzothiazepines	Excitation-contraction coupling; hormone release; regulation of transcription; sysnaptic integeration	**Timothy syndrome; cardiac arrhythmia with developmental abnormalities and autism spectrum disorders**
	Ca_v 1.3 (α1D)	Endocrine cells; neuronal cell bodies and dendrites; cardiac atrial myocytes and pacemaker cells; cochlear hair cells	Dihydropyridines; phenylalkylamines, benzothiazepines	Hormone release; regulation of transcription; sysnaptic regulation; cardiac pacemaking; hearing; neurotransmitter release from sensory cells	
	Ca_v 1.3 (α1F)	Retinal rod and bipolar cells; spinal cord; adrenal cells; mast cells	Dihydropyridines; phenylalkylamines, benzothiazepines	Neurotransmitter release from photoreceptor	**Stationary night blindness**
P/Q	Ca_v 2.1 (α1A)	Nerve terminals and dendrites: neuroendocrine cells	ω-Agatoxin IVA	Neurotransmitter release; dendritic Ca^{2+} transients; hormone release	**Familian hemiplegic migraine; cerebellar ataxia**

N	Ca_v 2.2 (α1B)	Nerve terminals and dendrites; neuroendocrine cells	ω-Conotoxin-GVIA	Neurotransmitter release; dendritic Ca^{2+} transients; hormone release	
R	Ca_v 2.3 (α1E)	Neuronal cell bodies and dendrites	SNX-482	Repetitive firing; dendritic calcium transients; hormone release	
T	Ca_v 3.1 (α1G)	Cardiac and smooth muscle myocytes; Neuronal cell bodies and dendrites	None	Pacemaking; repetitive firing	
	Ca_v 3.2 (α1H)	Cardiac and smooth muscle myocytes; Neuronal cell bodies and dendrites	None	Pacemaking; repetitive firing	**Absence seizures**
	Ca_v 3.3 (α1I)	Neuronal cell bodies and dendrites	None	Pacemaking; repetitive firing	

Table 1*: Classification of VGCCs based on their cellular function and pharmacologic properties.Although various subtypes of calcium channels are identified in different cells, only a few of them are functionally expressed in CMs.*

3.4. Voltage-Gated Calcium Channels in CMs:

The Ca^{2+} entry through the transmembrane voltage gated Ca^{2+} channels of excitable cells mediates a variety of biological functions like membrane excitability, cell cycle events,

enzyme regulation, muscle contraction, gene expression and hormone secretion. The L-type Ca^{2+} channel is ubiquitous and is dominant in mature CMs, whereas the expression of T-type Ca^{2+} channels varies among species and cardiac tissues. Although it has been shown that T-type Ca^{2+} channels have a possible involvement in pacemaker activity of the heart, their precise functions remain unclear.

The Ca^{2+} influx through L-type Ca^{2+} channels or the L-type Ca^{2+} current (ICa-L) largely determine the Action Potential (AP) amplitude and refractoriness in CMs as well as the automicity in sino-atrial cells. During action potential, I_{CaL} activates contraction by triggering Ca^{2+} release from sarcoplasmic reticulum (SR) this in turn regulates E-C coupling [30-31].

3.4.1. L-type Ca^{2+} channels:

L-type Ca^{2+} channels serve as mediators of Ca^{2+} influx and the cascade of regulatory events accompanying it. They play a pivotal role in the function and dysfunction of ventricular CMs. L-type Ca^{2+} channels are multi-subunit complexes that interact with several molecules involved in the cardiac function, notably by β-adrenergic signaling. The L-type Ca^{2+} channels incorporate the conduction pore, voltage sensor and gating apparatus and the known sites of channel regulation by second messengers, drugs and toxins. Two L-type channel isoforms, $Ca_v1.2$ and $Ca_v1.3$, are known to be present in CMs. The $Ca_v1.2$ gene encodes for the typical I_{CaL} in ventricular myocytes [32]. Experiments with knockout mice have proved that $Ca_v1.2$ knockout mice die during early embryonic development, from cardiovascular failure [33]. $Ca_v1.2$ is organized into four homologous domains (I–IV), each consisting of six-transmembrane α helices (S1 through S6) and a membrane-associated P loop between S5 and S6. Two size forms of the $Ca_v1.2$ subunit (240 and 210 kDa), are present in cardiac muscle and differ by truncation of the C-terminus by *in vivo* proteolytic processing. In ventricular CMs, the proteolytic fragment of $Ca_v1.2$ repressed its own transcription [34]. In order to form a functional L-type Ca^{2+} channel, this main and largest subunit co-assembles with auxiliary subunits in a 1:1:1 ratio: an entirely intracellular β subunit and a disulphide-linked α2δ subunit complex, with the carboxy-terminal transmembrane segment of δ anchoring the extracellular α2 to $Ca_v1.2$ [35]. $Ca_v1.3$ produces currents endowed with a more negative activation threshold

and faster kinetics compared to classical I_{CaL}. $Ca_v1.3$ is mainly expressed in atrioventricular and sinus nodes and also may play a role during development [36].

3.4.2. T-type Ca^{2+} channels:

The pharmacological and biophysical properties of T-type Ca^{2+} channels put them under the low voltage-activated channel class, which open at low membrane potentials and inactivate very rapidly. The T-type Ca^{2+} channels are composed of α_1 subunits, which are the pore-forming subunits that determine most of the characteristics such as channel selectivity for Ca^{2+}, voltage-dependent activation and the sensitivity to organic Ca^{2+} channel blockers. Two isoforms of T-type Ca^{2+} channels are identified in the heart, namely $Ca_v3.1$ and $Ca_v3.2$. Both of these isoforms are functionally expressed in embryonic hearts, but are silenced during the development. Although $Ca_v3.1$ and $Ca_v3.2$ have similar activation and inactivation kinetics, they can be differentiated by their recovery from inactivation and sensitivity to blockade by Ni^{2+}. Recombinant $Ca_v3.2$ currents are blocked by relatively low Ni^{2+} concentrations, while $Ca_V3.1$ currents are much less sensitive to Ni^{2+} [37]. It should be noted that recombinant Ca_v1 channels require auxiliary subunits for normal gating behavior, while $Ca_V3.1$ or $Ca_V3.2$ alone exhibits currents similar to native I_{CaT} [38]. Notably, the T-type Ca^{2+} channels are found to be re-expressed in adult atrial and ventricular myocytes, under various pathological conditions such as hypertrophy and heart failure. During such pathological conditions these channels contribute to abnormal electrical activity and excitation-contraction coupling [38-40]. It has also been shown that increased Ca^{2+} influx through $Ca_v3.2$ induces calcineurin/NFAT hypertrophic signaling [41]. Thus both L-type and T-type Ca^{2+} channels (along with the auxillary subunits in combination with the former) play a significant role in the pathophysiology of the heart.

3.5. Calcium signaling mediated by calcium binding proteins

Ca^{2+} binding proteins play an important role in the regulation of cardiac-signal transduction as well as in cardiac contractility. These proteins sense the Ca^{2+} concentration and bind specifically to signaling molecules, being involved in the establishment of signaling microdomains. The most prominent of Ca^{2+} binding proteins is

Calmodulin (CaM), which is a central mediator of Ca^{2+} dependent signaling, transducing local Ca^{2+} signals into specific cellular outcomes.

3.5.1. Calmodulin

Calmodulin is composed of 148 amino acids and is found to exist in two different configurations namely apocalmodulin and Ca^{2+}-calmodulin. Apocalmodulin lacks Ca^{2+} whereas Ca^{2+}-calmodulin binds with 4 Ca^{2+} ions per molecule- The shift from apo- to Ca^{2+} calmodulin involves substantial structural changes [42]. There are different Ca^{2+} Calmodulin dependent enzymes that play an important role in cardiac function. They are,

a. CaMKII :

One of the main functions of CaM is the regulation of ion channels by activating the Ca^{2+}/CaM- sensitive enzymes such as CaMKII. If intracellular Ca^{2+} concentration rises, activated calmodulin (Ca^{2+}/CaM) binds to CaMKII at the regulatory domain. Ca^{2+}/CaM binding disrupts the association of the regulatory and catalytic domain, and causes a conformational shift exposing the catalytic domain for substrate binding and relieves autoinhibition. Figure 5 shows the regulation of CaMKII by CaM, where the oxidation and autophosphorylation converts CaMKII into Ca^{2+}/CaM independent enzyme leading to many possible physiological and patophysiological outcomes [43].

CaMKII is in fact a serine/threonine kinase which phosphorylates several proteins that play a key role in Ca^{2+} handling and E-C coupling, including ryanodine receptors (RyRs), phospholamban and the LTCC [44]. CaMKII is known to be activated by high amplitude Ca^{2+} waves [45].

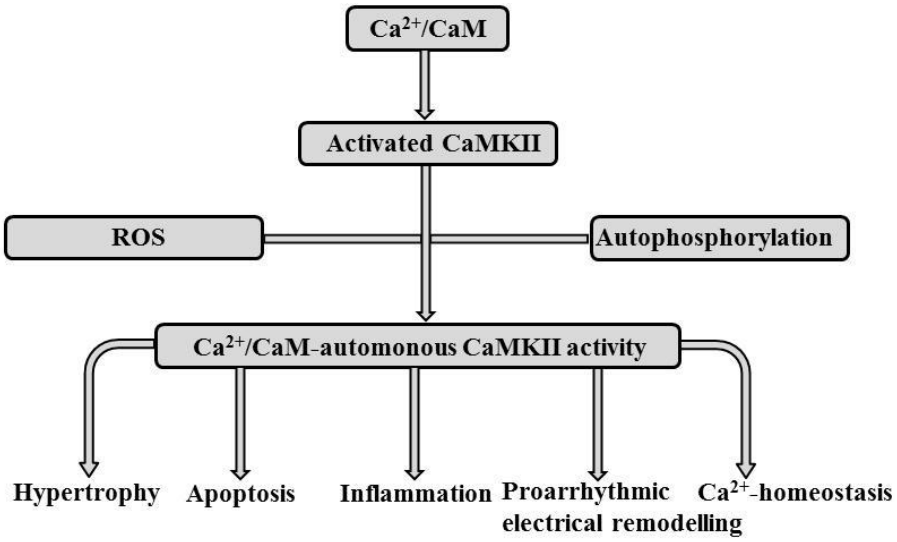

Figure 5: *CaM in the regulation of CaMKII adapted from Erickson et al. Oxidation and autophosphorylation of CaMKII convert it into Ca^{2+}/CaM independent enzyme leading to various arrhythmias. (Adapted from Erickson et al, 2011)*

CaMKII is sensitive to the frequency of Ca^{2+} transients and ideally responds to changes in cardiac rhythm, therefore providing an additional mode of Ca^{2+} regulation. CaMKII regulation of $Ca_v1.2$ channels is a major contributor to the positive force-frequency relationship of cardiac contraction. Direct interaction of CaMKII with $Ca_v1.2$ is necessary for Ca^{2+} dependent facilitation. CaMKII forms a complex with the cardiac $Ca_v1.2$ channel and the kinase activity is directly influenced by its interaction with α1C C terminus [46-47]. CaMKII integrates Ca^{2+} signals to control myocyte excitability. Thus, CaMKII modulates I_{CaL}, which may be important under pathophysiological conditions (e.g. arrhythmias). A transgenic mouse model of cardiac hypertrophy over-expressing CaMKIV showed an increase in CaMKII activity and also showed an increase in the propensity for ventricular arrhythmias, which has been attributed to increased activity of CaMKII resulting in enhanced opening frequency of L-type Ca channels[48].

T-type Ca^{2+} channels are expressed during cardiac development until the end of the neonatal period, then their expression decreases [49]. Significant I_{CaT} reappears in adult ventricular myocytes during the development of cardiac hypertrophy and failure [50]. T-type Ca^{2+} channels are phosphorylated by CaMKII, which increases the probability of single channel openings and that is also upregulated in the ventricles during cardiac hypertrophy[51]. It has been speculated that the enhancement of I_{CaT} in CMs may enhance

their autonomous activity contributing to arrhythmogenesis. However, the potential role of CaMKII signaling in the regulation of T-type Ca^{2+} channels has not been fully explored [52].

It has also been proved that CaMKII is responsive to high amplitude Ca^{2+} waves mediated by activation of β-adrenergic receptors. CaMKII activity is induced by heart failure, in turn inducing the activity of hypertrophic transcription factors NFAT and GATA4 [53-56].

b. Ryanodine receptors (RyR2):

CaM also regulates the SR Ca^{2+}-release channels, the ryanodine receptors (RyR2). Ryanodine receptors are proteins that trigger the release of most of the activator Ca^{2+} that mediates the final step in the E-C coupling. In the heart, RyR2 are localized within the sarcolemmal cisternae of the SR. Cardiac RyR2 are also present adjacent to plasma membrane Ca^{2+} channels. This facilitates spraying of a small amount of Ca^{2+} that enters via plasma membrane channels directly into intracellular release channels, thus resulting in the increase in cytosolic Ca^{2+} concentration, termed as Ca^{2+} sparks. These Ca^{2+} sparks provide signals that open the RyRs. RyR2 then release a much larger amount of Ca^{2+} from the SR, compared to the Ca^{2+} that entered the cell through the plasma membrane channels [57]. When Ca^{2+} binds to CaM, it displaces the autoinhibitory domain and exposes the catalytic activity site of CaMKII. CaMKII can also be autophosphorylated and partially activated in the absences of Ca^{2+}/CaM [58]. Wehrens *et al*. demonstrated that CaMKII mediated RyR2 phosphorylation at Ser-2815 increases the SR Ca^{2+} release by increasing the probability of opening of RyR2 [59]. CaMKII activity and subsequent phosphorylation of RyR2 are increased at faster heart rates [60] due to the "Ca^{2+} memory" properties of CaMKII, thereby during each contraction a fraction of the CaMKII monomers become activated and faster frequencies cause a stepwise increase in the number of activated monomers [61]. This led to the proposal that CaMKII-dependent phosphorylation of RyR2 contributes to the force-frequency response, the observation that cardiac contractility increases as a function of heart rate [60]. The levels of one of the isoforms of CaMKII, CaMKIIδ, are elevated in heart failure samples, suggesting that CaMKII phosphorylation of Ser2815 on RyR2 (increasing the SR-Ca^{2+} leak), may contribute to cardiac pathogenesis [62]. There are also contradictory evidences suggesting

that pathological consequences of CaMKII activation in heart failure are not a result of phosphorylation of RyR2 [63].

c. Calcineurin

In response to elevated levels of Ca^{2+}, calmodulin (CaM) binds to calcineurin (CaN), a serine/threonine phosphatase, leading to its activation. CaM binds to a regulatory domain within CaN leading to a conformational change that displaces the autoinhibitory domain from the active site, resulting in activation of phosphatase. This mechanism is the same as the activation of CaM-dependent protein kinases[64]. The highly conserved phosphatase CaN plays very important roles in numerous processes including T-cell activation, development and function of the central nervous system, and cardiac growth [65]. Dysregulation of CaN might lead to various pathological conditions including vardiac hypertrophy.

NFAT family of transcription factors is one of the principle targets of CaN. Followed by the dephosphorylation by CaN, NFATs translocate to the nucleus where they exert wide range of transcriptional effects. Figure 6 shows how Ca^{2+} entry influences CaN activation leading to NFAT dephosphorylation. It was speculated that GATA4 binding proteins might mediate certain aspects of the hypertrophic program and identified GATA4-NFATc4 interaction [66]. Overexpression of CaN *in vivo* resulted in drastic increases of cardiac hypertrophy, ventricular dilatation, cardiac fibrosis and pulmonary oedema, which led to premature death due to heart failure. This finding was reinforced by the discovery of increased CaN, NFAT and GATA4 activity in samples of failed human hearts [67]. It was also evident that in contrast to the activation of other regulators of hypertrophy such as CaMKII and MAPK, CaN is relatively insensitive to transient increases in $[Ca^{2+}]i$ and that it is rather activated by sustained levels of Ca^{2+} [68]. Several Ca^{2+} channels including TRPC transient receptor potential canonical channels, L-type Ca^{2+} channels and T-type Ca^{2+} channels may also have a role in CaN activation.

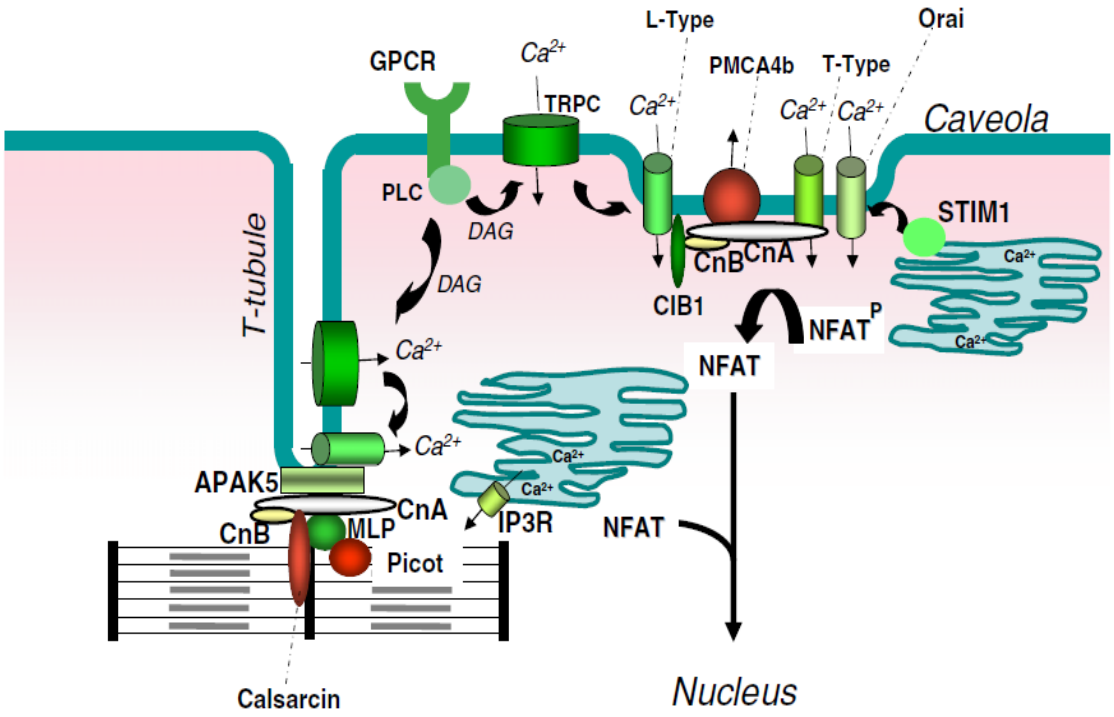

Figure 6: *The sarcolemmal microdomain of calcineurin. Calcineurin becomes activated by calcium that enters the cell through the TRPC, L-type or T-type calcium channels. These channels, in addition to other proteins influence calcineurin activation (green proteins have an activating role, while red proteins show inhibitory influence on calcineurin activity) that ultimately leads to NFAT dephosphorylation and its translocation to the nucleus. Adapted from Heineke J and Ritter O, 2012.*

Ca^{2+} entry via LTCC induces CaN activity and the physical interaction between CaN and $Ca_v1.2$ has been shown to enhance L-type Ca^{2+} currents[69-70]. CaN directly interacts with N- and C-terminal regions of the α1C unit. Through these interactions CaN is able to dephosphorylate the L-type Ca^{2+} channel and thereby modulate channel opening. Hence, activation of CaN enhances, while its inhibition reduces L-type channels currents, while its inhibition has the opposite effect [70]. Also, a CaN-dependent increase in L-type Ca^{2+} current was also reported in mouse hypertrophy models [71]. Cardiac overexpression of the pore-forming α1C subunit of the L-type Ca^{2+} channel in transgenic mice leads to 29-44% increase in Ca^{2+} currents in transgenic CMs and also leads to cardiac hypertrophy, which is associated with enhanced cardiac interstitial fibrosis [72]. Experiments have shown that the pharmacological inhibition of L-type Ca^{2+} channels leads to the reduction of cardiac hypertrophy in human patients [73-75].

While L-type Ca^{2+} channels play a key role in excitation-contraction coupling, T-type channels play only a minor role in the process and, instead, seem to be engaged primarily in Ca^{2+}-triggered signal transduction [76]. A recent report has shown the localization of α1H and α1G channels within the caveole in neonatal and adult CMs, which implies an important role in the modulation of caveolae-based signaling [77]. It has also been reported that mice with a genetic deletion of α1H show a dramatic reduction in the development of myocardial hypertrophy in response to pressure overload and angiotensin II stimulation. CaN also physically interacts with α1H, supporting the existence of both proteins within the same signaling domain [78]. Contrastingly, α1G T-type channel appears to mediate anti-hypertrophic functions through coupling activation of NO-synthase NOS3 [79]. These data show that CaN/NFAT signaling and cardiac hypertrophy at the sarcolemma are regulated by a specialized subset of L-type Ca^{2+} channels and a majority of T-type Ca^{2+} channels (most likely within caveolae) [80].

Thus, L-type and T- type Ca^{2+} channels play an important role in Ca^{2+} signaling via Ca^{2+} binding proteins. Any interference in Ca^{2+} signaling due to disfunction of these VGCCs will lead to distruption of Ca^{2+} homeostasis resulting in endoplasmic reticulum stress.

4. Endoplasmic reticulum stress:

4.1. Introduction

The endoplasmic reticulum (ER) is a dynamic intracellular organelle with multiple functions for cellular homeostasis, development and stress responsiveness. The ER plays a critical role in many cellular processes including synthesis, folding, modification and transport of proteins, synthesis and distribution of phospholipids and steroids and storage of Ca^{2+} ions within its lumen. Disturbance in any of these functions results in ER stress and aggregation of misfolded proteins. ER stress has been observed many pathophysiological conditions like nutrient deprivation, viral infection, ischemia/reperfusion and cardiomyocyte hypertrophy [81].

4.2. Endoplasmic reticulum and calcium homeostasis

Ca^{2+} being a ubiquitous second messenger, participates in a wide variety of cellular processes, including protein synthesis, muscle contraction, gene expression, secretion,

cell cycle, metabolism, etc. [82]. The ER is the principal organelle involved in Ca^{2+} homeostasis and one of the important functions of ER, that is protein folding, is Ca^{2+}-dependent. The cytoplasmic Ca^{2+} regulation depends on the activity of a series of transporters in the ER membrane. [The] SERCA pump imports Ca^{2+} from the cytoplasm into the ER lumen, whereas the RyR and inositol 1,4,5-triphosphate receptor are the Ca^{2+} channels that release the Ca^{2+} ions back into the cytoplasm [83-85].

Protein folding requires a highly oxidative, Ca^{2+}-rich environment and an abundance of ER-resident molecular chaperones, including glucose- regulated protein 78 (GRP78 or BiP), GRP94, calnexin, calrectulin and protein disulphide isomerase (PDI). The nascent polypeptides translocate into the ER where they mature to form their most thermodynamically stable native structure, before being secreted into the extracellular space or transported to other organelles. The molecular chaperone GRP78 facilitates the protein folding mechanism. Perturbation of the Ca^{2+} homeostasis results in protein misfolding or disruption in the ability of the ER to correctly fold proteins. Normally cells ensure that proteins are correctly folded using a combination of molecular chaperones, foldases and lectins. However, when proper folding cannot be restored, incorrectly folded proteins are targeted to ER-associated degradation pathways (ERAD) pathways for processing [86]. Any disruption in the Ca^{2+} homeostasis in the ER lumen will affect the protein folding activity of the ER, leading to ER stress. To monitor the protein folding process and to ensure that only native proteins are exported to their final destination, cells have evolved a sensitive quality control system called the unfolded protein response (UPR) system. This intricate mechanism is an important means of reestablishing cellular homeostasis and alleviating the inciting stress. The emerging evidences demonstrate that the UPR influences cellular metabolism through diverse mechanisms, including Ca^{2+} and lipid transfer, raising the prospect of involvement of these processes in the pathogenesis of disease, including cardiovascular disease, cancer, neurodegeneration and diabetes mellitus.

In mammalian cells, UPR is a complex signaling program mediated by three ER transmembrane receptors, namely activating transcription factor (ATF6), inositol requiring kinase 1 (IRE1), and double stranded RNA-activated protein kinase-like endoplasmic reticulum kinase (PERK). In the physiological state, GRP78/Bip binds to and suppresses the activity of these three proximal, ER-resident transmembrane UPR transducers [87].

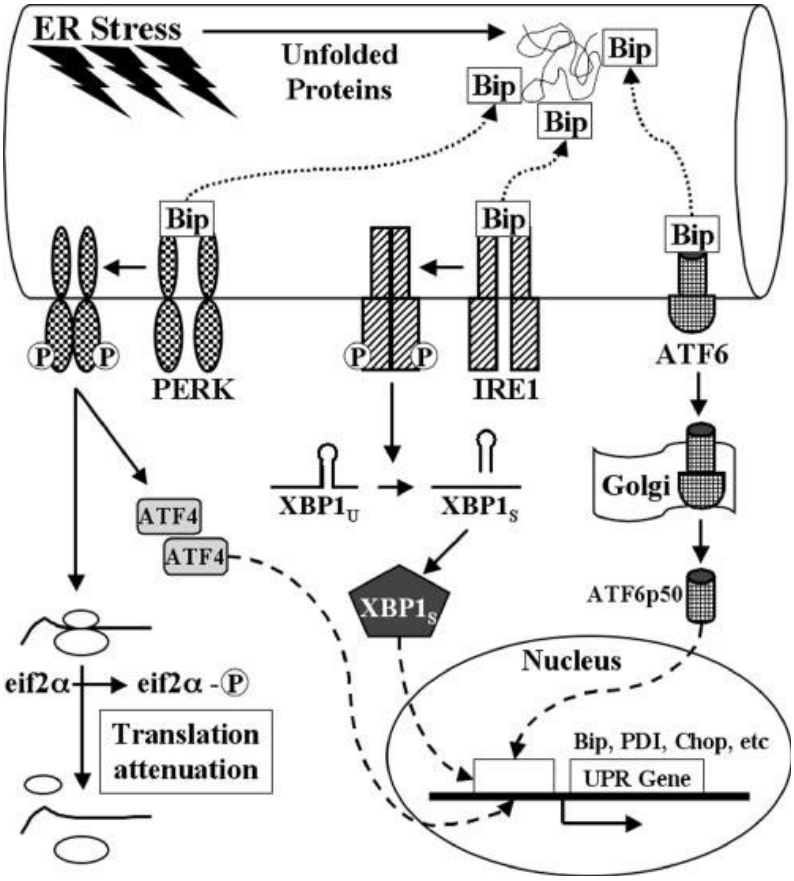

Figure 7: *Illustrative diagram representing ER stress and UPR activation. Binding of Bip to misfolded proteins results in phosphorylation of UPR transducers PERK, IRE1 and activation of ATF6, leading to the induction of various UPR genes. B.L.Williams and W.I. Lipkin,2006.*

During ER stress, Bip binds to misfolded proteins and is thereby sequestered from PERK, IRE1 and ATF6 (Figure 7)[88] . When released from GRP78/Bip, the kinase domain of the activated PERK phosphorylates Ser51 of the α subunit of the eukaryotic translation initiation factor1 (eif2α), thereby attenuating global translation initiation and protein synthesis [89]. PERK-mediated phosphorylation of eif2α preferentially induces translation of activating transcription factor 4 (ATF4)[90]. Followed by GRP78/Bip release, IRE1 undergoes dimerization and trans-autophosphorylation, activating its endoribonuclease activity, IRE1 then mediates the excision of a 26- nucleotide intron from X-box binding protein 1 (XBP1), resulting in a translational frameshift and formation of a potent transcriptional activator [91]. Bip-free ATF6 is transported to the golgi, where it is cleaved by site-1 and site-2 proteases, generating a 50 kDaKDa bZIP transcription factor (ATF6p50) that migrates to the nucleus [92]. The downstream nuclear effectors of the UPR

regulate the expression of genes that enhance the protein folding and degrading capacity of the ER, regulate amino acid metabolism, mediate resistance to oxidative stress and induce apoptosis [93].

4.3. ER Stress in the Myocardium

There are several studies that correlate ER stress with myocardial damage. For example the hearts of transgenic mice that overexpress monocyte chemoattractant protein-1[94]. ER stress is activated in such hearts resulting in heart failure. This experiment suggests that, in this model, the preapoptotic phase of ER stress contributes to the loss of myocardium associated with failure. On further exploration of the role of ER stress in heart failure, it has been found that the transgenic overexpression of a mutant KDEL receptor, an ER protein that facilitates ER protein targeting, activates the ER stress response in mouse hearts and causes dilated cardiomyopathy. Also, overexpression of the ER stress response gene p53-upregulated modulator of apoptosis (PUMA) contributes to ER stress-mediated apoptosis in cultured CMs [95] and targeted deletion of PUMA in mouse hearts attenuates CMs death during *ex vivo* ischemia/reperfusion (I/R) [96]. There are also contradictory results that suggest that ER stress might protect heart and even foster hypertrophic growth of the myocardium. Studies also suggest that the prosurvival phase of ER stress might help accommodate the increased protein synthesis that takes place during overload-induced hypertrophy [97].

ER stress might also play an important role in developing myocardium. GRP78 expression is upregulated in the neonatal mouse heart compared to the adult mouse heart[98]. Moreover, GRP78 is required for normal cardiac development[99].

It has also been shown that targeted disruption of XBP1 gene in mice proved to be embryonically lethal due to cardiac developmental defects[100]. This indicates that ER stress response is required for proper cardiac development. Since ischemia activates ER stress in the brain, several studies were done to assess the ER stress response in myocardium by ischemia or I/R. Studies revealed that numerous ER stress response genes were activated within 24 hours of *in vivo* myocardial infarction in mouse hearts [101]. Studies also showed that the expression of several ER stress markers increased in mouse hearts subjected to I/R. All these studies pointed towards the cardioprotective effect of ER stress response.

A further study in support of protective roles for ER stress showed that overexpression of activated ATF6 in transgenic mouse hearts decreased ischemic damage and increased ventricular pump function in an *ex vivo* I/R model [102] However, it's still not clear if the ER stress is protective or damaging. Perhaps mild and brief episodes of ischemia favour activation of prosurvival aspects of ER stress, whereas severe or long episodes of ischemia eventually activate proapoptotic aspects. Other factors including the presence of additional ER stress, or existent cardiac pathologies may influence the time to transition between the prosurvival and proapoptotic aspects of ischemia-activated ER stress [103]. Sustained UPR resulting from ER stress could also lead to the removal of misfolded poly-ubiquitinated protein aggregates by a self-eating process called autophagy which could be a prosurvival mechanism adapted by the cell. Basal autophagy is seen in the developing heart, which makes it important for protein quality control and the normal functioning of heart. Thus it becomes necessary to study about autophagy and the link between ER stress and autophagy.

5. Autophagy

5.1. Introduction

Autophagy, one of the major catabolic mechanisms of a cell, is an evolutionarily conserved mechanism of recycling long lived proteins and clearance of defective organelles [104]. Basal autophagy is known to be critical for the fundamental housekeeping function of cell survival and homeostasis [105]. In addition, autophagy also plays significant roles in metabolism by replenishing energy substrates and governing mitochondrial number and quality control [106]. It is a near-ubiquitous process of delivery of cytoplasmic materials, including proteins and organelles, to lysosomes for degradation[107]. Based on the differences in function and mechanism, autophagy has been divided into three types namely, microautophagy, macroautophagy and chaperone mediated autophagy. Macroautophagy (referred commonly as autophagy) is the most common form of autophagy.

Macroautophagy is a bulk degradation process for cytosolic proteins and organelles which involves 3 major steps: formation of ultrastructurally distinct double membranous vesicles called as autophagosomes, fusion of autophagosomes with lysosomes and degradation by the lysosomal acid hydrolases and proteases [108-109]. In macroautophagy,

the impaired cytoplasmic components are engulfed in an autophagosome, which then fuses with the lysosome to deliver its contents for degradation in the mature autolysosome.

The core autophagic machinery consists of evolutionarily conserved signaling molecules encoded by autophagy related genes (ATG) that governs the whole macroautophagic process. They are 1) the Atg1 kinase complex (composed of at least Atg1-Atg13-Atg17-Atg31-Atg29) and the mammalian ULK1/2 complex including ULK1/2-ATG13-RB1CC1-CC12 orf44/ATG10. 2) The phosphatidylinositol 3-kinase composed of Vps34-Vps15-Vps30/Atg6-Atg14 and the mammalian counterpart including PIK3C3/VPS34-PIK3R4/VPS15-BECN1-ATG14. 3) The ubiquitin-like protein conjugation cascades involving Atg3,Atg4, Atg5, Atg7, Atg8 (and the mammalian LC3 and GABARAP subfamilies), Atg10, Atg12 and Atg16 and the corresponding mammalian homologs, which are required for phagophore expansion, autophagosome maturation and cargo recruitment. 4) A recycling protein complex composed of Atg12, Atg9, Atg18, and Atg21 and the mammalian homologs including WIPI1/2, which participates in the transfer and recycling of components between the phagophore and the phagopore assembly site and membrane donor sites [110].

Autophagy plays a variety of functions. (1) Autophagy induced in response to starvation, promotes cell survival by allowing a cell to break down non-essential or excessive cellular components, thus releasing substrates that facilitate the generation of ATP and the recycling of molecules such as essential amino acids that the cell itself cannot manufacture *de novo*. (2) Autophagy that serves as a primary route for the removal of excess or damaged organelle, is capable of engulfing and degrading complex aggregates of misfolded or damaged proteins that are too large to be handled by the proteasome [111]. (3) It is involved in both innate and adaptive immunity by degrading invading pathogens and delivering self-antigens for MHC-class-II loading. (4) Autophagy may also contribute to cell death. Autophagy mediated cell-death has been termed as type-II programmed cell death in contrast to type-I apoptotic programmed cell death. In certain diseases, particularly in neurodegenerative diseases there is a clear correlation between cell death and abundance in autophagic vesicles. However, cell death could occur not because of abundance in autophagic activity; rather the inefficiency in processing the autophagic vesicles or deficient autophagic activity could affect the cell viability [112]. In the regulation of autophagic flux, the autophagosome processing involves three discrete steps, namely

nucleation, elongation and fusion. In addition, there are also three control check points in regulating autophagic flux namely, induction, substrate targetting and degradation.

a. Nucleation

The nucleation of an autophagic isolation membrane is initiated by the activation of a class III phosphoinositide 3-kinase (PI3K), called Vps34, by its binding partner Beclin1. Class III PI3 kinases phosphorylates the three position –OH group of the inositol ring of phosphatidylinositol (PI), a negatively charged membrane phopspholipid to produce PI(3)P. PI(3)P then recruits additional proteins required for the formation of isolation membrane [113]. This process of formation of the isolation membrane is regulated by a system of evolutionarily conserved proteins (Atg proteins). Beclin1 (Atg6), a part of a PI3-K plays an important role during the initial steps of autophagosome formation by mediating the localization of other Atg proteins to the isolation membrane.

b. Elongation

The synthesis of autophagosomes requires the Atg5-Atg12 and LC3 (Atg8) - phosphotidylethanolamine (PE) conjugation systems. The covalent conjugation between Atg12-Atg5 is similar to that of ubiquitination where Atg12 is first activated by Atg7, and then transferred to Atg10. Atg12 is then covalently conjugated to Atg5 at a lysine residue and Atg10 is released [114]. The Atg12-Atg5 complex interacts non-covalently with Atg16, and this complex recruits covalently linked phospholipid PE and LC3 (LC3-PE) to initiate the elongation process [115]. Lipidation of LC3 converts it from the LC3-I form to the LC3-II form and allow insertion of the protein into the growing autophagic membrane. The free cytoplasmic protein end of LC3-II identifies the membrane as an autophagosome and allows targeting selective substrates. LC3-II is therefore a potential avenue for targeting active autophagosomes prior to their fusion with lysosomes [116-117]. The basic method to monitor the regulation of autophagic flux is by monitoring the conversion of LC3-I to LC3-II by western blot and the use of green fluorescent protein fused to LC3 (GFP-LC3) to visualize the vesicle formation.

c. Fusion

The fusion of mature autophagosomes to lysosomes can be either direct or mediated by endosome fusion. Most of the components required for this process play a major role in vesicular trafficking in general and are not specific for autophagy.

d. Induction

Kinase mammalian target of rapamycin (mTOR) acts as a central control point for the induction of autophagy. mTOR lies downstream of insulin signaling and class I PI3K [118]. Many of the mechanisms that promote or inhibit autopahgy converge in some way on mTOR and the induction complex [119]. In contrast to class III PI3K, class I PI3K generates PI(3,4)P2 and PI(3,4,5)P3 in addition to PI(3)P from PI. Binding of insulin or other growth factors to receptors in the plasma membrane activate Class I PI3K. PI(3,4)P2 and PI(3,4,5)P3 formed at the plasma membrane, then recruit phosphoinositide-dependent kinase-1 and protein kinase B (AkT) to the membrane via their pleckstrin homology domains resulting in sequential activation [120]. The cascade of events activated by Class I PI3K at the plasma membrane leads to activation of mTOR and inhibition of autophagy. There are two distinct mTOR complexes, which target different downstream components. The mTORC1 complex is sensitive to rapamycin. It promotes cell growth by blocking autophagy through ULK1 phosphorylation and by increasing protein translation through phophorylation of ribosomal protein S6 kinase, eEf2 kinase and translational repressor 4E-BP1. Thus activation of mTOR could promote cellular catabolism, whereas, inhibition of mTOR could promote anabolism.

e. Substrate targeting

The autophagy that is induced by starvation is non-selective and it degrades a diversity of cellular components at one time to maintain the cellular homeostasis. However, autophagy can also selectively remove damaged or excess cellular components. Though a diversity of organelles and cellular components could be eliminated through selective degradation, cells recruit ubiquitination process to maintain specificity [121]. Adaptor proteins like p62/SQSTM1 contain both a ubiquitin binding domain and a LC3 interacting region. So the ubiquitination of misfolded protein aggregates or a protein in the outer

membrane of an organelle provides essential tagetting signals to attract such adaptor proteins. P62/SQSTM1 on the other hand recruits ubiquitinated targets to the nascent phagophore by binding to the cytoplasmic tail of the LC3 II in the membrane of the autophagosome. Selective specificity is based on the transmission of appropriate signals from the target component to recruit the appropriate ubiquitin ligase and the specific adaptor protein.

f. Degradation

The substrates recruited by the adaptor proteins are delivered to the autolysosome via LC3 II binding for degradation. The degraded components are released in to the cytoplasm by the permeases. Thus degradation process acts as a final step in controlling the autophagic flux.

The autophagic activivity has been measured by the presence of double membrane bound autophagosomes on electron micrographies. Importantly, the abundance of autophagosomes not only reflects the increase in autophagosome formation but also a decrease in the lysosomal processing of autophagosomes. Thus the ultrastructural changes resulting from an increase in autophagic activity can be indistinguishable from abundance in autophagosome caused by blocking the autophagic activity [116].

There are few techniques that are used for assessing changes in autophagic flux in cultured cells. 1) Addition of lysosomal protease inhibitors like Bafilomycin A1 to the media prevents the fusion of autophagosome with the lysosome, thereby blocking autophagy. The increase in LC3-II simply indicates the increase in autophagosome formation. But in the presence of a lysosomal protease inhibitor, LC3 II accumulates further, indicating the enhancement of autophagic flux. 2) Changes in the levels of adaptor proteins like p62/SQSTM1 is also useful in assessing the changes in autophagic activity. Inhibition of autophagy results in an accumulation of p62/SQSTM1 whereas increase in autophagic activity results in decrease of p62/SQSTM1. 3) New techniques involving GFPLC3 are also developed for studying the autophagic flux[122].

5.2. Autophagy and Calcium

The first report on the Ca^{2+}-dependent regulation of autophagy suggested that both the chelation of either intracellular or extracellular Ca^{2+} ions and the elevation of cytosolic

Ca^{2+} levels suppressed autophagy. After this, some reports suggested that cytosolic Ca^{2+} stimulates autophagy while others report that cytosolic Ca^{2+} and Ca^{2+}-handling proteins inhibit autophagy (see below). Indeed, Ca^{2+} signaling may have opposite effects in normal cells versus stressed cells, and differently regulate basal autophagy and augmented autophagic activity in response to stress.

5.2.1. Cytosolic calcium as an inducer of autophagy

Autophagy that is stimulated by vitamin D, ionomycin and thapsigargin has been known to be induced due to ER Ca^{2+} mobilization [123]. It has also been proved that autophagy occurred by the Ca^{2+}-dependent activation of AMP activated protein kinase (AMPK), which required upstream activation of Ca^{2+} / CaM kinase kinase β. AMPK is activated during starvation to inhibit the activity of mTOR. In addition, the calcium phosphate transfection method has been shown to induce a Beclin1 dependent autophagy in HEK-293 cells, proving the potential of Ca^{2+} as an autophagy inducer [124-125].

5.2.2. Cytosolic calcium as an autophagy inhibitor

Ionositol 1,4,5- trisphosphate (IP_3) receptor which is located at the ER is an ubiquitously expressed intracellular Ca^{2+} release channel. IP_3Rs may mediate Ca^{2+} release from the ER to the cytosol, in response to elevations in the cytosolic IP_3 levels produced in the cells after stimulation by hormones, growth factors or antibodies [126]. It has been shown that while moderate elevations of cytosolic Ca^{2+} activate IP_3Rs, higher Ca^{2+} levels exert the opposite effect [127-128]. Many cytosolic proteins including protein kinases and phosphatases, directly bind and regulate IP_3Rs, and in turn control ER Ca^{2+} flux properties. IP_3-induced Ca^{2+} release towards the mitochondria promotes ATP production, inhibition of AMPK and resulting in stimulation of mTOR activity. mTOR can stimulate the IP_3Rs by direct phosphorylation[129-130].

Thus, spontaneous Ca^{2+} signals may suppress basal autophagy in healthy cells through mitochondrial pathways, acting as a quality control system to maintain cell homeostasis; stress conditions may promote Ca^{2+} signaling and may elevate Ca^{2+} in the cytosol resulting in autophagy stimulation through cytoplasmic effector molecules. On the other

hand, $IP_3$3Rs can also inhibit the dissociation of Beclin1 from BCl-2, independently of its Ca^{2+} release activity [131]. It has been well established that a fraction of IP_3Rs present in ER domains are in close association with mitochondria[132]. These domains allow efficient transfer of Ca^{2+} ions from the ER to the mitochondria[133]. The spontaneous Ca^{2+} flux to the mitochondria indicates that the cells are healthy and they do not require activating autophagy. Reducing these Ca^{2+} signals activate autophagy. Further reduction of these Ca^{2+} signals lead to the activation of ER-stress-induced apoptosis[134]. Also, blockade of L-type Ca^{2+} channels will result in an abnormal low Ca^{2+} transfer to the mitochondria [135]. Although the exact mechanisms behind the Ca^{2+} signaling switch from anti-autophagic to pro-autophagic are yet to be clarified, it's clear that IP_3Rs combined with proteins like BCl-2 and Beclin1 play a central role in both the processes and regulate the Ca^{2+}-signaling in basal and stress conditions [136].

5.3. Autophagy in heart

Basal cardiomyocyte autophagy is a very important process for cardiomyocyte function and survival. It has been shown that vitiating autophagic pathways in adult heart by conditional inactivation of either Atg5 or Atg7 genes resulted in rapid-onset of cardiac hypertrophy, left ventricular dilation and diminished cardiac output [137]. It has also been observed that effect of aging (and a concomitant decrease in basal autophagy) leads to the accumulation of defective proteins and organelles leading to functional defects [138,139]. These observations show that the housekeeping cardiomyocyte autophagy is essential for protein quality control. Figure 8 illustrates the major molecules and molecular pathways that are known to regulate autophagy in ventricular CMs.

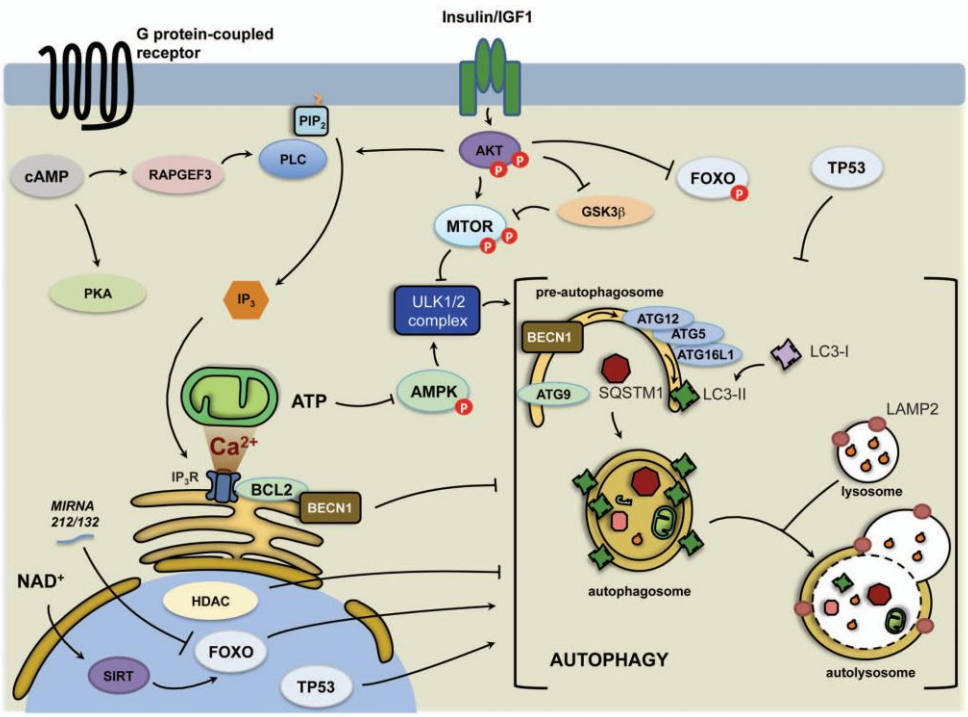

Figure 8: *Simplified scheme of the major cellular pathways governing autophagic flux in ventricular CMs. Adapted from Lavandero S et al. 2013.*

5.3.1. Afterload induced autophagy

Pathological stress due to nutritional scarcity or hypoxia results in a rapid increase in autophagic flux and help to replenish scarce nutrients [105,140]. On the other hand, suppression of autophagy during starvation reduces intracellular ATP levels and diminishes cardiac output [141]. In spite of this, pathological conditions resulting from elevated afterload, chronic ischemia and ischemia/reperfusion are associated with induction of high level autophagy. There are arguments that say cardiomyocyte autophagy could be adaptative or maladaptative depending on the context and amplitude of its induction during pathological conditions [142]. Activation of autophagy has proved to be protective during ischemic conditions whereas it could be detrimental in the load-stressed heart and during post-ischemic reperfusion [143].

Beclin1, a molecular element critical to initiate autophagy [144], upon overexpression specific for CMs, accelerated the load stress-induced autophagy, resulting in cardiac failure. Conversely, diminishing the autophagic response by 50% in Beclin1 haplosufficient mice attenuated pathological remodeling induced by after load stress [145].

Excessive autophagy can lead to the removal of key molecules and organelles, triggering autophagic cell death. On the other hand, in case of proteotoxic cardiomyopathy, an increased autophagic flux helps in the removal of toxic, misfolded, oxidized protein[146]. Thus the underlying cardiomyopathic stimuli lead to the functional differences in the actions of autophagy.

5.3.2. Autophagy in myocardial ischemia and ischemia/reperfusion

Hypoxia is capable of rapidly inducing a cell survival response engaging autophagy by activating the hypoxia inducible factor (HIF-1). This cell survival response is mediated by the BH3-only protein Bcl-2/E1B 19 kDa-interacting protein 3 (BNIP3/BNIP3L (NIX)) that is induced by HIF-1. Mitochondria-associated BNIP proteins also mediate mitophagy, a metabolic adaptation that controls ROS production and DNA damage. In addition, severe hypoxic conditions can induce HIF-independent autophagic response which is an outcome of extreme nutritional stress response involving AMPK-mTOR and UPR pathways[147-148].

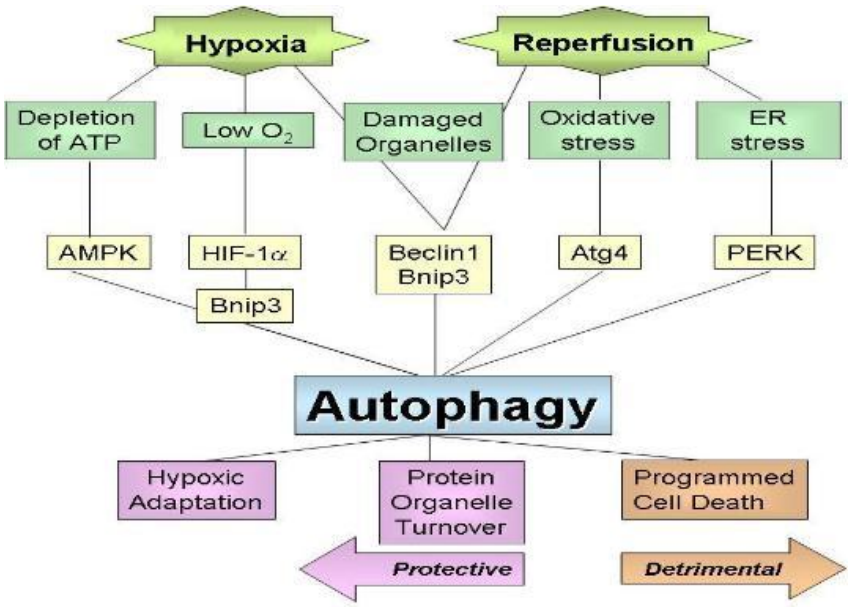

Figure 9: *Myocardial ischemia and reperfusion elicit conditions that strongly induce autophagy including energy starvation, ER stress, protein aggregation etc. Although autophagy induction by ischemia is protective, enhancement of autophagy during reperfusion could induce cell death in the heart. (Adapted from Matsui et al, 2008)*

Although there have been several reports on the induction of autophagy upon ischemic insult in various cell systems[149], there is a question of debate on the effects of autophagy in ischemia/reperfusion injury. During mild ischemia, cardioprotective autophagy is activated by AMP-activated protein kinase (AMPK) mediated inhibition of mTOR and this autophagy is adaptative and exerts a pro-survival effect. However, when oxygen and nutrients are restored during reperfusion, cardiomyocyte autophagy is upregulated dramatically involving the over-expression of Beclin1, with detrimental effects for CMs [143,150].

5.3.3. Autophagy in Cardiac hypertrophy

During myocardial infarction, the heart undergoes a compensatory hypertrophic growth response. This hypertrophic response might trigger myocyte death, ventricular dilation, diminished contractile performance, and a clinical syndrome of heart failure [151].

There are several humoral factors that also act as hypertrophy stimulants in CMs. First group of hypertrophic stimulants are growth factors such as fibroblast growth factor, insulin-like growth factor, and others [152-153]. These growth factors through several second messenger cascades activate physiological or adaptive hypertrophic growth. A second group of humoral stimulus arises from the activation of heptahelical G-protein coupled receptors like beta 1-adrenergic receptors, AT1 receptor for angiotensin II (Ang II) and ET receptor for endothelin-1[154]. Chronic elevation of plasma Ang II has been identified as a major cause in the pathogenesis of hypertrophy and is also known to play a role in cardiac remodeling. Activation of α-adrenergic receptors and in turn activation of PKC also is considered as a powerful stimulus for cardiac hypertrophy[155]. The third group of hypertrophy stimulus is activation of mineralocorticoid receptors by aldosterone. Aldosterone binds to mineralocorticoid receptor and enters the nucleus to regulate gene expression. Aldosterone signaling is associated with GATA4 transcription, which is induced during hypertrophic stimuli. Aldosterone also increases AT1 receptor density thereby leading to aldosterone-induced cardiac hypertrophy and myocardial fibrosis ultimately leading to heart failure[156-158].

Autophagy has been now known to play a critical role in heart failure. Experiments have shown that in isolated neonatal myocytes, inhibition of autophagy by knockdown of Atg7 induced hypertrophy and also that the conditional deletion of Atg5 increased the size of

myocytes [159]. It has also been shown that rapamycin, a potent inducer of autophagy, prevents cardiac hypertrophy induced by thyroid hormone treatment [160]. Thus autophagy might antagonize cardiac hypertrophy by increasing protein degradation and reducing cardiac mass. Disrupting the gene coding for Beclin1 decreases cardiomyocyte autophagy and diminishes pathological remodeling induced by severe pressure overload. On the contrary, Beclin1 over expression increases autophagic activity and accelerates hypertrophy [161].

5.4. Cardiac autophagy as a therapeutic target

The incidence of heart failure remains high in spite of significant advances in both pharmacologic and device based cardiovascular therapeutics [1]. Our level of understanding of cardiac plasticity and remodeling is insufficient for the utility of these advancements in therapeutics [162]. However, recent findings on cardiomyocyte autophagy could prove it to be a novel therapeutic target in treating heart failure. In the process of cell growth, both anabolic and catabolic pathways are activated. In the initial phase, the anabolic process is higher and cell growth emanates. When this cell growth reaches a steady state the autophagic flux increases. It has been shown that cardiomyocyte autophagy triggered by elevation in afterload has both adaptative and maladaptative features. Activation of autophagy during pressure stress maybe beneficial, but over-activation of autophagy has detrimental consequences [163]. The prevalence of autophagy in various cardiac disorders suggests the existence of a common cellular pathway that could be targeted for the therapeutic gain [164].

6. ER stress-induced autophagy

ER stress is caused by accumulation of unfolded, misfolded or damaged proteins that exceeds the capacity of protein folding chaperones in the ER. The unfolded protein response sets up to eliminate this stress and can also lead to the induction of autophagy. In mammalian cells, the UPR signaling is more complicated than in yeast [165]. The three ER stress transducers, namely PERK, ATF6 and IRE1, sense the level of unfolded protein in the ER and activate transcription of numerous genes. In addition to UPR, ER stress also results in release of Ca^{2+} from the ER and hence increases the cytosolic Ca^{2+} in the cell [5]. In resting conditions the ER-resident chaperone GRP78 binds to all three UPR

transducers and, during stress conditions, GRP78 binds instead to missfolded proteins [166]. Once released, PERK, IRE1 and ATF6 mediate the UPR survival response to restore the ER homeostasis [167]. To further reduce the ER load, the UPR encompasses the translocation of the ER proteins to the cytoplasm, where they are degraded through ERAD [168]. In situations of prolonged stress, upregulation of CHOP /GADD153 leads to the activation of apoptosis. But in some situations, autophagy can intervene and remove the accumulated polyubiquitinated aggregates thus preventing cell death [169].

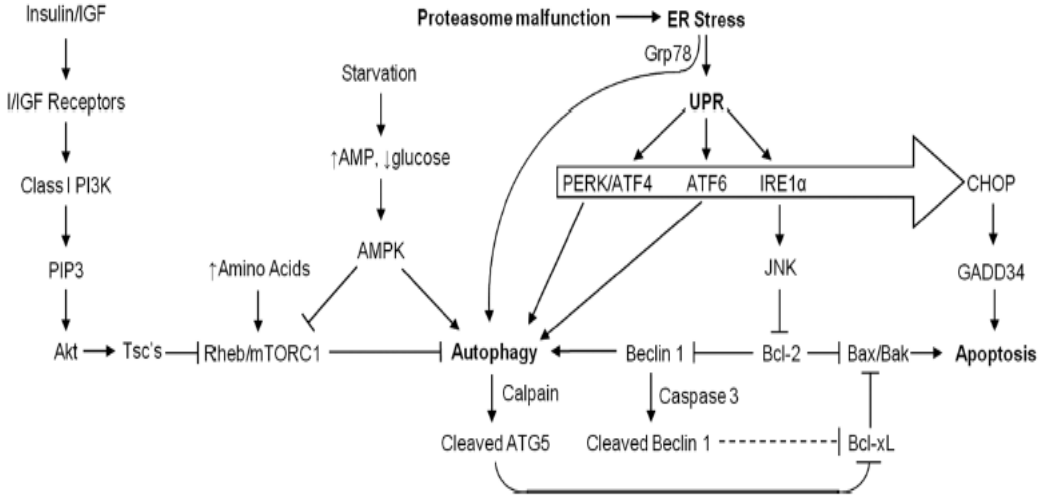

Figure 10: *Integration of ER stress and macroautophagy with the regulatory network controlling the maintenance of cellular homeostasis. During ER stress GRP78 induces both autophagic vesicle formation and UPR through different mechanism. Adapted from Benbrook et al, 2012.*

It has been demonstrated that ER stress induces autophagy directly through the upregulation of GRP78 and through mechanisms downstream of the GRP78 release of the three UPR transducers (Figure 9) [170]. The knockdown of GRP78 in normal and cancer cells has been shown to prevent the formation of autophagosomes in response to starvation. The dilated and distrupted ER and the deficient autophagosome formation induced by knockdown of GRP78 were known to be simultaneously alleviated by knockdown of XBP1- transcription factor [171], suggesting that an intact ER is maintained by and/or required for autophagy. The link between GRP78 and autophagy induction occurs downstream of nucleation, as the knockdown of GRP78 did not prove to have any

effect on the association between Beclin1 and Vps34 [171], a class III phosphatidylinositol 3-kinase (PI3K) critical for the initiation of autophagosome biogenisis.

The PERK-eIF2α signaling pathway is also known to mediate ER stress-induced autophagy in mammalian cells [169]. ER stress induced by polyglutamine repeats (PolyQ) upregulate Atg12 expression and induces autophagy as interpreted from the conversion of LC3 I to LC3-II and the increase in the LC3-positive vesicles in the mouse embryonic carcinoma cells and murine embryonic fibroblasts (MEFs) [172]. In addition, eIF2α mediates autophagy in systems that are not associated with ER stress as well. It has also been shown that PERK-dependent phosphorylation of eIF2α is essential for autophagy in MEFs infected with *herpes simplex* virus, and also that eIF2α phosphorylation is required for starvation induced autophagy [173]. Other studies have established the link between the PERK arm of UPR and the upregulation of autophagy through the ATF4-driven transcriptional upregulation of the ATG genes [174].

The UPR transducer IRE1α has been known to upregulate autophagy via IRE1α activation of c-Jun N terminal kinase (JNK). Studies have shown that pharmacological proteosomal inhibition induced ER stress and autophagy in colon cancer cells, but neither upon siRNA-mediated reduction of IRE1α nor in the presence of pharmacological inhibitors of JNK activity [175]. In this study, the JNK inhibitor did not have any effect on XBP1 activation and was equally effective in XBP1-positive and –negative cells, indicating that the UPR mediated upregulation of autophagy occurs through the JNK but not the IRE1α arm of UPR. Thus, like GRP78, the function of XBP1 maybe required to maintain the ER in the functional state and to support autophagic vesicle formation. Both the knockdown of IRE1α, PERK or ATF6 and the use of a JNK inhibitor showed that ER stress-induced autophagy is dependent on IRE1α activation of JNK, but independent on PERK and ATF6 [169]. On the other hand, studies on breast cancer cells have shown that all the three UPR transducers appear to be involved in the induction of autophagy [176].

From all these previous studies, it can be concluded that ER stress can induce UPR mediated transcriptional regulation of pro-autophagic genes, leading to the upregulation of autophagy. Also, it becomes clear that Ca^{2+} has its role to play in all these processes. The core idea of this thesis is to study the role of voltage gated Ca^{2+} channels in the regulation of Ca^{2+} homeostasis and macroautophagy in CMs. This can be achieved by pharmacologic or gene manipulation of the VGCCs, which will be discussed in the further chapters.

Objectives

Objectives

The global objective of this study was to elucidate the involvement of voltage-gated Ca^{2+} channels (VGCCs) in the regulation of Ca^{2+} homeostasis in neonatal ventricular CMs cultured *in vitro*, and study the mechanisms underlying the presumed cytoprotective effects due to their blockade.

The experimental goals to achieve this objective were:

1. To study the effects of the pharmacological blockade T-type and L-type VGCCs in cell viability.
2. To study the induction of *ER stress* by VGCCs blockade, given the Ca^{2+}-dependence of ER homeostasis and its impact on cell viability. This goal was pursued through the study of the UPR and macroautophagy pathways, as likely outcomes of ER stress.
3. To study the effects of gene silencing of VGCCs on cell homeostasis (a term encompassing UPR and autophagy), in order to identify the Ca^{2+} channel isoforms mediating the effects of the pharmacological blockers.
4. To analyze the putative induction of UPR and macroautophagy upon hypoxia and hypoxia-reoxygenation, as *in vitro* experimental paradigms of chronic ischemia and ischemia-reperfusion, respectively.
5. To analyze the putative induction of UPR and macroautophagy upon different hypertrophic stimuli.
6. To analyze the expression profile of VGCCs in CMs subject to hypoxia, hypoxia-reoxygenation or hypertrophic stimuli.
7. To study the effects of VGCCs blockade on the viability of CMs subject to hypoxia, hypoxia-reoxygenation or hypertrophic stimuli and to study the mechanisms for a presumed cardioprotection of VGCC pharmacological blockers against detrimental effects of hypoxia, hypoxia-reoxygenation and hypertrophic stimuli

Materials

Table 2:

1. Chemicals, reagents and cell culture materials

Company	Product
Applied Biosystems(New Jersey, USA)	TaqMan Universal PCR Mastermix First strand c DNA synthesis kit for RT-PCR
BD Biosciences (Bedford, MA, USA)	Plates (100X20) Serological pipettes
Thermo Scientific	EZ ECL Chemiluminescence Detection kit for HRP
Biorad Laboratories(CA,USA)	30% Acrylamide/Bis solution 29:1
Falcon(BD Labware , USA)	Serological pipet (different volume) Plates 100X 20 mm 6 well plates for cell culture 96 well plates for cell culture 24 well plates for cell culture
Fisher Scientific (Madrid ,Spain)	Centrifuge tubes (different volume) Methanol
GIBCO-Invitrogen(Carlsbad ,USA)	Dulbecco's modified Eagles medium (DMEM) 254 medium supplemented with human melanocyte growth supplement (HMGS-2) Fetal bovine serum (FBS) Fungizone amphotericin B OptiMEM FURA-2/AM L-Glutamine LipofectamineRNAiMAX reagent Lipofectamine 2000 Lysotracker red HEPES Horse serum (HS) Medium 199 (M199) Pencilin/ Streptomyicin Trypsin EDTA SYBR safe DNA gel stain Low molecular weight protein bench mark
Merck (Barcelona, Spain)	β Mercaptoethanol
Millipore (Bedford, MA)	Polyvinylidine fluoride (PVDF) membrane
Roche (Germany)	2-(2-Methoxy-4-nitrophenyl)-3-(4-nitrophenyl)-5-(2,4-disulfophenyl)- 2H-tetrazolium (WST-1)
Sigma Aldrich (Barcelona ,Spain)	Ammonium persulfate (APS) Caffeine D-glucose Disodium Hydrogen Phosphate Calcium chloride Sodium hydroxide Manganese chloride Magnesium chloride Potassium chloride Dimethyl sulfoxide (DMSO) Dodecyl sodium sulfate (SDS) Gelatin from porcine skin

	Glycerol Glycine Hoechst (Bisbenzimide H) 33258 N,N,N',N'-tetramethyl-ethane-1,2-diamine (TEMED) Sodium chloride (NaCl) Thapsigargin Tris base Triton X-100 TRIzol reagent Tween-20 Nimodipine Nifedipine (S)-())-Bay K 8644 Kurtoxin Mibefradil Poly-D-Lysine hydrobromide Monodansyl cadavarine (MDC) Aldosterone Angiotensin Phenylephrine Isoprenaline Chloroquine
Panreac (Barcelona, Spain)	Ethanol Hydrochloric acid (HCl) Isopropanol
Sakura Finetechnical (Tokyo, Japan)	Tissue Tek OCT
Cascade Biologicals Inc.(Portland ,OR,USA)	Neonatal human epidermal melanocytes(HEMn-Lp)
Gene Craft (Germany)	Taq DNA polymerase
GE healthcare	50 base pair DNA ladder
Thermo Scientific	EZ ECL Chemiluminescence Detection kit for HRP SuperSignal® West Dura Extended Duration Substrate
Worthington, Lakewood, NJ, USA	Type II collagenase

Table 3:

2. Antibodies

Primary Antibody	Molecular weight	Dilution	Company	Secondary Antibody
Atg5	Complex-56; 33	1: 2000	Sigma Aldrich	**Anti-mouse**
Beclin1	55	1: 10,000	Novus Biologicals	**Anti-rabbit**

P62/sqstm1	47	1: 4000	Novus Biologicals	**Anti-rabbit**
LC3	19;17	1: 3000	Novus Biologicals	**Anti-rabbit**
GRP78	78	1: 3000	Santa Cruz	**Anti-goat**
Gadd 153	31	1: 1000	Santa Cruz	**Anti-mouse**
Ubiquitin	115	1: 500	Santa Cruz	**Anti-mouse**
α-actin	45	1: 5000	Sigma	**Anti-mouse**
β-actin	45	1: 5000	Sigma	**Anti-mouse**

Table 4:

3. **Sequence of short interfering RNA:**

Product name	Sequence	Company
siRNA Ca_v 3.1	5'-CGAUUCCUGUCCAAUGCUAtt-3' 3'-UAGCAUUGGACAGGAAUCGta-5'	**Applied Biosystems**
siRNA Ca_v 3.2	5'-GCAUUGUAGACAGCAAGUAtt-3' 3'-UACUUGCUGUCUACAAUGCga-5'	**Applied Biosystems**
siRNA Ca_v 3.3	5'-GCCUGUCACUCACAUCUCUtt-3' 3'-AGAGAUGUGAGUGACAGGCtg-5'	**Applied Biosystems**
siRNA Ca_v 1.2	5'- CUCUAUACCUGUUCGGAUAtt-3' 3'- UAUCCGAACAGGUAUAGAGAGct-5'	**Applied Biosystems**
siRNA Ca_v 1.3	5'-GGAAGUUCAAUUUCGAUGAtt-3' 3'-UCAUCGAAAUUGAACUUCCct-5'	**Applied Biosystems**

Table 5:

4. **Oligonucleotides used to amplify transcripts of pore-forming Ca^{2+} channel subunits**

	Acc. no.	Sequence	Length (bp)	Temp.
Ca_v1.2	NM_012517	5'-CTCGAAGTTGGGAGAACAGC-3' 3'-GACGAAACCCACGAAGATGT-5'	233	**58°C**
Ca_v1.3	NM_000720	5'-TCCAGCAGGAAATTCGGTGTGTCA-3'	189	**55°C**

		3’-TCGGTCGTGCTTGTAGGAGTAATG-5’		
$Ca_v3.1$	NM_031601	5’-CATCCTGGTCTCCATGGTCT-3’ 3’-GCAAATGACCACAATGTTGC-5’	178	**55°C**
$Ca_v3.2$	NM_153814	5’-ATCCTGGTCACTCTGCTGCT-3’ 3’-ACCCTCCTCCGTCTCGTAGT-5’	201	**55°C**
GAPDH	NM_017008	5’-TCCCTCAAGATTGTCAGCAA-3’ 3’-AATGTATCCGTTGTGGATCTCT-5’	308	**55°C**
XBP1		5’-AAACAGAGTAGCAGCGCAGACTGC-3’ 3’-GGATCTCTAAAACTAGAGGCTTGGTG-5’	290	**63ºC**

Acc. no.: Accession number of the amplified gene; Length: length in base-pairs of the PCR product; Temp.: annealing temperature used in the PCR

Methods

1. Cell culture

The neonatal rat ventricular CMs were obtained as described by Pellieux *et al*[177]. The neonatal rat ventricles from 2 days old Sprague Dawley rats were separated from the atria by dissection and digested thrice at 37ºC by using 0.45 mg/ml type-2 collagenase (Worthington, Lakewood, NJ, USA) and ADS buffer containing 116 mM NaCl, 1mM NaH_2PO_4, 5.4 mM KCl, 0.8 mM $MgSO_4.7H_2O$, 5.5 mM glucose and 20MM Hepes at pH 7.4. Dissociated cells were washed by low-centrifugation in medium consisting of 3:1 mixture of DMEM 1g/L glucose and M199 (GIBCO) supplemented with 10% horse serum, 5% foetal calf serum, 2mM/L Glutamine, 10 mg/mL Streptomycin and 100 units of Penicillin. Cardiomyocytes were separated from non-myocytes by 2 rounds of differential plating for 45 mins each. Cells were plated at a density of 10^3 cells/mm^2 in 2 g/l gelatin-coated FALCON polystyrene dishes in the presence of 10 μM BrdU, to prevent the proliferation of non-myocytes. After 24h, the media was changed to remove BrdU from the culture. After 96h of culture, the CMs are treated with the respective calcium channel blockers or hypertrophic stimuli at a specific concentration, mentioned in the table 1, for 24 h.

Where indicated, hypoxia (0.2% O_2, 93% N_2, 5% CO_2) was achieved using an In Vivo2 hypoxic workstation (Ruskin Technologies, Leeds, UK), after depriving the media of serum and glucose.

All procedures involved in obtaining CMs from the animals were performed in this study followed National Institute of Health Guide for the Care and Use of Laboratory Animals.

2. Cell Viability test

2.1. TUNEL assay

Cardiomyocytes were checked for viability upon calcium channel blockade by TUNEL assay using the *In-situ* cell death detection kit (Roche). The cells were plated in M24 plates and after 96h they were treated with T-type and L-type Calcium channel antagonists and after 48h treatment were fixed with 4% Paraformaldehyde (PFA) for 20 min at RT. After rinsing with PBS, the cells were permeabilized with a solution containing 0.1% Sodium citrate and 0.1 % Triton in PBS. The cells were then incubated

with the TUNEL reaction mixture containing TdT (enzyme solution) and fluorescein-dUTP in 1:10 ratio for 1h at 37º C in a dark humid chamber, according to the manufacturer's instructions. Subsequently, the cells were washed and stained with Hoechst and mounted with mowiol. During this incubation period, TdT catalyzes the addition of fluorescein-dUTP at free 3'-OH groups in single- and double-stranded DNA. After mounting, the cell viability was assessed by counting the TUNEL positive and TUNEL negative nuclei using fluorescence microscopy.

3. Auto-fluorescence assay

In this study, acidic organelles were labeled with Monodansylcadavarine (MDC) and LysoTracker® Red DND-99 (LR), as per manufacturer's instructions.

3.1. Monodansylcadavarine

Acidotropic labeling allows the observation of autophagosome formation in live cells. Autophagy can be quantified based on the number of MDC-positive vesicles per cell or the percentage of cells with MDC-positive vesicles. The cells were seeded in M24 plates. After 48 h of treatment with specific calcium channel inhibitor, the cells were incubated with Hoestch (10 μg/ml) in culture media for 5 mins. The cells were then washed with warm PBS 1X and incubated with MDC in the culture media at a final concentration of 100 μM for 45 min in dark at 37ºC. After incubation, the cells were washed three times with PBS 1X and are observed for autophagic vacuoles under fluorescence microscope (excitation wavelength 380-420nm).

3.2. LysoTracker® Red DND-99

Weak basic amines selectively accumulate in the cellular compartments with low internal pH and the acidotropic labeling can be used in the investigation on biosynthesis and pathogenesis of lysosomes. In this experiment, the cells that were plated in M24 plates were incubated with Hoestch after 48h treatment as mentioned above for MDC labeling. After 5 min of Hoestch, the cells were washed with PBS 1X and incubated with LysoTracker® Red DND-99 at a final concentration of 100nm in culture media for 10

min. After incubation, the cells were washed thrice with PBS 1X and were observed for acidotropic labeling under fluorescence microscope in the presence of Tyrode solution.

4. Western blot analysis

At the end of the corresponding treatments, the CMs were washed twice with cold PBS. The corresponding CMs lysates were obtained by adding adequate lysis buffer [2% Sodium dodecyl sulphate (SDS), 125 mM Tris-HCl, pH 6.8], depending on the nature of the experiment. Protein extracts were denatured by heat shock at 95ºC for 3 min and quantified by a Lowry assay (Bio-Rad). Equal amounts of proteins were subjected to SDS–polyacrylamide gel electrophoresis (PAGE) and transferred to polyvinylidene difluoride membranes (Millipore, Bedford, MA, U.S.A.) using semidry Trans-Blot apparatus (Hoefer, Amersham Pharmacia Biotech). Non-specific binding was blocked by incubation with TBST (20 mM Tris-HCl, 150 mM NaCl, 0.1% Tween-20, pH 7.4) plus 5% nonfat milk. Immunodetection was performed using the appropriate primary antibodies given in the table 3. Immunoblots were developed with an appropriate secondary Peroxidase-conjugated antibody, and the bound antibody was visualized using the chemiluminescent substrate Super Signal (Thermo Scientific, Rockford, U.S.A.) and EZ-ECL (Biological Industries, Israel). Levels of α-actin (CMs) signal as well as Naphthol blue were used to verify equal protein loading in each lane.

5. Gene knockdown by siRNA

Briefly, CMs were plated at 80% confluence. 48h after seeding the cells, transfection was performed in serum free DMEM low glucose medium along with OptiMEM® medium containing 50-100 nM siRNA and Lipofectamine™ RNAiMAX™ reagent (Invitrogen) following the manufacturer's instructions. After 6h the medium was topped up with DMEM low glucose medium and 10% horse serum and 5% foetal calf serum without antibiotics. Cells were processed after 48h of transfection. In each experiment, the efficiency of knockdown was analysed by qPCR. The sequence of short interfering RNA is given in table 4.

6. Polymerase chain reaction

The polymerase chain reaction (PCR) technique is applied for rapid enzymatic proliferation of a given segment of DNA. In this study, reverse transcription, semi-quantitative and real time qPCR techniques were employed.

6.1. Isolation of RNA and cDNA synthesis

The total RNA was prepared from the treated CMs using Macherey-Nagel Total RNA and protein isolation kit, coupled with rDNase digestion, to prevent genomic DNA contamination, according to the manufacturer's instructions. The concentration of RNA was determined by a Nanodrop (ND-1000) spectrometer. The cDNA synthesis was performed by reverse transcribing mRNA using Taqman Reverse Transcriptase enzyme (Applied Biosystems, Carlsbad, CA, USA). Negative control (RT-) was maintained to make sure that the target RNA was not contaminated with genomic DNA.

6.2. Semi-quantitative PCR

The synthesised cDNA was used as a template for subsequent PCR amplification of specific VGCC pore-forming subunits. Primers were designed to be complementary to the published sequences of each of the VGCC pore-forming subunits, and also some sequences were obtained from the published literature. The housekeeping gene GAPDH was used as a loading control. The primers, sequences, product sizes and amplification conditions are mentioned in Table 5. 20 µL of reaction mixture contained 10x reaction buffer (2µL), 1.25µL $MgCl_2$ (25mM), 1µL dNTPs (10mM), sterile water (22.55µL) and Taq polymerase (0.2µL). The PCR reaction was run in a thermocycler (Gene Amp® PCR System 2700 from Applied Biosystems). 38 cycles of PCR amplification include initialization at 95°C for 5 minutes, denaturation at 94°C for 30 seconds, annealing (temperature as mentioned in table 5) for 30 seconds, elongation at 72°C for 30 seconds and final elongation at 72°C for 7 minutes. Equal volumes of PCR products (20µL) were loaded and electrophoresed in a SYBR Safe (Life Technologies)-stained 3% agarose gel. The images of agarose gel illuminated by UV light were taken using Kodak EDAS 290

imaging system with Kodak 1D 3.6 software. Experiments were performed in triplicates and the representative images were presented.

6.3. XBP1 splicing assay

Under endoplasmic reticulum (ER) stress conditions, XBP1 mRNA is processed by unconventional splicing and translated into a functional transcription factor[178]. The procedure for XBP1 splicing assay was adapted from previous literature[179]. The sequence of the XBP1 primer is given in Table 5. The PCR product was amplified upto 35 cycles including initialization at 94°C for 4 minutes, denaturation at 94°C for 10 seconds, annealing at 63°C for 30 seconds, elongation at 72°C for 30 seconds and final elongation at 72°C for 10 minutes. XBP1 processing is characterized by excision of a 26-bp sequence from the coding region of XBP-1 mRNA. To distinguish the unspliced from the spliced band, the PCR product was digested with Pst-1 for 2.5 h at 37ºC, because the cleaved product contains a Pst-1 restriction site. The resulting digests were run on a 3% agarose gel, to resolve the two digested products of length 290 bp and 183 bp. In contrast the products amplified from spliced XBP-1 mRNA were resistant to digestion and remained 473 bp long.

6.4. Quantitative PCR (Real Time PCR)

Predesigned gene-specific primer pairs and probes were selected for one target gene (GADD153, GRP78, XBP1, Beclin1, Atg5, Atg12) and a endogenous control (β-actin) within a list of predesigned assays (Assays-on-Demand; Applied Biosystems). The relative quantification study was performed using TaqMan universal PCR master mix in an ABI prism 7000 sequence detection system (Applied Biosystems). This complete realtime PCR system enables detection and absolute quantification of nucleic acid sequences, by cycle-by-cycle detection of accumulated PCR products facilitated by detecting the changes in fluorescence signalling during the amplification. The qPCR allows the detection of PCR amplification in the exponential growth phase of a reaction. All assays were based on TaqMan hydrolysis probes labelled with FAM (green fluorescent fluorophore 6-carboxyfluorescein). The PCR reaction was performed with 1μL of cDNA for 40 cycles at 95ºC for 15 seconds and 60ºC for 1 minute. The results were obtained in the form of a Ct value (cycle threshold), which represents the cycle

number of the PCR during which the exponential growth of PCR product starts. Therefore, the higher the expression of the gene in the sample, the lower Ct value will be obtained as a result. The relative quantity of mRNA for every gene was calculated in the following manner: ΔCt=Ct of the target gene - Ct of GAPDH gene; Δ(ΔCt) = ΔCt of sample - ΔCt of the control. Relative mRNA levels were calculated and expressed as fold induction over contralateral controls (value=1.0) following the formula $2^{-\Delta(\Delta Ct)}$. Every experiment was repeated three times and all samples were amplified in triplicates and data were normalized using GAPDH as endogenous control.

7. Transfection with ptfLC3 plasmid

The ptfLC3 is a tandem flagged plasmid construct obtained as a gift from Dr. Tamotsu Yoshimori. This plasmid contains the green fluorescent protein pEGFP-LC3 and the red fluorescent protein mRFP-LC3. The cells were seeded in 24 well plates with the normal culture media and after 24h the cells were transfected with OptiMEM® medium containing 1 μg of the plasmid and Lipofectamine 2000 (Invitrogen). The media was replaced by normal culture media after 6h of transfection. The cells were left overnight in the incubator, and after 24h of transfection, the cells were treated and observed for evaluation of the autophagy flux from the co-localisation of both pEGFP-LC3 and mRFP-LC3, at different time intervals of 4, 8 and 24h, under fluorescence microscope.

8. Statistical analysis

Statistical significance was evaluated by Student's t-test or by one- way ANOVA, as appropriate. Values of $P< 0.05$ were considered statistically significant. All data examined were expressed as mean ± standard error of the mean (SEM).

Results and Discussion

Chapter-1

Distinct roles for L- and T-type Ca^{2+} channels in the regulation of Ca^{2+}-homeostasis in neonatal cardiomyocytes

1. Introduction

Voltage-gated Ca^{2+} channels that are widely distributed throughout the myocardium play a very important role in the proper development and functioning of the heart. During a cardiac action potential, Ca^{2+} influx through L-type Ca^{2+} channels enables Ca^{2+} loading into the sarcoplasmic reticulum and also triggers Ca^{2+} release from the SR enabling EC coupling. L-type Ca^{2+} channels are considered to be the key target to regulate inotrophy in the treatment of cardiovascular diseases. Ca^{2+} entry through the T-type Ca^{2+} channels plays an important role in the development of heart throughout the neonatal period and also modulates the pacemaker activity[180]. T-type channels disappear during the end of the neonatal period, and are known to be re-expressed in the adult CMs under pathological conditions.

L-type and T-type Ca^{2+} channel antagonists are known to be potent vasodilators and have been widely used in the treatment of various cardiovascular diseases such as hypertension, coronary artery disease, angina, hypertrophic cardiomyopathy, and others. The dihydropyridines nifedipine and nimodipine, which are potent L-type channel blockers, and the non-dihydropyridines mibefradil and bepridil, as T-type channel blockers, were used in this study. Particularly, mibefradil was initially identified as a dual T/L type Ca^{2+} channel blocker. Later, studies have shown that mibefradil blocks T-type channels with higher sensitivity of 10 to 30 fold over L-type channels[181-182].

This chapter deals with the effect of pharmacological blockade of T- and L-type VGCC on cell viability and on the disruption of Ca^{2+} homeostasis, and the possible outcomes of the unfolded protein response and/or deregulation of the autophagic flux in neonatal CMs.

2. Results:

2.1. Expression of L-type and T-type Calcium channels in ventricular CMs

Molecular cloning studies have revealed 10 genes encoding pore-forming α1 subunits. These 10 genes are classified into 3 major families based on their sequence similarity. The HVA channels comprise the L-type channels ($Ca_v1.1$–1.4), and the P/Q- ($Ca_v2.1$), N- ($Ca_v2.2$) and R- ($Ca_v2.3$) type channels. The LVA channels form the third family

comprising the T-type channels or $Ca_v3.x$ family. Out of these, it has been shown previously that the L-type channels $Ca_v1.2$ and $Ca_v1.3$, as well as the T-type channels $Ca_v3.1$ and $Ca_v3.2$, are expressed in neonatal CMs. We performed a series of PCR reactions to check the expression of T-type and L-type channels in our cell model of rat ventricular neonatal CMs. The cDNAs obtained from the CMs were amplified with the specific primers for the VGCC pore-forming subunits and the PCR product was run on a 3% agarose gel. We found that the four channel types namely $Ca_v3.1$, 3.2, $Ca_v1.2$ and 1.3 are expressed in the neonatal CMs as previously reported (Figure 1).

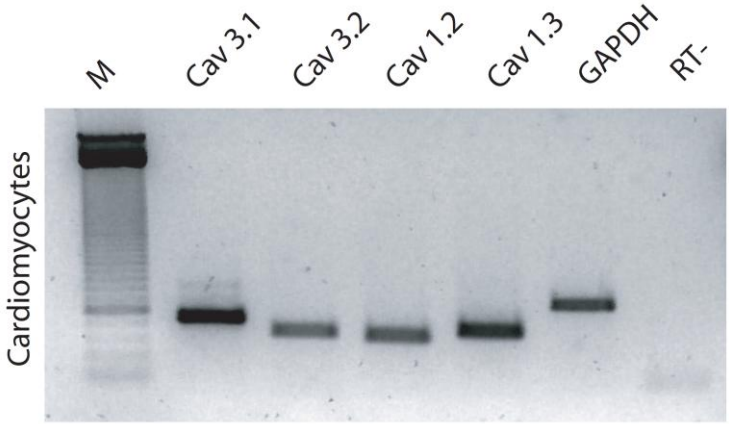

***Figure 1**: RT-PCR to check the expression of the VGCC pore-forming subuints in neonatal rat ventricular CMs. As reported previously, $Ca_v3.1$, $Ca_v3.2$, $Ca_v1.2$ and $Ca_v1.3$ are expressed in CMs.*

2.2. Effects of VGCC blockers on the viability of CMs

Apoptosis and necrosis play a key role in the pathogenesis of cardiovascular diseases. Cell death resulting from apoptosis is due to the loss of terminally differentiated CMs and it can be mediated by the apoptotic death receptors in the plasma membrane, as well as due to the release of apoptotic factors from mitochondria. Many factors such as stress proteins, growth factors and intracellular Ca^{2+} levels are known to regulate apoptotic cell death [183]. Therefore, we wanted to study the effect of VGCC blockers on the viability of CMs.

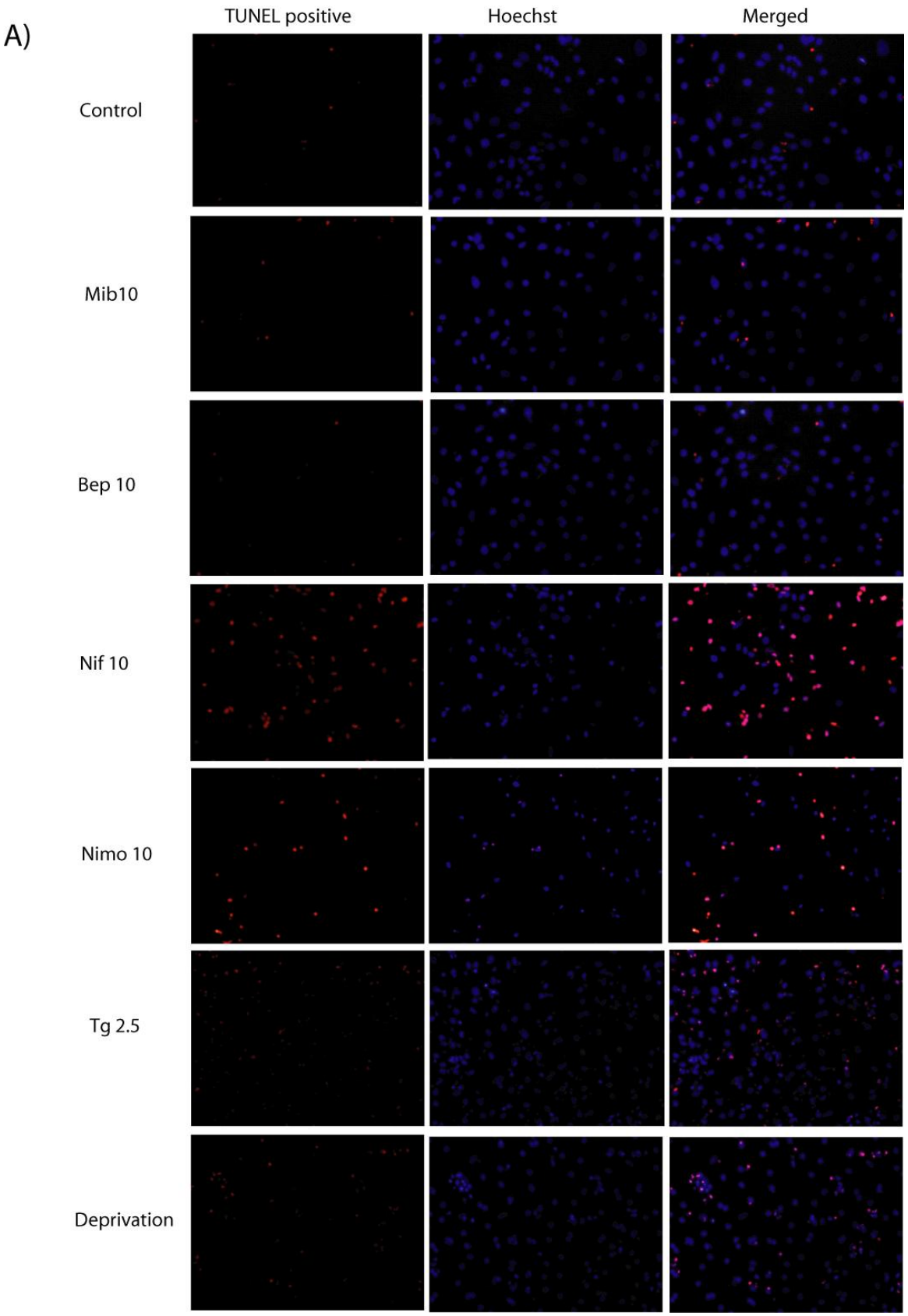
A)
TUNEL positive
Hoechst
Merged
Control
Mib10
Bep 10
Nif 10
Nimo 10
Tg 2.5
Deprivation

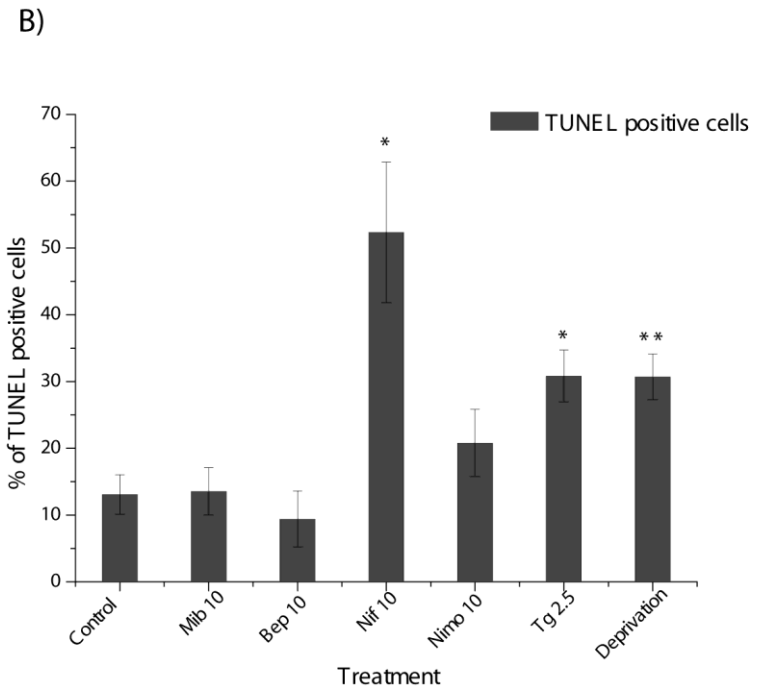

***Figure 2**: Viability of CMs in the presence of T-type and L-type calcium channel blockers. A) The fluorescent microscopy images show the effect of the drugs on the viability of cells, the dead cells represented by TUNEL positive cells along with pignotic nuclei (revealed by Hoechst staining). B) The percentage of death induced by the T-type and L-type channel blockers compared to the control.*

The cells were treated with the L-type and T-type channel blockers, along with thapsigargin and deprivation as positive controls, for 48 hours. The DNA fragmentation induced by the VGCC blockers was studied using TUNEL immunostaining assays. We found that the L-type channel blockers (nifedipine and nimodipine) significantly increased the TUNEL positive cells, with nifedipine decreasing the viability of CMs to 50%, which was higher than that of thapsigargin and deprivation (~30%) (Figure 2A). However, neither T-type Ca^{2+} channel blocker mibefradil nor bepridil did significantly decrease the viability of CMs when compared to the untreated controls (Figure 2 B).

2.3. VGCC blockers induce a transient unfolded protein response

Ca^{2+} entering through the L-type Ca^{2+} channels regulates Ca^{2+} loading in the SR and subsequent EC coupling in CMs. Thus, we reasoned that disturbance in the Ca^{2+} influx via L-type channels would lead to disruption of the Ca^{2+} homeostasis in ER, leading to ER stress. A sustained ER stress induces the Unfolded Protein Response (UPR). We thus

proceeded to the analysis of three main UPR markers, namely the molecular chaperone GRP78 and the transcriptional regulators GADD153 and XBP1.

Induction of UPR upon treatment of CMs with L-type and T-type Ca^{2+} channel blockers was studied by checking the expression of these three UPR markers, by q-PCR, RT-PCR and western blot, at two different time points (8h and 24h).

The q-PCR experiments to quantitate the expression of three UPR genes showed a low level upregulation of the 3 genes at 8h by application of both L-type and T-type channel blockers (Figure 3A). This UPR induced by both type of channel blockers was of a transient nature, as the expression of two of the UPR genes, XBP1 and GRP78 dropped down to near control levels at 24h (Figure 3 B), whereas that of GADD153 was maintained only upon T-type channel blockade. In contrast, the positive controls, thapsigargin and deprivation showed a sustained upregulation of all the three UPR genes.

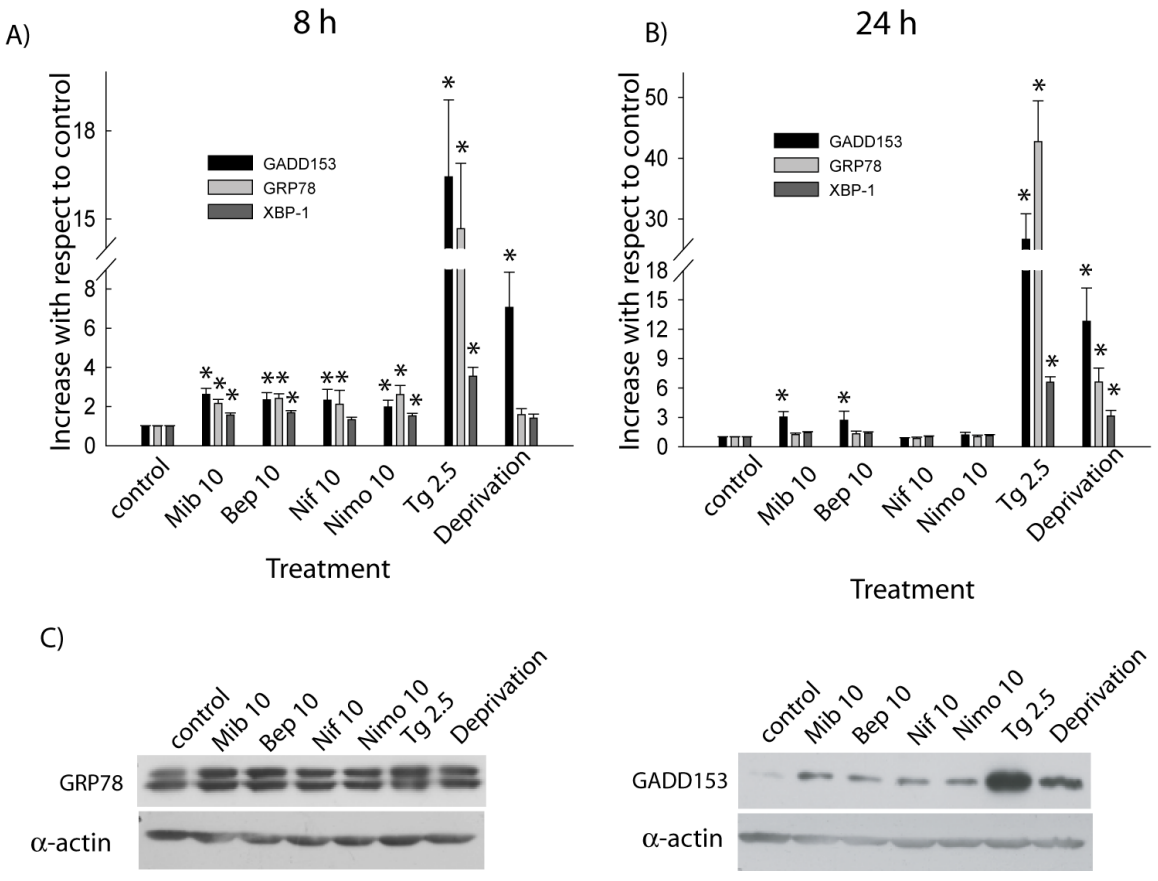

Figure 3*: Transient UPR induced at 8h, comes down to normal levels at 24h. A) Low level UPR is induced at the transcriptional level at 8h by T-type and L-type channel blockers. B) The transient UPR induced by the T-type and L-type channel blockers dropped down to near control levels at 24h. C) Western blots at 8h show induction of*

*both GADD153 and GRP78. β- actin is used as a house-keeping control in q-PCR experiments. Histogram bars represent mean ±SD values from at least 5 independent experiments *Significant differences related to untreated control, P< 0.05.*

The detection of protein levels by WB assays confirmed the induction of UPR, showing moderate GADD153 and GRP78 upregulation at 8h treatments with L-type and T-type channel blockers, in contrast with a stronger and sustained upregulation by thapsigargin and deprivation treatments (Figure. 3C).

2.4. The number of acidic organelles and autophagic vacuoles increases in the presence of VGCC blockers

It has been shown that a sustained UPR may either lead to cell death by apoptosis or cell survival by autophagic clearance of accumulated unfolded proteins. Also, previous studies have shown that ER stressors induce the formation of autophagosomes that can be observed at the ultrastructural level[169]. We wanted to study if the UPR induced by L-type and T-type Ca^{2+} channels could in turn trigger a macroautophagic process. Initially, we studied this issue by labelling the CMs with autofluorescent acidotropic compounds like LysoTracker® Red DND-99, targeting acidic organelles, and MDC (monodansyl cadaverine) which accumulates in autophagic vacuoles.

A)

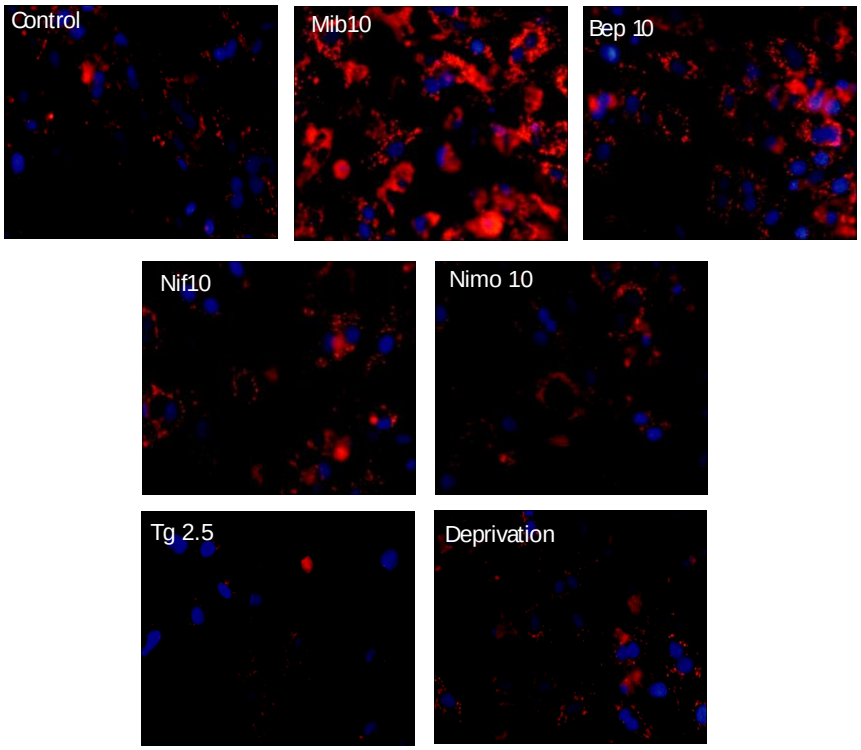
Control
Mib10
Bep 10
Nif10
Nimo 10
Tg 2.5
Deprivation

B)

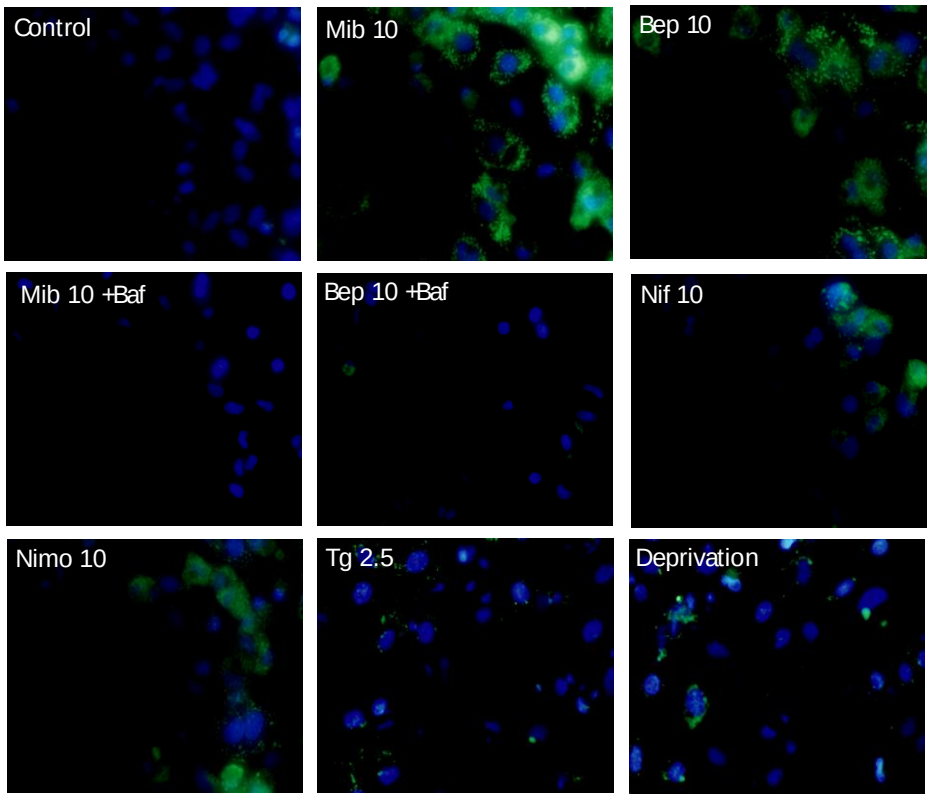
Control
Mib 10
Bep 10
Mib 10 +Baf
Bep 10 +Baf
Nif 10
Nimo 10
Tg 2.5
Deprivation

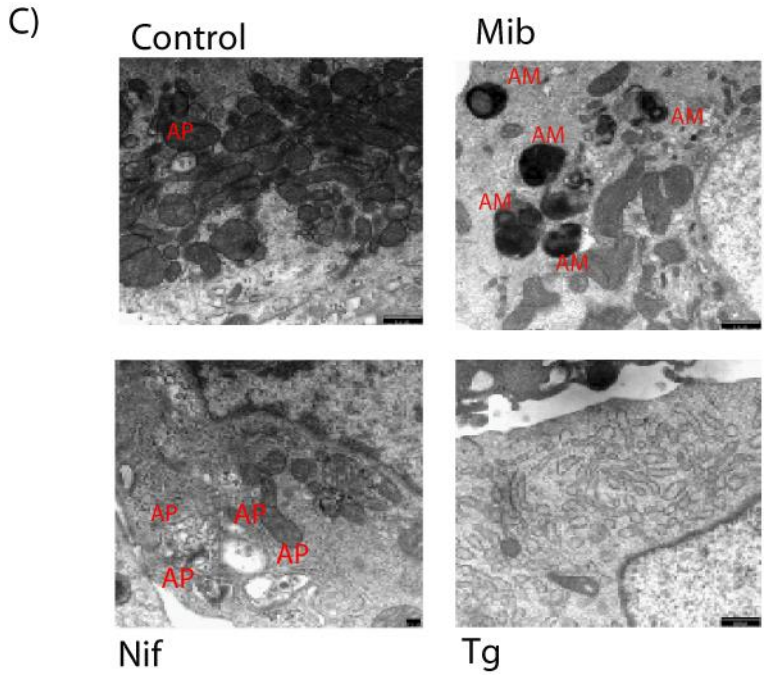

Figure 4: *Increased acidotropic labelling induced by both T-type and L-type calcium channel blockers. A) Lysotracker red assay under fluorescent microscopy showing increased acidotropic staining in cells treated with L-type or T-type calcium channel blockers, compared to untreated cells. B) MDC, targeting autophagic vacuoles, also displayed an increased staining in CMs subject to treatment with L-type and T-type channel blockers. Note that addition of vATPase inhibitor bafilomycin prevented any Lysotracker red or MDC staining. C) The transmission electron microscopy photographs reveal amphisomes (AM) with mibefradil treatment, autophagosomes (AP) with nifedipine. Thanpsigargin treatment resulted in swollen ER. The images are representative of at least 3 independent experiments with duplicates for each individual treatment.*

We found that the L-type and T-type channel blockers induced a strong acidotropic labelling by both MDC and LR, CMs displaying a punctate fluorescent pattern at 400x optical magnification (Figure. 4). In comparison, deprivation of CMs increased the level of LR and MDC labelling to a lesser extent, whereas the fluorescence levels for both dyes were below those of control when the cells were incubated with autophagy inhibitor thapsigargin.

To complement the fluorescence experiments referred above, we examined CMs ultrastructure by transmission electron microscopy, which remains an utmost reliable

method to detect alterations in the autophagic flux, while not readily quantifiable[184-185]. The cytoplasm of CMs treated with mibefradil (or bepridil, not shown) was plagued with amphisomes/MBVs, as evidenced by the presence of large electrondense double-membrane vacuoles with mitochondria and other cellular organelles inside (Figure 4 C). In contrast, the cytoplasm of CMs treated with L-type channel blocker nifedipine (or nimodipine, not shown) displayed numerous double-membrane autophagic vacuoles surrounding diverse cytoplasmic components, compatible with autophagosomes. The cells treated with thapsigargin displayed swollen ER.

2.5. Autophagy is differentially regulated by T-type and L-type calcium channels

We studied the autophagic process in CMs at the molecular level by analyzing the expression of 3 key mediators of canonical macroautophagy at the transcriptional level by q-PCR, using specific probes for the inducible genes Beclin1 (Atg6), Atg5 and Atg12. At the peak of the UPR (8 h), none of VGCC blockers had induced the expression of Atg genes significantly. However, there was a significant upregulation of Atg5 and Atg12 genes at 24 h, displaying a nearly 2-fold induction with respect to control cells. Like for UPR genes, these increases were moderate compared to those induced by deprivation or thapsigargin (Figure 5A, B). At the protein level, the WB results at 24 h treatments show that L- and T-type channel blockers increased the levels of autophagosome nucleation/initiation protein Beclin1, but not Atg5 or the tandem Atg5-Atg12, opposite to the effects of deprivation, that surprisingly decreased the lebels of all analyzed Atgs (Figure. 5C).

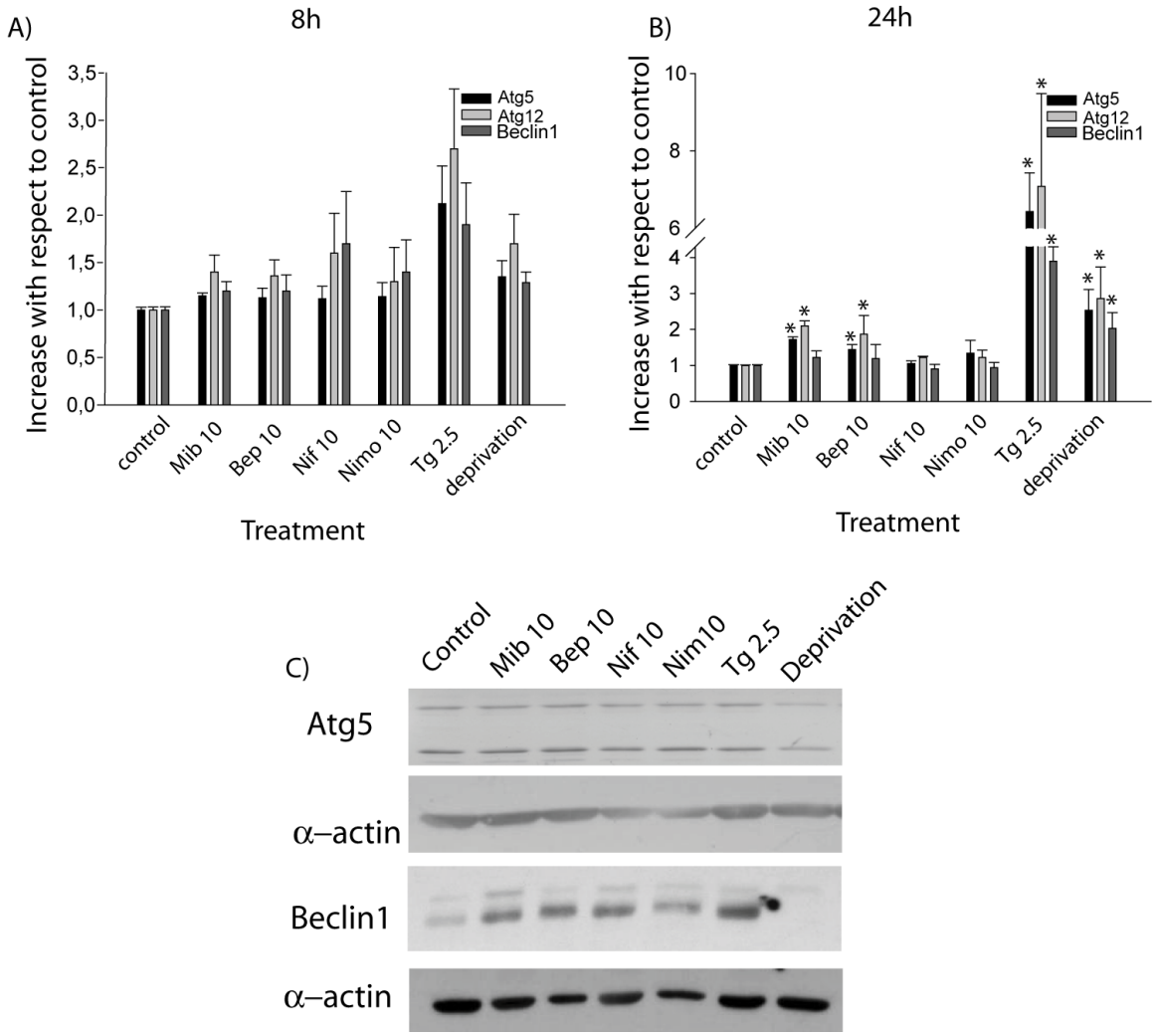

Figure 5: *The expression of Atg genes is induced by T-type and L-type channel blockers at the transcriptional and protein level. A) q-PCR analysis of the cells treated with the drugs does not show any significant increase of Atg genes compared to that of thapsigargin and deprivation at 8h. B) Only the treatments with T-type channel blockers show a little induction of Atg5 and Atg12 genes at 24h. C) Western blot analysis at 24h shows increase of only Beclin1 but not Atg5 with both the T-type and L-type channel blockers. β- actin is used as a house-keeping control Histogram bars represent mean ±SD values from at least 5 independent experiments *Significant differences related to untreated control, P< 0.05. The western blots are representative of at least five independent experiments.*

We also performed WB assays to quantify the conversion of LC3 (Atg8) from the soluble form (LC3-I) to the autophagosomal-associated lipidated form (LC3-II).

We could observe a robust LC3 conversion to its lipidated form (LC3-I to LC3-II) due the effect of L-type and T-type channel blockers, such that the LC3II/I ratio values displayed the following order, from highest to lowest: mibefradil> deprivation> nifedipine> thapsigargin> nimodipine> bepridil > control (Figure 6 A,B). Based on the level of LC3-II conversion and also the differential effect of the drugs on the viability of the cells in TUNEL assay, mibefradil and nifedipine were chosen for further comparative studies on the effect of T-type and L-type Ca^{2+} channel blockers on CMs autophagy.

As the LC3-II ratio provides information only about the number of autophagosomes[186] but is not indicative of their biogenesis, the autophagic flux can be more accurately studied in the presence or absence of lysosomal protease inhibitors or Bafilomycin A1, which is a v-ATPase inhibitor thus preventing autophagosome-lysosome fusion. Increase in autophagic flux as a result of a pharmacological challenge can be interpreted from the further increase in LC3-II ratio upon addition of Bafilomycin A1, whereas an unaltered LC3-II ratio upon addition of Bafilomycin A1 is interpreted as inhibition of autophagy and accumulation of autophagosomes[187].

To distinguish between these two possibilities, we applied a selection of the usual treatments in the absence or presence of bafilomycin A_1, which is a stablished inhibitor of autophagosomal-lysosomal fusion. In the treatment with L-type channel blocker nifedipine, the LC3II/I ratio was largely increased by co-application of Bafilomycin A_1. In contrast, in the treatments with T-type channel mibefradil or thapsigargin, the intensity of the LC3II band was not further increased by bafilomycin, indicative of a suppression of autophagy rather than an enhancement of lysosomal clearance (Figure. 6C).

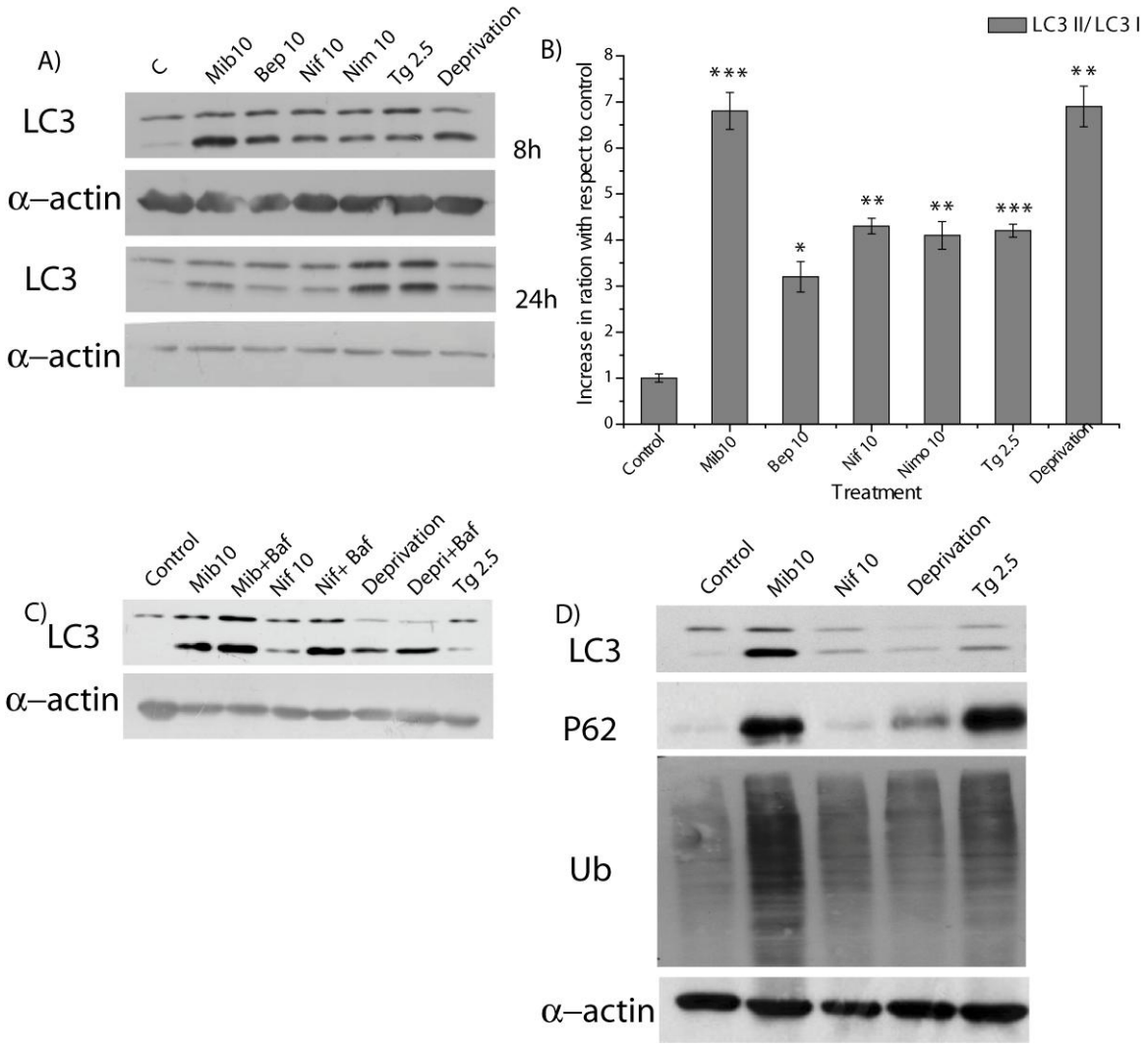

***Figure 6**: Autophagy is differentially regulated by T-type and L-type Ca^{2+} channel blockers. A) Both at 8h and 24h, both T-type and L-type channel blockers increase the conversion of LC3-I to its lipidated form LC3-II. B) The ratio of LC3-II/LC3-I in the presence of drugs shows a higher conversion with mibefradil 10µM and a moderate increase with nifedipine 10µM and nimodipine 10µM. C) Co-application of bafilomycin A1 does not increase the LC3-II conversion ratio due to mibefradil any further, but it does for nifedipine. D) Mibefradil 10 µM promotes the accumulation of p62/SQSTM1 and ubiquitin aggregates whereas nifedipine 10 µM induces a decrease in both p62/SQSTM1 and ubiquitin aggregates. These western blots are representative of at least five independent experiments. Histogram bars represent mean ± SD values from at least 5 independent experiments *Significant differences related to untreated control, $P< 0.05$.*

The autophagic flux is reflected in the degradation and autophagic clearance of ubiquitinated proteins and is better studied by the involvement of p62/SQSTM1. During autophagy stimulation, p62/SQSTM1 is degraded since the interaction of LC3-II with p62/SQSTM1 targets ubiquitin-conjugated protein for turnover, and p62/SQSTM1 becomes an autophagy substrate along the aggregates [188]. Conversely, autophagy inhibition results in the accumulation of p62/SQSTM1proteins.

Examination of p62/SQSTM1 protein expression by western blot showed that, at 24 h, the L-type channel blocker nifedipine significantly decreased the intensity of the p62/SQSTM1 band, which was otherwise increased by treatment with the T-type channel blocker mibefradil. Western blot results with a monoclonal antibody against ubiquitin were consistent with the p62/SQSTM1 band intensity variation: whereas nifedipine either decreased or maintained the ubiquitin intensity, mibefradil increased ubiquitin labelling in the entire lane when compared to the untreated control (Figure 6 D). The application of thapsigargin also increased the p62/SQSTM1 and ubiquitin aggregates, whereas deprivation of the CMs maintained or increased both labels at 8 and 24 h time points.

2.6. Autophagic flux accessed by tandem flagged LC3 constructs

We wanted to confirm the results described above by transfecting in CMs the pft-LC3 tandem construct, in which LC3 is tagged with both green fluorescent protein) GFP and monomeric red fluorescent protein (mRFP). The GFP helps in the localization of LC3 and has been widely used as an autophagosome marker. Whereas the GFP fluorescence is lost under acidic conditions and is degraded by lysosomal hydrolases, the mRFP fluorescence remains stable[189-190].

CMs were plated in M24 wells, and after 24h of culture, they were transfected with plasmids encoding ptf-LC3 in the presence of Lipofectamine 2000. After 24 h of transfection, the cells were treated with mibefradil and nifedipine along with rapamycin (100 nM) or Hanks buffer as positive controls of autophagy flux, and bafilomycin A1 (5nM) as an autophagy inhibitor. The cells were observed under fluorescence microscopy after 24h of treatment. The yellow puncta that is observed upon merging green and red images indicates autophagosomes and the red puncta indicates autophagolysosomes[191]. Thus, the increase in both yellow (a merger of GFP and mRFP in autophagosomes) and red puncta (mRFP in autolysosomes) is indicative of an enhanced autophagic flux,

whereas the increase of yellow (but not red) puncta indicates inhibition if autophagy[192-193].

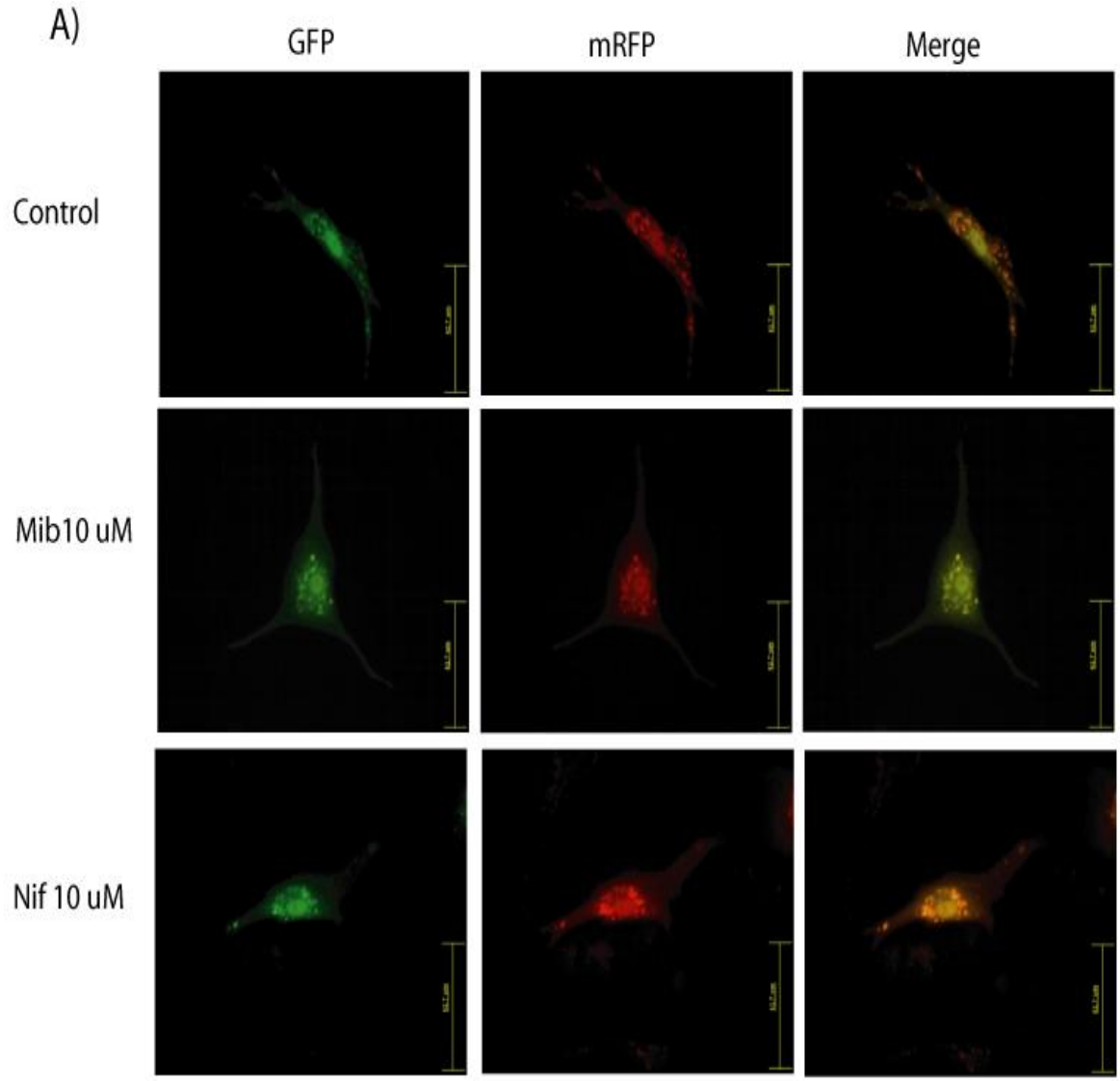

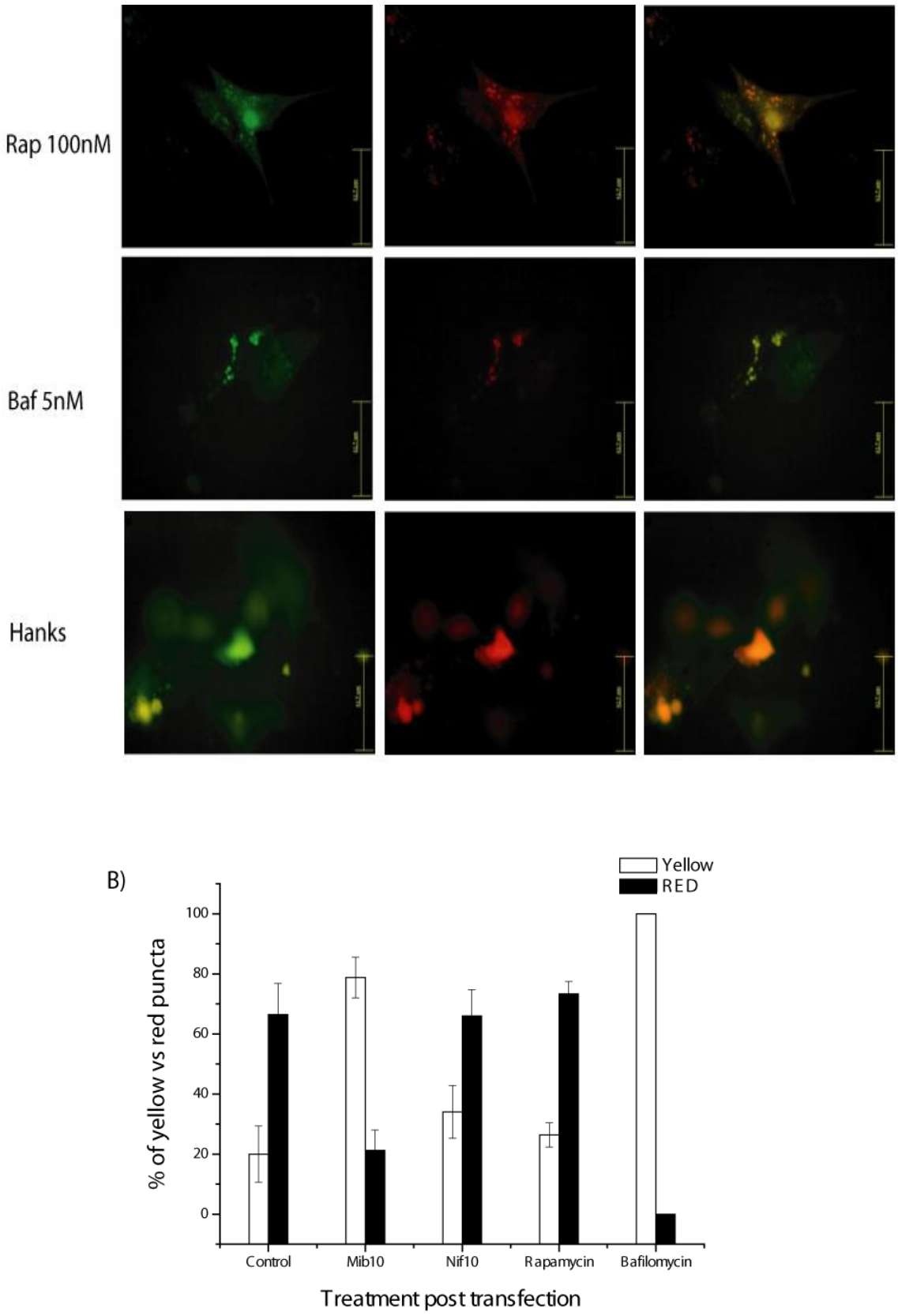

***Figure 7**: Determination of autophagic flux using tandem flagged LC3. A) Mibefradil 10µM induced an increase in the ratio of yellow to red puncta, indicating inhibition of*

autophagy, whereas nifedipine 10 μM induced an increase in red over yellow puncta, indicative of autophagy induction. The autophagy inducer rapamycin induced an increase in the number of red puncta, whereas the autophagy inhibitor bafilomycin A1 induced an increase in the number of yellow puncta. B) A graphical representation of the percentage of fluorescent structures present inside the cells 48h after transfection with ptfLC3, which includes 24h of treatment with VGCC blockers post transfection.

In our experiments we found that mibefradil increased the ratio of yellow over red puncta drastically at 24h, whereas nifedipine exerted the opposite effect (Figure 7). The results attained by treating the CMs with mibefradil were similar to those obtained using bafilomycin A1. Conversely, the results from nifedipine treatments were consonant with rapamycin-treated CMs. These data, in accordance with the western blot results in the presence of bafilomycin and also with the p62/SQSTM1 and ubiquitin western blot data clearly indicates an opposite effect of T-type and L-type Ca^{2+} channel blockers on macroautophagy in CMs.

2.7. Comparison of pharmacological blockade and gene silencing of VGCCs

In order to confirm that the pore-forming subunits of the L-type and T-type channels were the real molecular targets of the pharmacological blockers, we wanted to check the expression of UPR genes and assess the autophagic flux in CMs subject to VGCC knockdown with the RNAi technique. RNAi helps in the understanding of the functional role of a specific gene by specific gene silencing. siRNAs (small interfering RNAs) were designed specifically for the individual Ca^{2+} channel isoforms, namely T-type $Ca_v3.1$, $Ca_v3.2$ and L-type $Ca_v1.2$ and $Ca_v1.3$, channels, encoded by the genes Cacna1g, Cacna1h, Cacna1c and Cacna1d respectively.

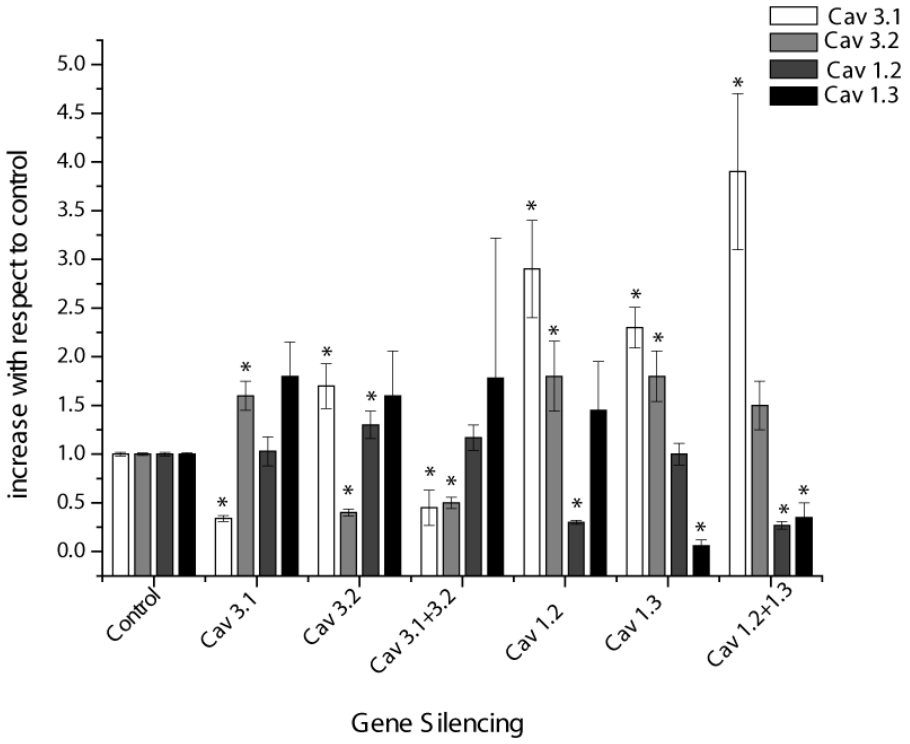

Figure 8*: Knockdown efficiency of the gene specific siRNA. q-PCR results obtained after gene silencing by using specific probes for the genes encoding the T-type and L-type calcium channels showed that the silencing of the channels induced a significant knockdown of the specific genes, ranging from 60% to 95%. β- actin was used as a house-keeping control. Histogram bars represent mean ±SD values from at least 5 independent experiments *Significant differences related to untreated control, P< 0.05.*

After 48h in culture, the CMs were transfected with siRNA specific for T-type and L-type Ca^{2+} channels and the effects of knockdown on UPR and autophagy were elucidated by q-PCR and western blot assays. 48h after transfection, the efficiency of the knockdown was measured by using the q-PCR technique and the results showed a transfection efficiency ranging from 95% ($Ca_v1.3$) to 60% ($Ca_v3.2$) (Figure 8). Importantly, the q-PCR results also showed that upon knockdown of one channel type, the expression of others is upregulated. For instance, the knockdown of $Ca_v3.1$ resulted in the upregulation of the expression of both $Ca_v3.2$ and $Ca_v1.3$; in a similar way, $Ca_v3.2$ knockdown resulted in the upregulation of $Ca_v3.1$ and $Ca_v1.3$. Co-transfection of $Ca_v3.1$ and $Ca_v3.2$ siRNA resulted in a 50% knockdown of both the channels and a near 2-fold increase in $Ca_v1.3$ expression. The knockdown of $Ca_v1.2$ channels exacerbated the expression of all other Ca^{2+} channels, whereas the knockdown of $Ca_v1.3$ increased the expression of only T-type

$Ca_v3.1$ and $Ca_v3.2$ channels. Here also, co-transfection of $Ca_v1.2$ and $Ca_v1.3$ rendered a 65-70% knockdown of both channels and resulted in a 1.5 to 3-fold induction of T-type Ca^{2+} channel expression. Thus, our data indicated that the expression of the different VGCC types in CMs is regulated in a concerted manner, so that compensatory mechanisms are unleashed upon knockdown of specific isoforms.

We performed XBP1 splicing assay for the knockdown samples. XBP1 mRNA is processed by unconventional splicing and translated into a functional transcription factor[178]. In our experiments the knockdown of $Ca_v3.1$ or $Ca_v3.2$ induced a moderate splicing of XBP1 splicing that did not occur with the knockdown of $Ca_v1.2$ or Cav1.3 (Figure 9A).

Western blot results were unconsistent for GRP78, but showed a steady upregulation of GADD153 upon knockdown of all channel types (Figure 9B).

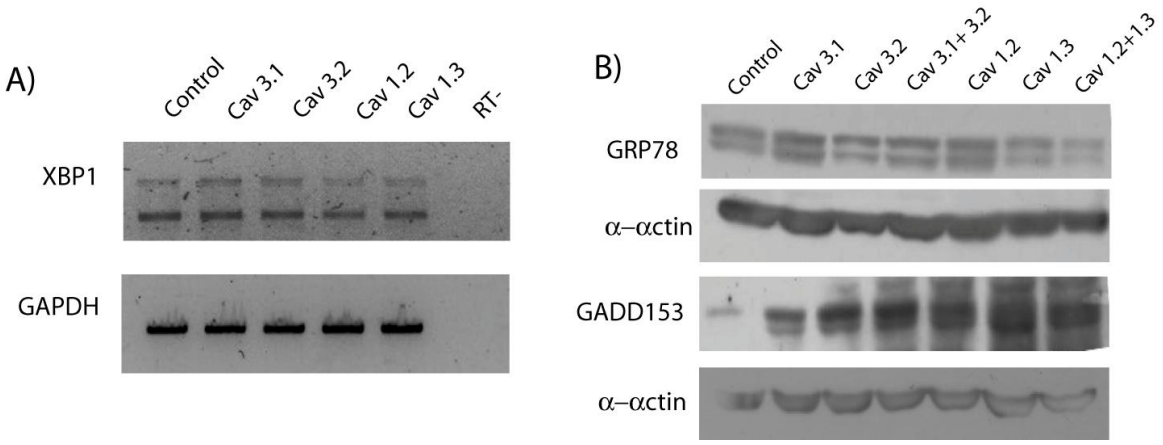

***Figure 9**: Monitoring UPR by gene silencing. A) The XBP1 splicing assay show a stronger intensity of the upper band (sXBP1) due to the knockdown of $Ca_v3.1$ and $Ca_v3.2$ channels, in contrast with a lack of effect for the knockdown of $Ca_v1.2$ or $Ca_v1.3$. B) The western blot results show unconsistent results for GRP78, but a clear increase of GADD153 protein expression due to the knockdown of all VGCC genes.The western blots are representative of at least five independent experiments.*

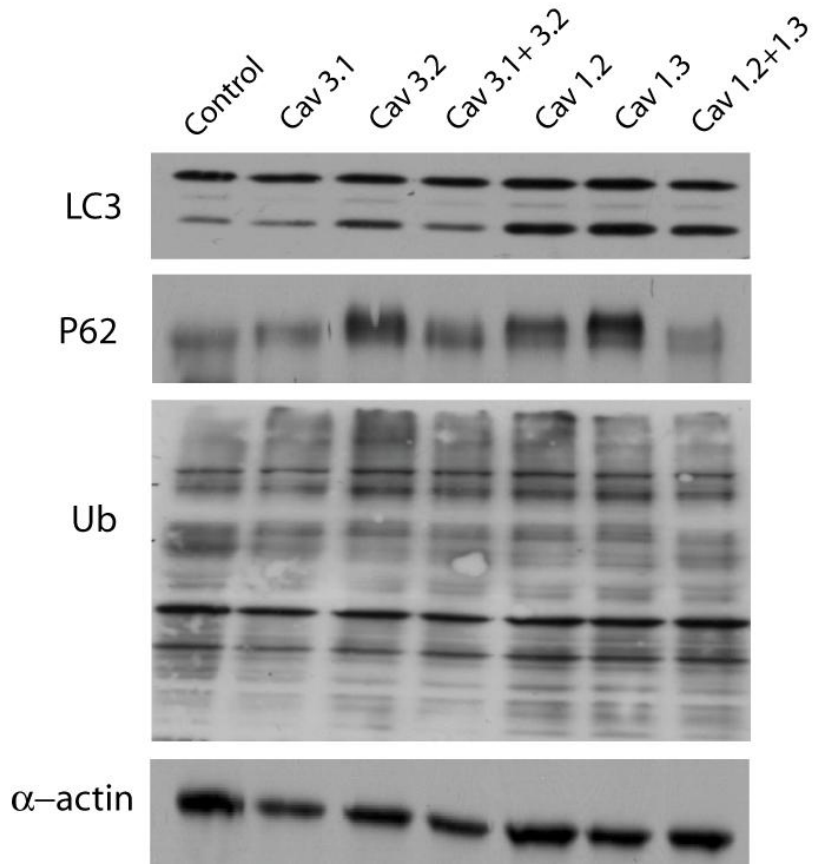

***Figure 10**: Autophagic flux upon silencing the channels. Western blots results displaying the de-regulation of autophagy due to VGCCs gene silencing. The knockdown of $Ca_v3.2$ mimicked the effects of mibefradil, whereas the knockdown of $Ca_v1.2$ or $Ca_v1.3$ channels also increased the p62/SQSTM1 and ubiquitin band intensities, contradictory to the pharmacological blockade of L-type Ca^{2+} channels. The western blots are representative of at least five independent experiments.*

The analysis of LC3 by western blot showed an increased LC3-II conversion due to the knockdown of $Ca_v1.2$, $Ca_v1.3$ and $Ca_v3.2$ channels. In an apparent contradiction with the pharmacological data, the knockdown of L-type Ca^{2+} channels increased the accumulation of p62/SQSTM1 and ubiquitin aggregates. The knockdown of $Ca_v3.2$ also increased p62/SQSTM1 levels and ubiquitination of protein aggregates, in good correlation with the data provided by mibefradil treatment (Figure 10).

2.8. Effect of VGCC blockers at therapeutic concentrations

In an attempt to shed light to the contradictory results of L-type channels pharmacological blockade and gene silencing on autophagy regulation, we performed a series of experiments to compare the effects of T-type and L-type channel blockers applied at high and low concentrations. The rationale was that, at lower concentrations, the putative overlap between the two drugs would be reduced as the target specificity would be increased.

The cells were treated with mibefradil and nifedipine at a concentration of 1µM (close to the concentration achieved in the blood of human patients, i.e. *therapeutic concentration*) for 24h, along with the drugs at 10 µM and thapsigargin as a positive control for UPR induction, and the results were analysed by western blot assay.

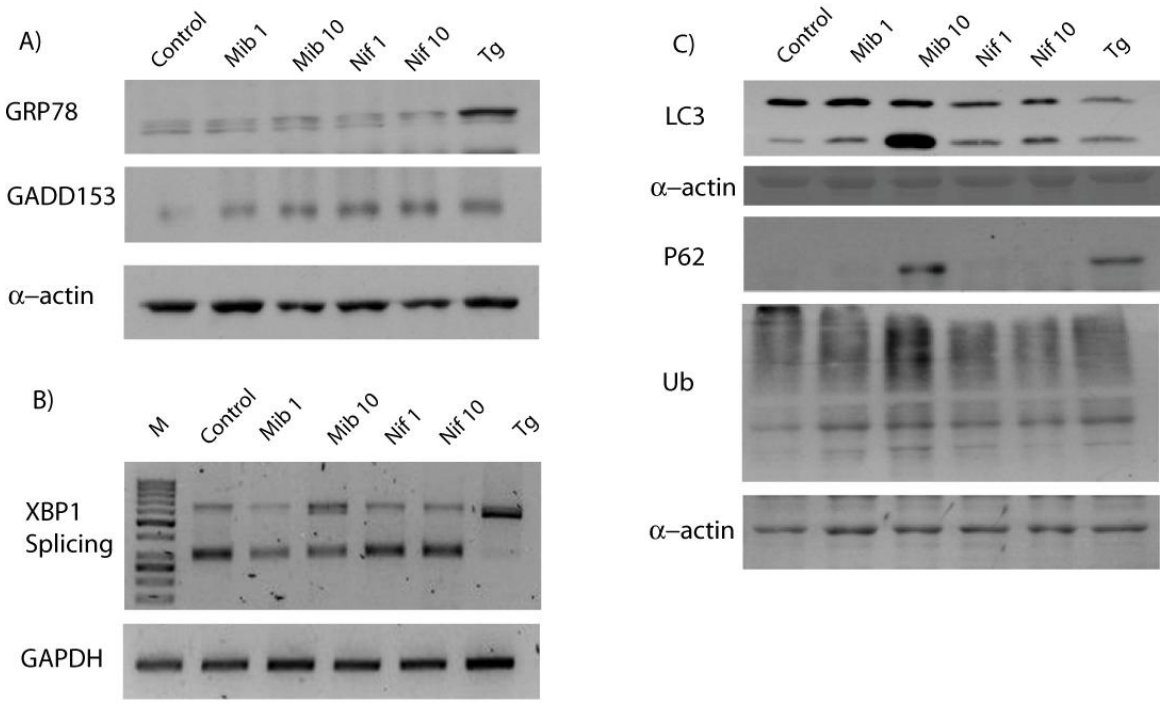

Figure 11*: Comparison of the effects of 2 different concentrations of drugs. A) Mibefradil and nifedipine only increased the protein band for GRP78 at the concentration of 10 µM (see the top band). The band corresponding to GADD153 shows clear increases with both drugs at 1 and 10 µM concentrations. B) The XBP1 splicing assay also shows the absence or a low level splicing with both nifedipine 1 µM and 10 µM, whereas splicing is induced by mibefradil 10 µM. C)Mibefradil and nifedipine at both concentrations*

induced LC3 II conversion. Mibefradil at 1 µM induced a slight increase in p62/SQSTM1 which was further increased by the higher concentration, while nifedipine did not induce an increase of p62/SQSTM1 at both lower and higher concentrations. The western blots are representative of at least five independent experiments.

Our data showed that T-type and L-type Ca^{2+} channel blockers at 1 µM had the same qualitative effect on the expression of UPR and ATG genes measured at the protein level, as that of 10 µM, but with less intensity. One of the UPR markers GADD153 was found to be induced with 1 µM and 10 µM of both mibefradil and nifedipine. The levels of GRP78 were moderately increased only at 10 µM treatments (Figure 11A). This could be due to the feedback mechanism activated that controls GRP78/BiP levels at a translational level[194]. The XBP1 splicing assay showed an increased splicing with respect to control with both concentrations of mibefradil, whereas both concentrations of nifedipine were refractory to induce XBP1 splicing in correlation with L-type Ca^{2+} channels knockdown (Figure 11B).

Mibefradil and nifedipine both at high and low concentrations increased the expression of Beclin1. In contrast, the expression of Atg5 and formation of the Atg5-Atg12 complex was increased by nifedipine at 1 µM, and surprisingly reduced by nifedipine at 10 µM concentration (Figure 11C).

In the case of LC3, mibefradil and nifedipine induced LC3-II conversion at both 1 µM and 10 µM concentrations, with mibefradil 10 µM showing a higher ratio of conversion. The band for P62/SQSTM1 was increased upon treatment with mibefradil 1 µM, being the effect further enhanced at 10 µM. In clear contrast, treatment with nifedipine did not increase the intensity of the p62/SQSTM1 band at any concentration. The p62/SQSTM1 results were in line with the level of ubiquitinated aggregates for both drugs.

3. Discussion

This chapter deals with the study of the effect of VGCC blockers on the viability and homeostasis of the neonatal rat ventricular CMs. The role of VGCC blockers in cardioprotection has long been reported and this study was intended to lay the grounds for a putative cardioprotective strategy.

The viability assays performed in the presence of the VGCC blockers showed at the first instance that the T-type and L-type channels affect the viability of the cells differently: T-type channel blockers did not affect the viability of the cells in any direction, whereas the L-type channel blockers induced a higher degree of cell death (Figure 2).

Since the main functions of endoplasmic reticulum are Ca^{2+}-dependent, we set out to study the effect of blocking VGCCs on ER homeostasis. As expected (but not investigated previously), the pharmacological blockade of VGCCs induced the UPR in CMs. Clearly, this shows that Ca^{2+} influx through VGCCs plays an important role in the maintenance of Ca^{2+} homeostasis beyond its well-known role in E-C coupling. The UPR response induced by application of VGCC blockers was transient, as the maximum levels of induction of two of the UPR markers XBP1 and GRP78 at the RNA level was seen at 8h, and reduced to near control levels at 24h with both T-type and L-type channel blockers. However, the higher level of GADD153 attained at 8h was maintained at 24h in the presence of T-type channel blockers. At the protein level, GRP78 showed a moderate increase upon 24 h treatment with either T-type or L-type Ca^{2+} channel blockers. Gulow *et al.*[194] postulated that translational and transcriptional upregulation of GRP78 are independent events and also that there is a possible regulatory mechanism that acts in a stress-dependent manner and specifically controls GRP78/BiP expression at the translational level during UPR. The translational rate of GRP78 mRNA could be controlled either by some signalling by the protein or by some structural motifs present in the mRNA[194]. Another aspect deserving consideration is that mibefradil induced XBP1 splicing whereas nifedipine did not. Under prolonged ER stress, XBP1u operates negatively by enhancing XBP1s degradation, which may lead to termination of UPR[195] . XBP1u is also shown to induce autophagy by regulating FOXO1 expression[196-197]. Thus, XBP1u may interconnect and regulate various homeostatic pathways in mammalian cells, by linking ER stress pathway and autophagy[198].

Both T-type and L-type channel blockers that induced a transient UPR also increased the presence of autophagosomes/autophagic vacuoles, in agreement with a previous study by Ogata *et al.* 2006[169], showing that ER stressors induced the formation of autophagosomes. As a matter of fact autophagy is an important cell process utilized by the heart for the maintenance of cellular homeostasis in both basal and stressed conditions. Previous studies have reported that induction of autophagy in response to cardiac stress is essential for cardioprotection and for minimizing the myocardial damage[199-200].

Our study of autophagy markers in the transcriptional and the protein level initially suggested that there could be an induction of autophagy by both T-type and L-type channel blockers. However, an increase in Atg12-Atg5 expression or induction of Beclin1 does not give a complete picture of the autophagy status[188]. There are previous reports stating that in some mouse and human cancer cell lines, ER stress may increase the transcription of Atg5 and Atg12 in response to UPR[201] . Initially, the LC3-II conversion induced by the drugs confirmed to us the deregulation of autophagy in CMs. In addition, our experiments in the presence of an autophagosome-lysosome fusion inhibitor suggested that the T-type channel blocker mibefradil inhibited autophagy whereas the L-type channel blocker nifedipine enhanced autophagic flux. This result was further supported by monitoring p62/SQSTM1 levels and ubiquitin aggregates. Previous studies have shown that p62/SQSTM1 depletion decreases LC3-II[202]. Interestingly, studies from Bjorkov *et al*, also show that p62/SQSTM1 depletion leads to induction of cell death by polyglutamine[203]. Thapsigargin, a SERCA pump inhibitor and ER stress inducer, also induced an increase in the levels of p62/SQSTM1 and ubiquitin aggregates, thus appearing to block autophagy as previously reported by Ganley *et al.*[204]. Previous studies in mouse embryonic fibroblasts have also shown that thapsigargin inhibits autophagosome-lysosome fusion[205]. But the autophagic flux induced by deprivation switched from an increased autophagic flux to a decreased autophagic clearance from shorter to longer time points. After 24 h of deprivation the level of LC3-II was increased, but the levels of p62/SQSTM1 were not decreased and, in some cases, even augmented when compared to untreated control cells. Consistent with this, Ramirez-Peinado *et al.* reported that LC3-II accumulation in cells starved for a long time may mean that autophagy is reduced compared to basal autophagy[206]. A review by Klionsky and Nemchenko, suggests that this autophagic *rollercoaster* induced by deprivation is to maintain the autophagy at an optimal level and not excessive level, as excessive autophagy might be detrimental[207]. Also, a previous work from Komatsu *et al.* with p62/SQSTM1 deficient mice has shown that deprivation-induced-autophagy, being nonselective, does not require p62/SQSTM1 for autophagic clearance[208].

The application of VGCC blockers to CMs that had been transfected with ptfLC3 plasmids showed an increase in mRFP labelling for nifedipine, and yellow puncta for mibefradil, reinforcing the concept that nifedipine enhances autophagy whereas mibefradil negatively regulates the autophagic flux.

The bacterial macrolide rapamycin is known to induce macroautophay by inhibiting mTOR activity. Previous reports indicated that rapamycin not only promotes formation of autophagosomes but also enhances autophagosome-lysosome fusion[209]. Hence, rapamycin is considered as one of the best positive controls to study autophagic flux via ptfLC3 experiments. In the presence of nifedipine a substantial population of tfLC3-transfected cells displayed only RFP signal, indicating enhancement of autophagic flux. The results attained in these experiments point to a similar efficacy of rapamycin and nifedipine in increasing the red puncta in CMs.

Our experiments dealing with VGCCs gene silencing were meant to shed light on the differential role of the Ca_v1 and Ca_v3 channels in Ca^{2+} homeostasis (and thereby on the regulation of macroautophagy), but proved not to be consistent with the pharmacological blockade data. The interpretation of these data is rather difficult, because of the incapacity to use a crucial assay to assess the autophagic flux; unfortunately and, given the technical impossibility of simultaneous gene overexpression and silencing, we could not perform the tfLC3 test in knocked-down CMs. Due to the fact that the p62/SQSTM1 gene may be induced to enhance cardiac autophagy[202], it is not possible to conclude that an increase in p62/SQSTM1 protein is necessarily the result of autophagy inhibition. However, the concomitant increase in poly-ubiquitinated aggregates, strongly suggests that the increase in p62/SQSTM1 due to $Ca_v3.2$ and $Ca_v1.2$ knockdown is the result of lack of degradation. Thus, whereas gene silencing of T-type $Ca_v3.2$ channels was consistent with pharmacological data at all levels, that of L-type channels was unconsistent regarding the regulation of the autophagic flux. The interpretation of these experiments is further complicated by the unexpectedly found interrelationship between the different VGCC isoforms. In this regard, we believe that the cross-regulation displayed by the genes encoding VGCCs should be taken into consideration. As a matter of speculation, the seemingly inhibitory effect of $Ca_v1.2$ knockdown on autophagy could be due to the concomitant overexpression of Ca_v3 channels. Nonetheless, a corollary of these results is that both systolic Ca^{2+} influx through L-type channels and -presumably diastolic-Ca^{2+} influx through T-type channels control Ca^{2+} homeostasis in neonatal CMs.

Generally speaking, autophagy is regarded as a cell survival mechanism. Studies on diseases caused by protein aggregates like Huntington's and parkinson's disease point to ER-stress induced autophagy as a way to promote removal of protein aggregates and thereby enhance cell survival [210]. In case of heart failure, the role of autophagy remains less clear or double edged. While some studies suggest that autophagy is beneficial,

others indicate that cardiac autophagy might be detrimental. The effect of autophagy on cardioprotection has been widely studied under various cardiomyopathies and it can be stated that impairment of autophagy contributes to morbidity and mortality associated with cardiovascular diseases[211]. Matsui *et al.* showed that autophagy was beneficial during ischemia and detrimental during reperfusion injury[143]. Zhu *et al.* postulated that increased autophagosome abundance in pressure-overload animals is a reflection of compensatory autophagy that becomes ineffective due to impairment of autophagic flux mediated by Beclin1[145]. They also concluded that autophagy negatively regulates cell size, antagonising cardiac hypertrophy, and also it is protective in some forms of cardiomyopathy like desmin-related cardiomyopathy and ischemia/reperfusion injury. Kanamori *et al.* investigated the function of autophagy in cardiac remodelling using a mouse myocardial infarction model. They found that blocking of autophagy with bafilomycin A_1 exacerbated cardiac dysfunction, whereas enhancement of autophagy alleviated cardiac remodelling and dysfunction[212-213]. Gottlieb *et al.* also recently reported that upregulation of autophagic flux mitigates post-infarction remodelling[214]. Although all these cases clearly indicate that activation of autophagy might be cardioprotective, there are also reports that associate autophagy with progressive destruction of CMs in the failing heart. The hamster model of dilated cardiomyopathy studied by Miyata *et al.* revealed the presence of autophagy vacuoles and degraded mitochondria in the CMs under ultrastructural analysis. In this model, the heart failure was found to be progressive leading to 50% mortality at 30 weeks[215]. Wang *et al.* has shown that the induction of excessive autophagy in late-stage hypertrophy leads to cardiac failure[142]. Interestingly, experiments by Kinoshita *et al.* showed that T-type channel blockade prevents sudden death in heart failure mice by reducing arrhythmias in dilated cardiomyopathy[216].

In this line, our data suggests that the autophagy induced by pharmacological blockade of L-type channels might be detrimental, as it dramatically lowers the viability of cultured neonatal CMs. In open contrast, the pharmacological blockade of T-type channels seems to block the strong constitutive autophagy present in neonatal cells in a sustainable manner, ensuring cell viability 48 h into the treaments.

T-type Ca^{2+} channels are sensitive to depolarization and they provide a transient current by activation and inactivation at a fast rate[29]. In addition, the steady-state activation and inactivation curves overlap, providing a constant inward window current which may facilitate slow diastolic depolarization contributing to automicity, and also help in Ca^{2+} homestasis mantainance in the ER[217-218]. T-type channels are abundantly expressed in

embryonic and neonatal ventricles[180,218], but in adult animals their expression in the heart is restricted to the conduction system[219-220]. Relevantly, T-type channels are however found to be re-expressed in the hypertrophied and failing hearts[78,221]. The I_{CaT} found in the pressure overload-induced hypertrophic heart is involved in pathological process that leads to systolic dysfunction and arrythmogenesis[78,216]. Furthermore, Chiang *et al.* demonstrated that genetic deletion of CACNA1H rendered resistance to pathological cardiac hypertrophy. The pharmacological blockade of T-type channels has also been shown to limit cardiac remodelling and improve the function or viability of heart cells subject to hypertrophic stimuli[220,222-223 224-225] and post myocardial infarction[224]. In addition, Kinoshita *et al*. reported that the pharmacological blockade of T-type channels with mibefradil prevented sudden death induced by non-ischemic or ischemic myocardial injury. While blockade of T-type channels appears to be cardioprotective, previous studies from Hong *et al*. suggest that impairment of membrane trafficking of L-type $Ca_v1.2$ channels leads to heart failure[226].

Consistent with these reports our results show, for the first time, that pharmacological blockade or genetic silencing of T-type Ca^{2+} channels induce a mild and transient ER stress that results in the subsequent inhibition of the macroautophagy pathway, probably by preventing the autophagosome-lysosome fusion. This late-stage autophagy inhibition is consistent with the mantainance or even upregulation of Atgs like Beclin1 or Atg5/Atg12, strong conversion of LC3-II (not further enhanced by Bafilomycin A1) and accumulation of p62/SQSTM1. Importantly and, given the fact that the viability of the ventricular CMs is not affected *in vitro*, we propose that such blockade of autophagy might be cardioprotective against certain stumuli unleashing an excessive or unspecific autophagy.

Chapter- 2

T-type Ca^{2+} channel blockade protects cardiomyocytes against hypoxia/re-oxygenation mediated cell death

1. Introduction

Ischemic heart disease is one of the highly prevalent diseases in the society. Organs and cells that depend highly on a continuous supply of oxygen adapt to multiple responses against hypoxia or ischemia for their survival. Cardiac cells show a remarkable ability to survive hypoxia. Although chronic hypoxia reduces or temporarily stops myocardial contractility, the cells can show a full recovery when hypoxia is eased[227]. Hypoxia, in spite of activating a series of cell survival mechanisms, also activates autophagy in the myocardium. Amino acids and fatty acids recovered by autophagy are utilized for ATP production. In most of the clinical instances, ischemia is followed by spontaneous or therapeutic restoration of arterial blood supply termed as *reperfusion*. Reperfusion also elicits a series of cellular responses, including accumulation of reactive oxidative species (ROS) and activation of signaling cascades. It has been claimed that the autophagy induced during ischemia is further enhanced during reperfusion in the heart in vivo in mouse and human heart[143,228]. Cultured neonatal and adult CMs have also been shown to experience an enhanced autophagy during ischemia and reperfusion (I/R)[150].

Generally speaking, cellular stressors that impair the ability of ER to confer post-translational changes and lead to ER stress, are potential autophagy inducers[229]. Accumulation of unfolded proteins, such as polyglutamine repeat (PolyQ72) in the ER, activates one of the UPR transducers PERK, which in turn induces autophagy to eliminate polyQ72 aggregates[172]. ER stress triggered by I/R has been shown to lead to increased autophagy in the heart[230]. However, autophagy maintains a complex functional role in I/R in the heart. The enhancement and the pathophysiological effects of autophagy could be directly proportional to the severity and duration of ischemia and consequent damage caused by reperfusion injury in the heart[231]. It has been reported that the enhanced autophagy during I/R, involving overexpression of Beclin1, is detrimental for CMs[150].

In the pathogenesis of I/R injury, intracellular Ca^{2+} overload plays an important role[232]. Pluteanu and Cribbs reported that T-type Ca^{2+} channels are regulated by hypoxia/reoxygenation (H/R) in ventricular myocytes[233]. They also reported that, under chronic hypoxic conditions, $Ca_v3.1$ mRNA levels decreased (with a subsequent decrease in T-type Ca^{2+} channel current density) in a HIF-1α dependent manner. Upon reoxygenation, the levels of $Ca_v3.1$ mRNA were restored. From the reports of Pluteanu and Cribs and Pastukh *et al.* [234]., it can be postulated that $Ca_v3.1$ channel downregulation acts as a protective mechanism to counteract tha Ca^{2+} overload during hypoxia[233-234].

Regarding L-type channels, although a protective effect of L-type Ca^{2+} channel blockers from I/R has been demonstrated in a wide variety of experimental models[235], recently it has been reported that the expression of L-type channels either decreased or remained unchanged during the I/R episode [236-237]. As a matter of fact the use of L-type channel blockers in humans for myocardial I/R has yielded deceiving results with little or no beneficial effects to patients[238]. On the contrary, the T-type channel blocker mibefradil is regarded as an effective antiarrythmic compound [239] , and is also known to reduce the infarct size in adult heart after myocardial infarction [240-242].

Taking into account that hypoxia/reoxygenation induces ER stress and autophagy, in addition to the reshuffling of the expression of voltage-gated calcium channels, we aimed to characterize these cell responses in our experimental setup, but also to break down the effects due to deprivation from those due to hypoxia (which is performed under serum deprivation, simulating the blockade of blood flow that characterizes ischemia) or reperfusion. The ultimate goal was to check if the pharmacological blockade of T-type channels would lead to cardioprotection in a situation of simulated ischemia or ischemia/reperfusion by inhibiting an exacerbated autophagy.

2. Results

2.1. Simulated ischemia induces the unfolded-protein response

Compared to the CMs maintained in complete media under normoxic conditions, the CMs subject to chronic hypoxia (0,2% O_2 for 24 h) induced a near 2-fold upregulation of GRP78 and XBP1, and a 6-fold upregulation of GADD153. Upon reoxygenation for 2-4 h, the induction of XBP1 and GRP78 was maintained, whereas the levels of GADD153 dropped below the control levels. Yet, the expression levels of all three UPR markers remained considerably below those displayed for CMs deprived from glucose and serum and cultured under normoxic conditions.

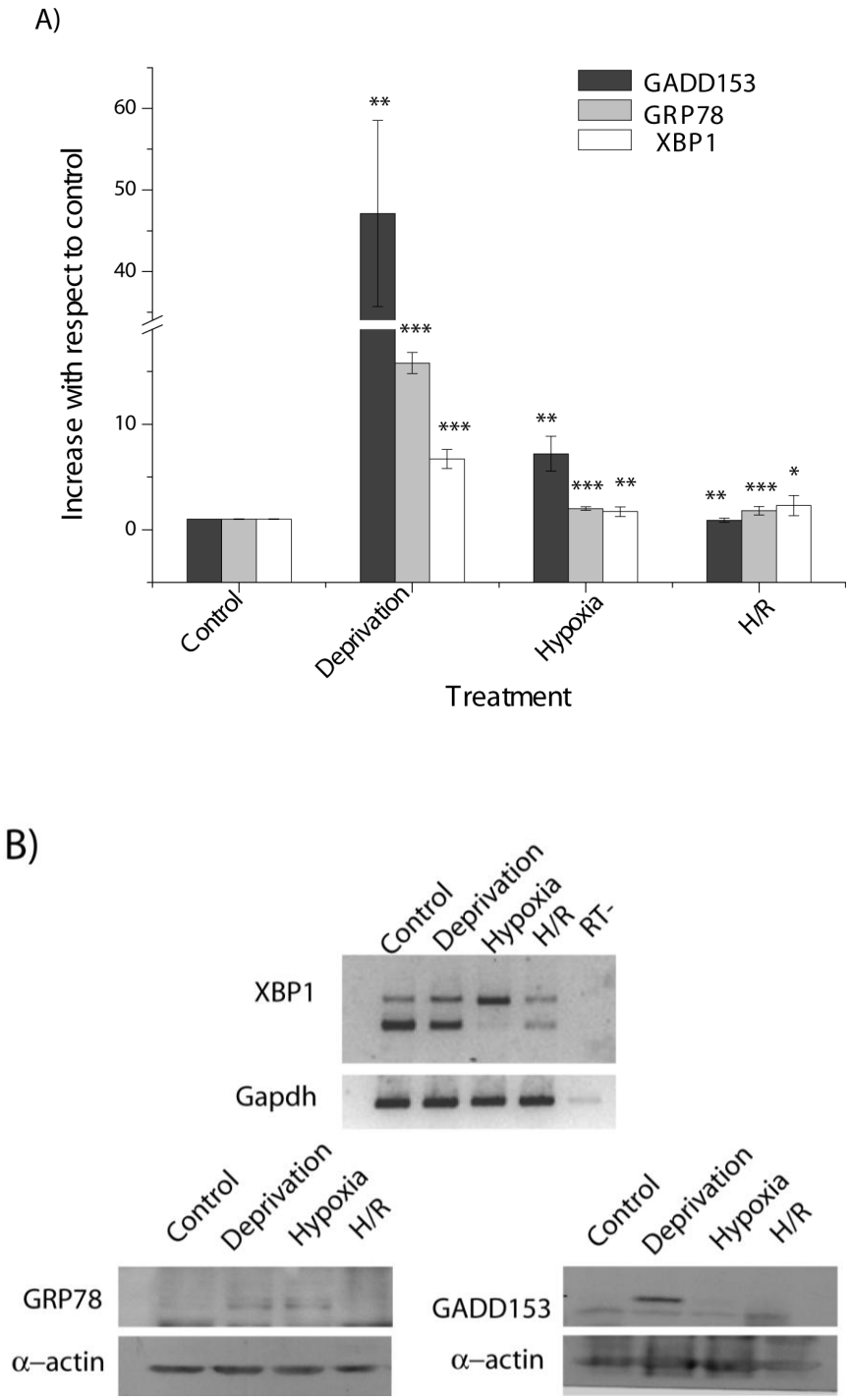

Figure 1*: Unfolded protein response induced in the CMs subjected to hypoxia. A) q-PCR results show that GRP78 and XBP1 are induced to 1.5-2 fold upon hypoxia as well as upon re-oxygenation, whereas GADD153 that was induced by hypoxia to near 6 fold, returned to control levels upon re-oxygenation. B) Hypoxia induced a complete splicing of XBP1, whereas both forms of XBP1 were reduced by reoxygenation. Both GRP78 and GADD153 protein levels were induced by deprivation. Only hypoxia induced an increase in GRP78, while it returned to control levels upon reoxygenation. GADD153 was not*

*induced either by hypoxia or reoxygenation and was maintained at control levels. Histogram bars represent mean ± SD values from at least 3 independent experiments with duplicate measurements of each treatment (n=3). *Significant differences related to untreated control, P< 0.05. Western blots are representative of at least 4 consecutive experiments.*

At the translational level, the expression of GRP78 was also increased by deprivation, maintained in hypoxia, and restored to control levels by reoxygenation. The levels of GADD153 were also increased by deprivation and restored to control values in CMs subject to hypoxia or reoxygenation.

2.2. Simulated ischemia induces autophagy

The expression of Atg genes was analysed for CMs that were maintained in normoxia vs hypoxia overnight, and also for those reoxygenated for 4h after hypoxia. Hypoxia and to a lesser extent reoxygenation, induced a moderate upregulation of Atg5 and downregulation of Beclin1. Following a similar pattern to the one for UPR genes, hypoxia and reoxygenation actually counteracted partially (for Atg5) or completely (for Beclin1) the deprivation-mediated increases of Atg genes (Figure. 2).

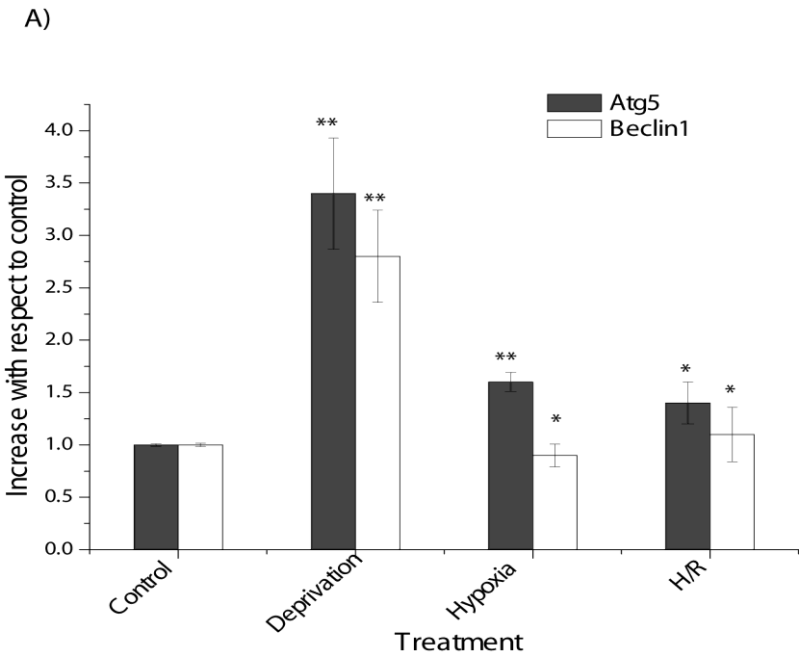

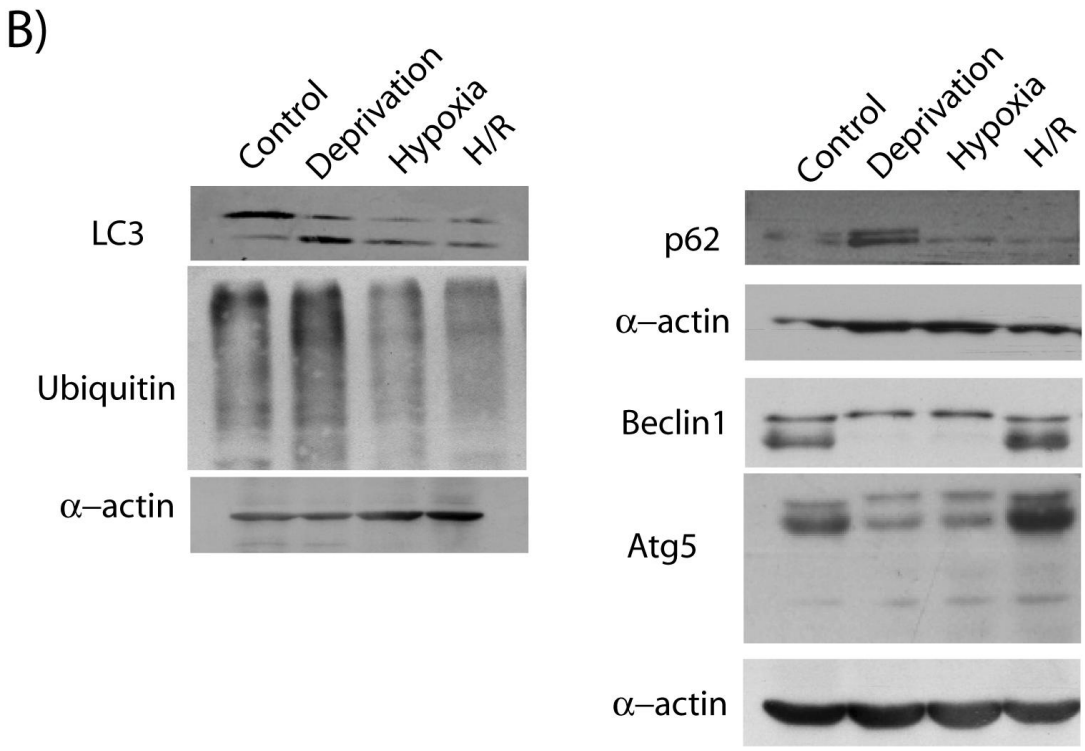

Figure 2: *Regulation of autophagy markers by ischemia reperfusion. A) q-PCR results show that both Atg5 and Beclin1 are induced by deprivation, and that hypoxia and reoxygenation bring the levels back to the ones displayed in normoxia (partially for Atg5, fully for Beclin1). B) Western blot results show that LC3-II is induced upon deprivation, hypoxia and re-oxygenation. Compared to deprivation, hypoxia or re-oxygenation clearly decreased the p62/SQSTM1 band intensity, and also the poly-ubiquitinated aggregates. The Beclin1 band disappeared with deprivation and hypoxia, whereas reoxygenation induced a strong upregulation of Beclin1. The complex Atg5-Atg12 was also reduced by deprivation and hypoxia, and increased by reoxygenation. Histogram bars represent mean ± SD values from at least 3 independent experiments with duplicate measurements of each treatment (n=3). *Significant differences related to untreated control, P< 0.05. Western blots are representative of at least 4 consecutive experiments.*

At the posttranslational level, we found that deprivation induced the LC3-II conversion, which was somewhat mitigated by hypoxia and, especially, reoxygenation. Similarly, while deprivation induced an increase in the p62/SQSTM1 levels, hypoxia and reoxygenation approached the p62/SQSTM1 band intensity to that from CMs cultured in complete media. This result was also supported by the clearance of poly-ubiquitinated aggregates by hypoxia and reoxygenation. In an apparent paradox, deprivation and

hypoxia suppressed the expression of Beclin1 protein and decreased the formation of the Atg5-Atg12 tandem, whereas reoxygenation induced a strong upregulation of both Atg proteins.

2.3. Reshuffling of the expression of VGCCs by hypoxia

T-type $Ca_v3.2$ channels have been reported to be upregulated under hypoxic conditions in different cell types[243-245], while $Ca_v3.1$ has been shown to be downregulated in neonatal CMs under sustained hypoxia[233].

CMS subjected to deprivation, hypoxia or reoxygenation protocols, including those that were pre-conditioned with mibefradil, were analyzed for a putative induction of transcripts for VGCCs by q-PCR. We found that deprivation upregulated all T-type isoforms including $Ca_v3.1$, $Ca_v3.2$ and $Ca_v3.3$, as well as the L-type channel $Ca_v1.2$. Hypoxia and reoxygenation alleviated VGCC upregulation, although the values for $Ca_v3.3$ remained higher than in CMs cultured in serum-containing medium.

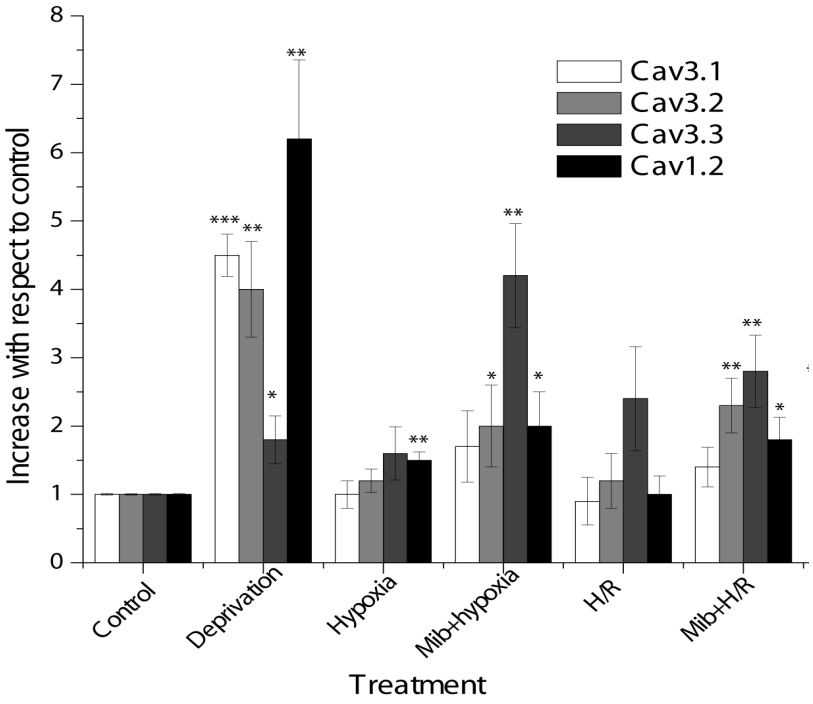

***Figure 3**: Deprivation significantly raised the mRNA levels for T-type as well as L-type calcium channels. The upregulation of all channel isoforms, except of $Ca_v3.3$, was largely reduced by hypoxia and reoxygenation treatments. Histogram bars represent mean ± SD*

*values from at least 3 independent experiments with duplicate measurements of each treatment (n=3). *Significant differences related to untreated control, P< 0.05.*

However, taking into account that the CMs subject to hypoxia or reoxygenation were also maintained in serum and glucose-deprived media most of the time (all of it for the hypoxia condition), we can attribute the VGCC channel expression reshuffling to the effect of glucose and serum deprivation. In fact, when considering the deprived CMs as the bona fide control condition for these experiments, we can conclude that the expression of all Ca^{2+} channel isoforms was reduced by both hypoxia and reoxygenation.

2.4. Mibefradil augments cell death induced by hypoxia and mitigates cell death induced by reoxygenation

Considering that T-type and L-type Ca^{2+} channels are upregulated under hypoxia and reoxygenation compared to control cells grown in rich medium, and that both conditions have been reported to decrease the viability of CMs, we pre-conditioned the cells with mibefradil for 2h before hypoxia or reoxygenation. We then performed TUNEL assays on the cells after hypoxia or reoxygenation, and compared the results with those from cells incubated in normoxia (Figure 4).

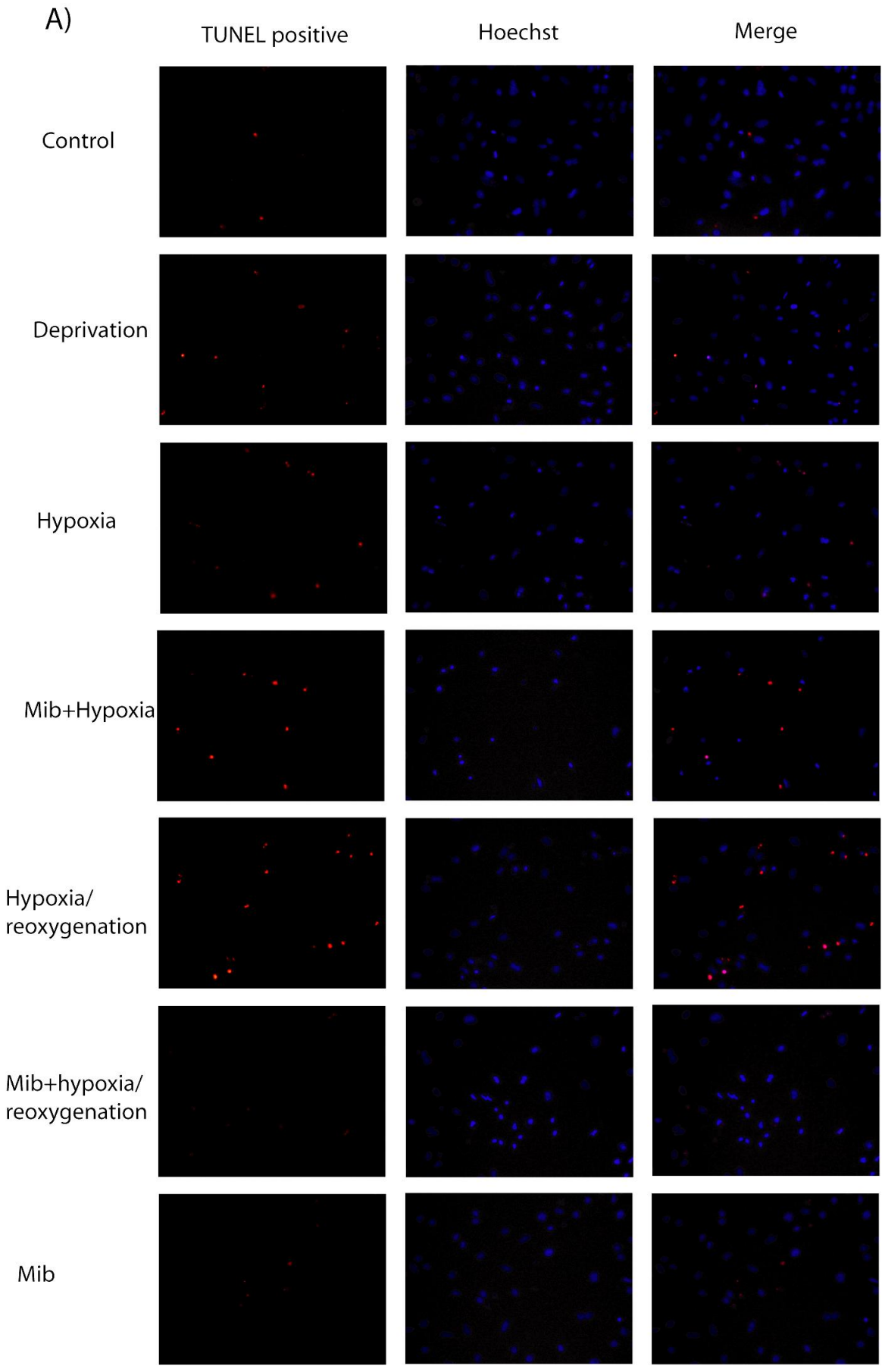
A)
TUNEL positive
Hoechst
Merge
Control
Deprivation
Hypoxia
Mib+Hypoxia
Hypoxia/
reoxygenation
Mib+hypoxia/
reoxygenation
Mib

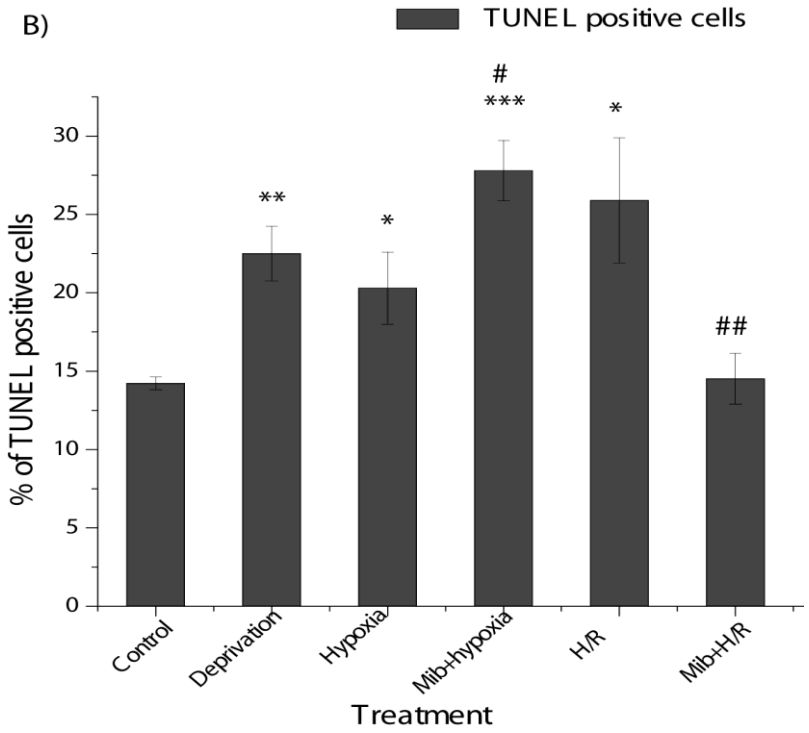

Figure 4*: T-type channel blockade confers protection against cell death caused by hypoxia/reoxygenation. Deprivation and reoxygenation increased the percentage of tunel positive cells significantly. Preconditioning with mibefradil increased the cell death due to hypoxia, and, in open contrast, protected against cell death caused by re-oxygenation. Histogram bars represent mean ± SD values from at least 3 independent experiments with duplicate measurements of each treatment (n=3). *Significant differences related to untreated control, P< 0.05. # Significant differences related to deprivation, P<0.05.*

We found that as expected deprivation, hypoxia (to a lesser extent) and reoxygenation induced the death of CMs. Preconditioning with mibefradil significantly increased the percentage of TUNEL positive cells in the cultures subject to hypoxia, whereas, rather paradoxically, it decreased the TUNEL positive cells to near control levels in cultures subject to reoxygenation.

2.5. T-type channels blockade increased UPR upon ischemia and Reperfusion

Upon preconditioning the cells with the T-type channel blocker mibefradil, hypoxia as well as reoxygenation increased the expression of UPR transcripts to the same level or even higher than hypoxia or reoxygenation alone (Figure 5A).

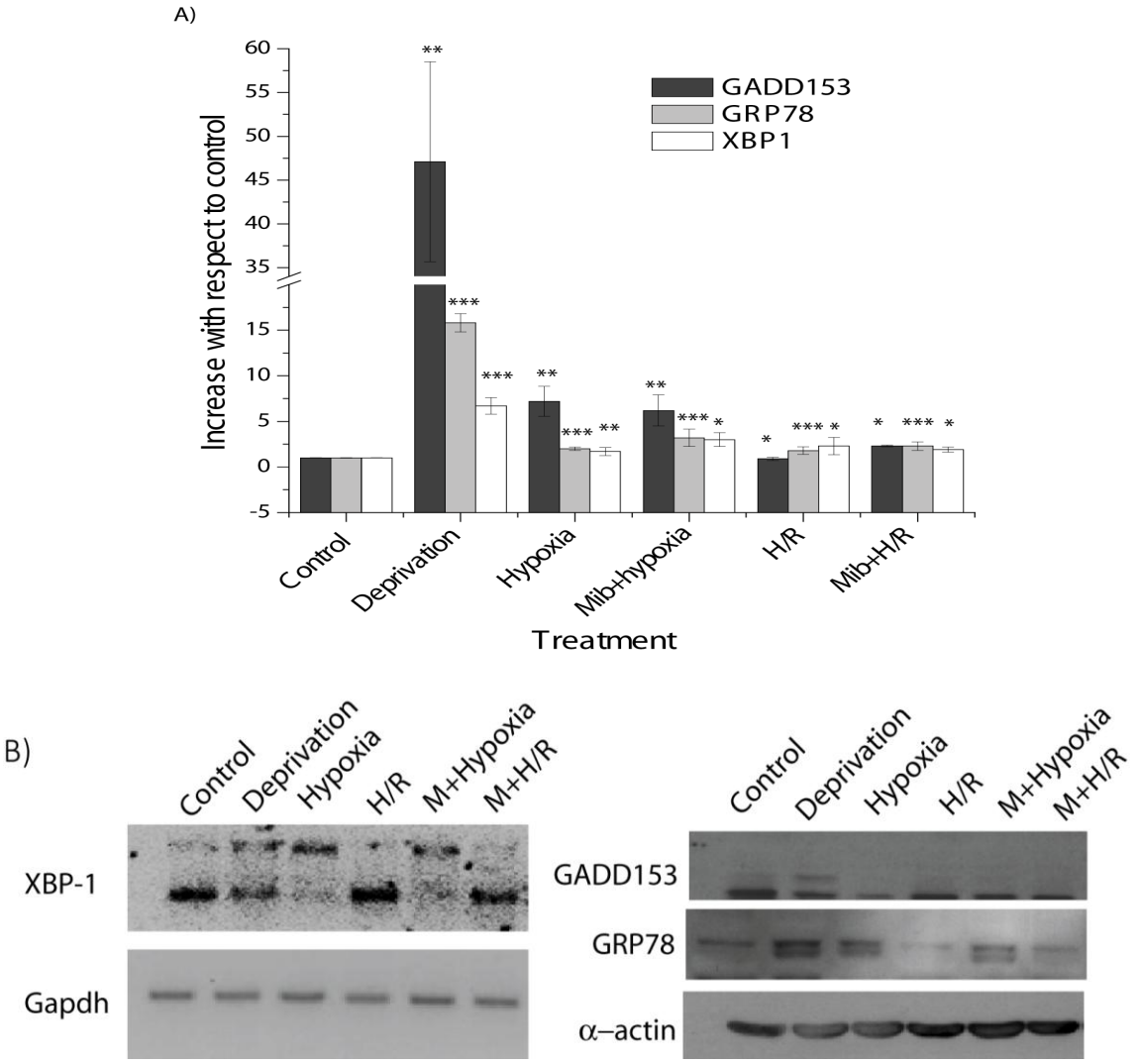

Figure 5*: Unfolded Protein Response upon T-type channel blockade under hypoxia and reoxygenation conditions. q-PCR data shows that XBP1 and GRP78 expression levels under hypoxia and reoxygenation were increased in the presence of mibefradil, whereas the level of GADD153 trancripts was grossly maintained. Histogram bars represent mean ± SD values from at least 3 independent experiments with duplicate measurements of each treatment (n=3). *Significant differences related to untreated control, P< 0.05. Western blots are representative of at least 3 different experiments.*

At the translational level, GRP78 was induced by deprivation and the upregulation was maintained in hypoxia, but not in reoxygenation. Mibefradil preconditioning did not change the expression of GRP78 in either cells subjected to hypoxia or reoxygenation. The GADD153 band was downregulated by hypoxia and re-appeared with mibefradil

preconditioning. Although re-oxygenation did not alter the levels of GADD153, under mibefradil treatment, re-oxygenation induced the upregulation of GADD153.

2.6. T-type calcium channel blockade altered the expression of Atg genes upon hypoxia or reoxygenation

Mibefradil preconditioning upregulated the expression of both Atg5 and Beclin1 transcripts compared to the cells subjected to hypoxia and reoxygenation (Figure 6A).

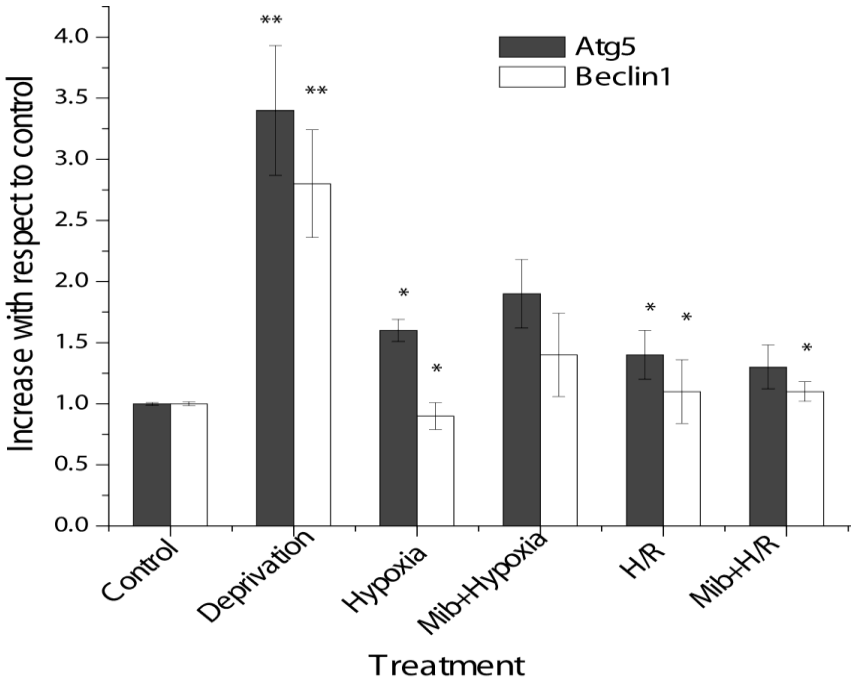

***Figure 6**: Regulation of autophagy genes by T-type calcium channel blockade under hypoxia. A) Application of mibefradil induced the expression of both Atg5 and Beclin1 genes under hypoxia, while it only induced the expression of Beclin1 upon reoxygenation. Histogram bars represent mean ± SD values from at least 3 independent experiments with duplicate measurements of each treatment (n=3). *Significant differences related to untreated control, P< 0.05.*

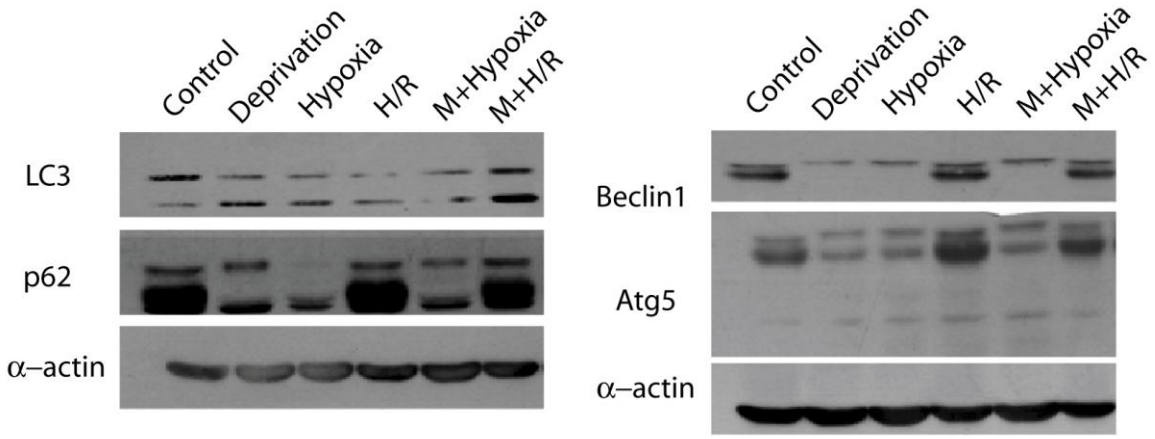

Figure 7*: the western blot results show that Beclin1 and Atg5 that were induced by reoxygenation were kept near control levels by preconditioning with mibefradil. On the other hand, LC3-II was induced by all the experimental conditions. The band corresponding to p62/SQSTM1 (top one) was reduced by hypoxia compared to deprivation, and restored in the presence of mibefradil. The p62/SQSTM1 levels were not increased by reoxygenation, while they were further increased by the presence of mibefradil upon reoxygenation. Western blots are representative of at least 3 consecutive experiments.*

At the protein level, the expression of Atg5 and Beclin1 in hypoxia or reoxygenation was reduced to control levels by mibefradil preconditioning. Similarly, both the LC3II/I ratio and the p62/SQSTM1 protein levels were increased by mibefradil preconditioning in CMs cultured in hypoxia or reoxygenation conditions (Figure.7).

2.7. Assessment of autophagic flux with tandem flagged- LC3

The autophagic flux was further analyzed by overexpression of tandem flagged LC3 constructs.

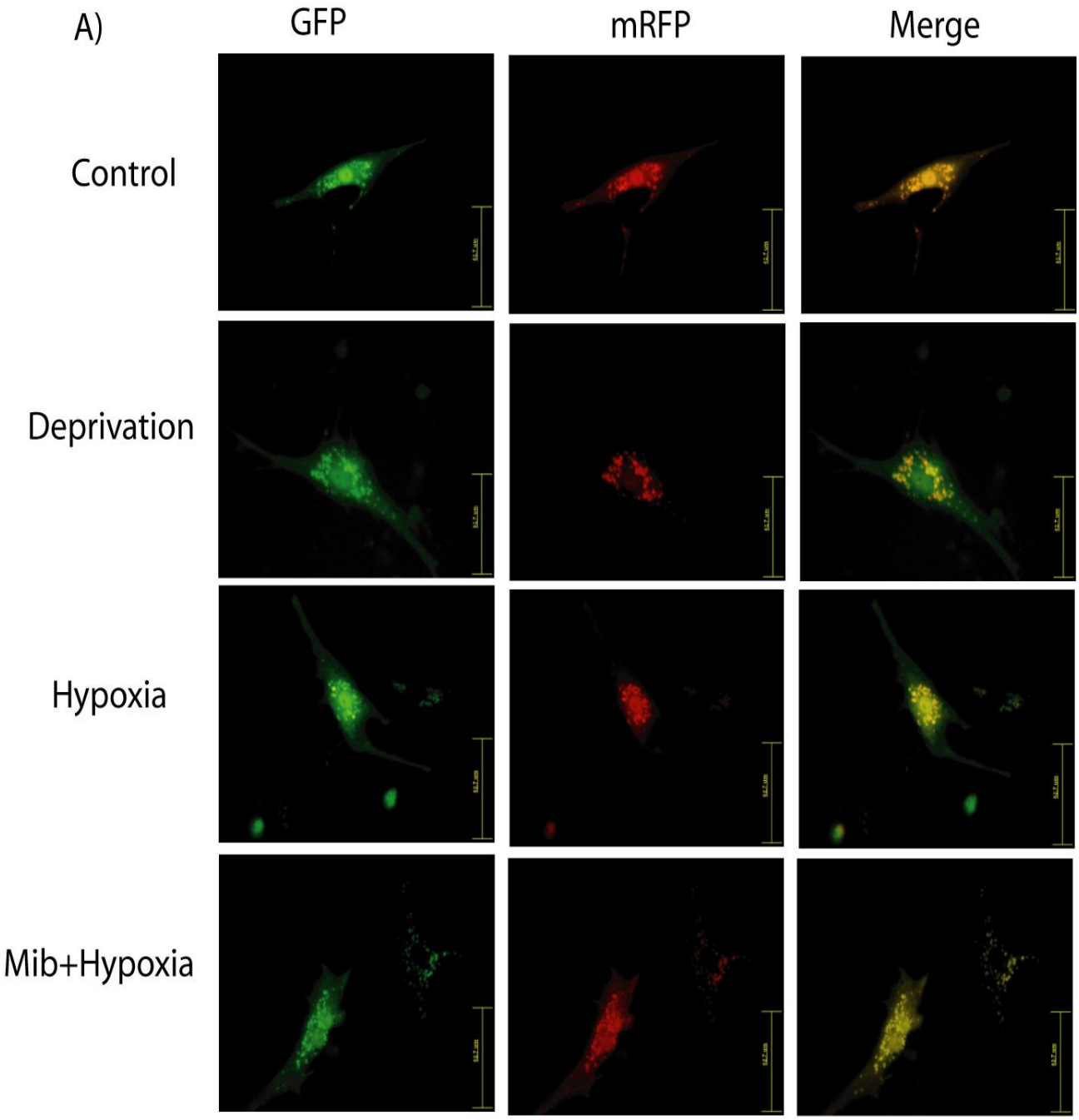
A)
GFP
mRFP
Merge
Control
Deprivation
Hypoxia
Mib+Hypoxia

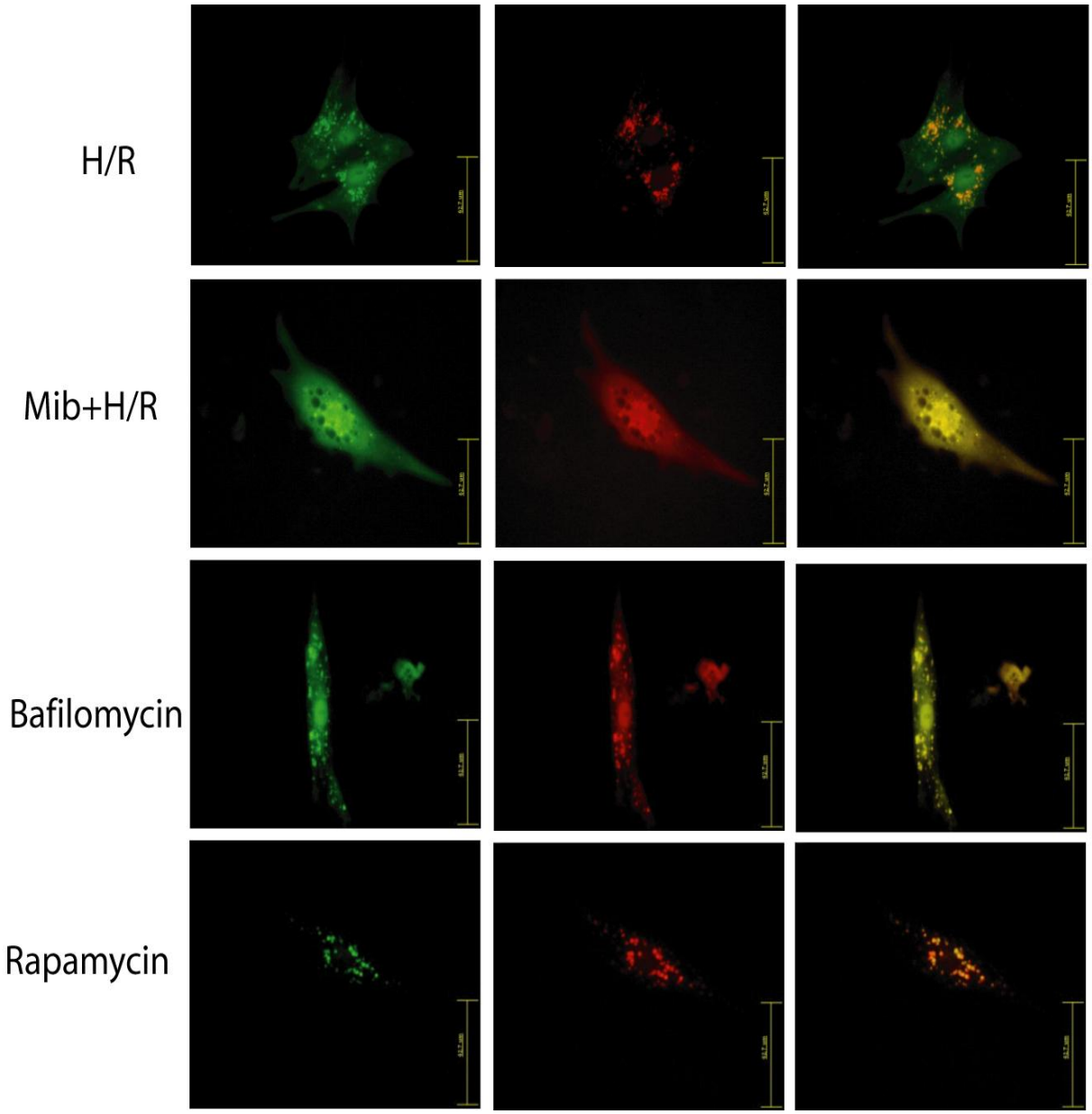
H/R
Mib+H/R
Bafilomycin
Rapamycin

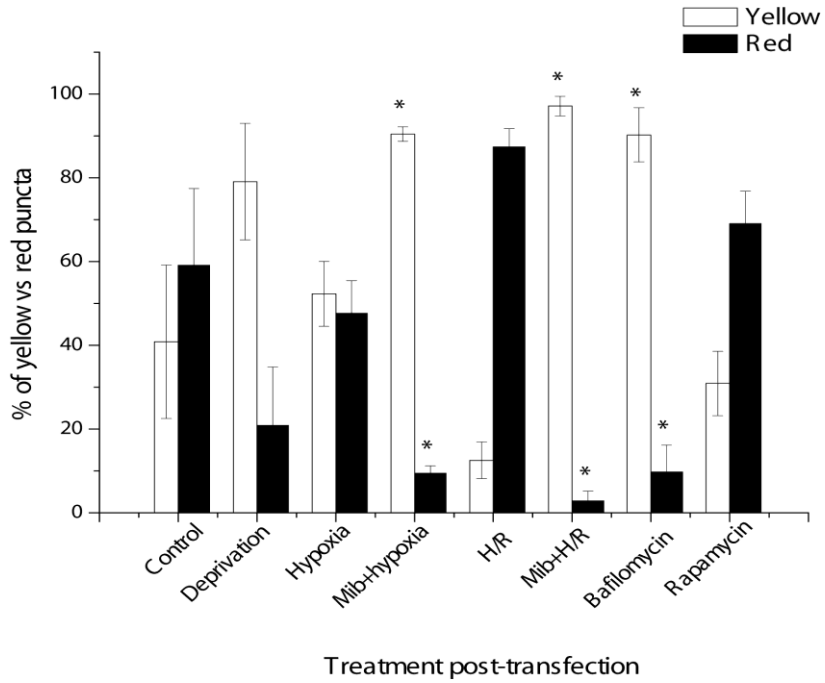

***Figure 8**: Autophagic flux assessed by tandem flagged LC3. A) The level of induction of autophagy by reoxygenation was much higher than that of the positive control for autophagy, rapamycin. Autophagy under deprivation, hypoxia and reoxygenation was inhibited by preconditioning with mibefradil. B) The graph shows the percentage of yellow and red puncta over the total number of LC3-labelled autophagic vacuoles. The high ratio of red over yellow in re-oxygenation was reversed by the addition of mibefradil. The lower-level autophagy induced by hypoxia was also blocked by the presence of mibefradil.*

As a proven inhibitor of the autophagic flux we used the v-ATPase inhibior bafilomycin A1, which prevents the fusion of autophagosomes and lysosomes; as expected, bafilomycin increased the percentage of yellow puncta (Figure 8). In contrast, rapamycin, a known autophagy inducer by inhibiting the mTOR complex-1, increased significantly the percentage of red puncta when compared to untreated CMs. We found that the ratio of yellow over red puncta was almost 1:1 in CMs cultured in hypoxia, similar to CMs cultured in normoxic conditions. However, in the former the total number of puncta was largely increased, indictative of autophagy induction[246]. Application of mibefradil under hypoxia resulted in inhibition of autophagy which was evident from the increase in the ratio of yellow to red puncta up to 9:1. On the other hand, hypoxia followed by subsequent reoxygenation induced a strong autophagic flux by increasing the ratio of red

over yellow, while preconditioning with mibefradil induced a drastic reversal of the ratio, indicative of a halt in the autophagy flux.

3. Discussion

From the previous chapter, it is clear that the T-type channel blockers can potentially inhibit autophagy in CMs. In this study, we examined the effects of T-type channels blockade on the CMs homeostatic cell mechanisms and viability, when challenged with hypoxia or reoxygenation.

Initially the presence of transcripts for T- and L-type Ca^{2+} channels was analyzed in CMs that were subjected to chronic hypoxia or reoxygenation. When comparing cells grown in rich medium and cells starved from serum and glucose, in normoxic conditions, we could appreciate a drastic increase in the expression of L-type $Ca_v1.2$ channels, and also of T-type $Ca_v3.1$, $Ca_v3.2$ and (to a lesser extent) $Ca_v3.3$ channels in the latter. We found that neither the expression of $Ca_v3.1$ nor of $Ca_v3.2$ channels was induced by hypoxia or reoxygenation by themselves (Figure 3). In fact and, taking into account that hypoxic and reoxygenated cells were also deprived from serum and glucose, we found that all channel types were rather downregulated in hypoxia or reoxygenation, when compared to the cells that were starved under normoxic conditions, except $Ca_v3.3$ For the first time we found that $Ca_v3.3$ channels, expressed at very low levels in CMs, are upregulated under deprivation and that their expression is mantained under hypoxia as well as reoxygenation. Pluteanu and Cribbs reported that T-type channel isoforms are differentially regulated during ischemia and reperfusion, so that the expression of $Ca_v3.2$ rises and that the expression of $Ca_v3.1$ mRNA is lowered, being either levels restored upon re-oxygenation [233]. It has been suggested that T-type channels may act as *in vivo* oxygen sensors, controlling excitability in hypoxic environments[247-248].

During hypoxia, Ca^{2+} homeostasis is disrupted through inhibition of sarcoplasmic/endoplasmic reticulum Ca^{2+}-ATPase pump due to intracellular ATP depletion[249]. We found that the mRNA/protein levels of all the three UPR markers were upregulated by deprivation (Figure 1), and that they came back to control (rich medium and normoxia) values during hypoxia or reoxygenation. In this regard, it had been previously reported that ischemia directly activates the ER stress response in the heart by inducing one of the UPR branches, ATF6, that in turn triggers the upregulation of GRP78[250]. However, upon reperfusion, the ATF6 activity and GRP78 activity are

attenuated[251]. It has also been reported that hypoxia induces the AMPK signaling cascade possibly HIF-1-mediated, that protects CMs against hypoxic injury by attenuating ER stress and apoptotic signals[252-253].

.

Available evidences also indicate that autophagy is induced during ischemia through an AMPK-dependent mechanism, whereas reperfusion further enhances autophagy through Beclin1 dependent mechanism[143,254]. Matsui et al. reported that autophagy has distinct roles during ischemia and reperfusion: while autophagy induced during ischemia might be protective, autophagy induced during reperfusion might be detrimental and induce cell death. It has been claimed that inhibition of autophagy induced by 3-MA or knockdown of Beclin1 led to increase in cell survival *in vitro*[150]. We observed that deprivation increased the levels of Beclin1 and Atg5, concomitantly to an increase in LC3-II and an increase in p62/SQSTM1. The levels of p62/SQSTM1 are double edged: on the one hand and, as commented earlier, p62/SQSTM1 is a macroautophagy susbtrate and so it is degraded faster when the autophagy flux is augmented [201,208,255]; on the other being p62/SQSTM1 an inducible gene, its upregulation has also been related to autophagy induction[202]. We also found that, under hypoxia or reoxygenation, the mRNA levels of Beclin1 came down to control (rich medium, normoxic) levels, while Atg5 was still upregulated in hypoxia. However and, in open contrast, Beclin1 and Atg5-Atg12 protein levels were largely decreased by deprivation; these decreases were mantained in cells subjected to hypoxia, but not in reoxygenation.

In apparent consonance with the drop of the Atg5-Atg12 protein levels by deprivation, in the light of the level of ubiquitinated aggregates and numbers of autolysosomes (monitored by tandem flagged LC3) we could conclude that, under our experimental conditions and in the 18-24h time point, deprivation slowed down the autophagic flux and that the autophagy process was restarted and shaped by hypoxia or reoxygenation. Considering that autophagy induced by reoxygenation is regarded as detrimental, we set out to investigate if T-type channel blockade may help in protecting CMs against this type of a stimulus, which is the experimental paradigm for ischemia/reperfusion injury. Parvinder et al. had suggested that T-type channels are more influential in mediating depolarization-evoked Ca^{2+} influx following a period of chronic hypoxia[256]. The viability assays performed on the cells exposed to chronic hypoxia followed by reoxygenation may indicate that hypoxia acts in a protective manner by reducing cell death induced by deprivation, while reoxygenation promotes cell death to a level similar to deprivation

(Figure 4). It also regulated the viability of the cells in an opposite manner in hypoxia or reoxygenation. Preconditioning with mibefradil in hypoxia induced cell death more than hypoxia or even deprivation, whereas preconditioning with mibefradil during H/R reduced cell death below the values seen with H/R or deprivation. As a matter of fact, mibefradil has been reported to be cardioprotective against ischemia/reperfusion by reducing the infarcted area[257]. It has also been shown that the blockade of I_{CaT} reduces both apoptosis and necrosis in CMs under excessive β-adrenergic stimulation [258].

The preconditioning with mibefradil only changed marginally the expression of the analyzed UPR or Atg genes in hypoxia or reoxygenation conditions (Figure 6). Nonetheless, the p62/SQSTM1 protein levels that had fallen drastically during hypoxia were restored by the presence of mibefradil.

Mibefradil preconditioning during reoxygenation increased both LC3-I and LC3-II bands, raising doubts over the autophagic status of the cells. However, from the overexpression of ptf-LC3 constructs, it was clear that the preconditioning was inhibiting the formation of autophagosomes (Figure 7). Whereas hypoxia clearly increased the percentage of red punta compared to that of deprivation, indicating an increased autophagic flux, mibefradil preconditioning increased significantly the percentage of yellow puncta. Similarly, while reoxygenation increased the ratio of red over yellow, the application of mibefradil upon reoxygenation reversed the ratio, blocking autophagolysosomes formation by an estimated 95%.

In summary, our experiments show that deprivation induces the expression of all VGCC channel types in cardiomyocytes, along the development of a strong ER stress that turns maladaptive and leads to disruption of the autophagic flux and subsequent cell death. The effects of hypoxia *per se*, probably via the induction of hypoxia-inducible factors, would be to restore the levels of VGCCs, downregulate the UPR and restart the autophagic flux. In this scenario, the addition of mibefradil in preconditioning treatments would bring the cell to a halt in the autophagic flux at a late stage, ultimately jeopardizing the viability of the cardiomyocytes. The situation is strikingly different upon reoxygenation. Here, the UPR is similar to the one measurable in hypoxia, except for the induction of GADD153. The autophagic status, though, is considerably different, as the autophagic flux is very much increased in a Beclin1-dependent fashion. In this scenario, mibefradil would favour the viability of the CMs by inhibiting an *excessive* autophagy.

In conclusion and, taking into account that reperfusion after chronic ischemia induces cell death by strongly enhancing autophagy in a Beclin1 dependent manner, and that preconditioning with mibefradil inhibits the autophagy flux, it can be concluded that de-regulation of autophagy is a likely cell mechanism through which T-type channel blockers exert their cardioprotective actions against ischemia/reperfusion injury.

Chapter 3

Cardiac hypertrophy mediated regulation of UPR and autophagy involves upregulation of voltage-gated calcium channels.

1. Introduction

The deficiency in the capability of the heart to adequately pump blood in response to systemic demands results in heart failure. Heart failure is induced by various stimuli such as hypertension, myocardial infarction, hypertrophic and dilated cardiomyopathies and diabetic cardiomyopathy[259]. Most of the above mentioned stimuli first induce a phase of cardiac hypertrophy. A major fraction of the ventricular CMs that is incapable of proliferation respond to stress by inducing a hypertrophic growth response. Cardiac hypertrophy is characterized by growth in length or width of individual CMs as a means of increasing cardiac pump function and decreasing ventricular wall tension and also thickening of left ventricular myocardium. Apart from this, a shift in glycolytic metabolism, alterations in Ca^{2+} storage and handling, changes in contractility and reactivation of a fetal gene program can be observed[162]. Moreover, in the long term, cardiac hypertrophy may lead to heart failure, arrhythmia and even sudden death [260-261].

Until now there are no therapeutic agents developed to target directly the hypertrophic growth. However, certain strategies are known to alter the hypertrophic growth which include suppression of neurohormones release (particularly of catecholamines, angiotensinII or aldosterone), Ca^{2+} influx (using Ca^{2+} channel blockers, specifically for L-type channels) or preload (using vasodilators or diuretics)[262]. Increase in cell mass during cardiac hypertrophy means increase in protein synthesis, which is also accompanied by structural remodeling and dysfunction of intracellular organelles. CMs might adapt to some cellular mechanisms against structural remodeling due to increase in protein synthesis, by inducing autophagy. Autophagy is reported to be activated during the acute and chronic phases of cardiac hypertrophy[145,263]. Oyabu *et al.* has reported that autophagy mediated degradation is necessary for hypertrophy regression during ventricular unloading[264]. A possible involvement of ER stress has also been reported in models of cardiac hypertrophy. Apart from autophagy and ER stress, the altered Ca^{2+} influx through T-type channels[222 78,265] and L-type channels[266-267] are also known to induce cardiac hypertrophy.

We set out to check a possible linkage between cardiac hypertrophy, ER stress, autophagy and the VGCCs. We used a selection of cardiac hypertrophy inducers namely angiotensin II, aldosterone, phenylephrine (α-adrenergic receptor agonist) and isoprenaline (β-adrenergic receptor agonist) on cultured neonatal rat ventricular CMs, with the objectives of characterizing channel expression, ER-homeostasis and autophagy regulation. Before starting these experiments, we realized that most published research works dealing with

cardiac hypertrophy *in vitro* are performed with CMs cultured in serum-free conditions, presumably to decrease the chance of growth of any contaminating fibroblasts. On the other hand, starvation is a known ER stressor and autophagy inducer in CMs and other cell types, and we reasoned that serum deprivation could be inducing some effects that would overlap with those due to hypertrophic stimuli. We consequently performed all the experiments both in the absence and presence of serum.

2. Results

2.1. Hypertrophy stimuli induce an increase in the frequency of cell beating

CMs were treated with the hypertrophy stimulants in the absence of serum, namely angiotensin II at 100 µM, aldosterone at 1 µM, phenylephrine at 10 µM and isoprenaline at 10 µM, 72h after culture. To monitor the induction of cardiac hypertrophy as a preliminary screening, the number of cell beats per minute was counted after 48h of treatment.

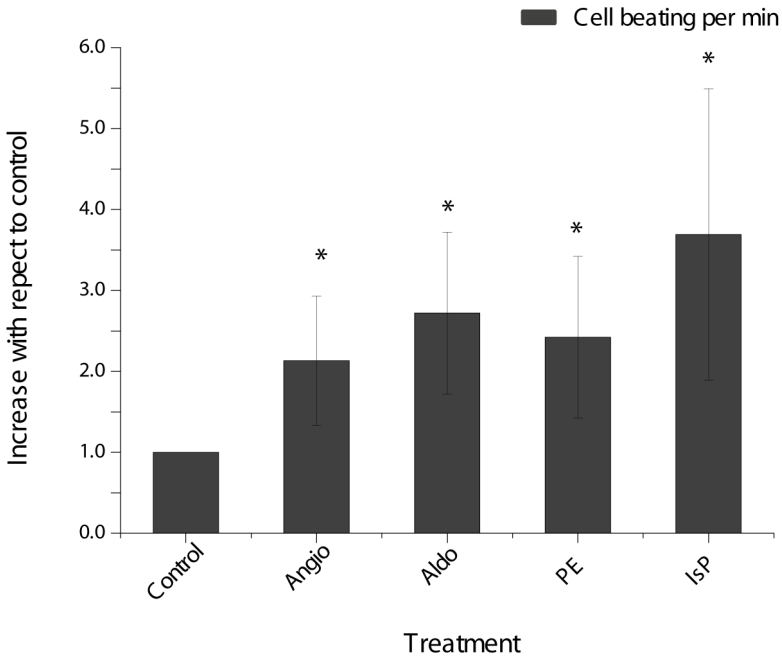

***Figure 1**: Hypertrophic stimuli induce a higher cell beating frequency. Histogram bars represent mean ± SD values from at least 4 independent experiments with duplicate measurements of each treatment (n=4). *Significant differences related to untreated control, P< 0.05.*

All four hypertrophic stimuli induced an increase in the number of beats/minute. Cells treated with angiotensin II showed a 2-fold increase in cell beating compared to that of untreated control (Figure 1). Aldosterone increased the beating frequency nearly 3-fold, phenylephrine 2.5-fold and isoprenaline treated cells showed a 4-fold higher beating frequency. A similar pattern of induction of cell beating was also observed in the cells treated with the hypertrophy agonists in the presence of serum (data not shown).

2.2. Hypertrophy markers are induced by the hypertrophy agonists

Natriuretic peptides, namely atrial netriuretic peptide (ANP) and brain natriuretic peptide (BNP), are known to be involved in the regulation of cardiac hypertrophy and their expression is reported to be induced in angiotensin II- and phenylephrine- induced cardiac hypertrophy. Cardiomyocytes that were treated with hypertrophic agonists were analyzed for the induction of hypertrophy markers ANP and BNP.

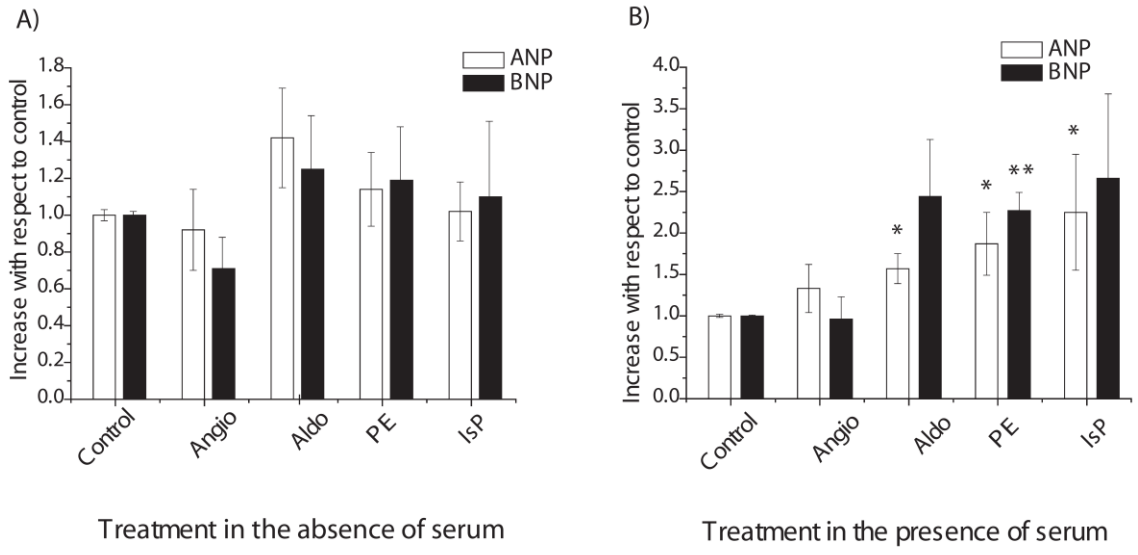

***Figure 2**: Expression of ANP and BNP in the presence of hypertrophic stimuli. A) A moderate expression of ANP and BNP was induced by aldosterone and adrenergic agonists (PE and IsP), but not angiotensin II, under serum deprivation.B) Aldosterone and adrenergic agonists induced the expression of ANP and BNP in the presence of serum. β-actin was used as a house-keeping control. Histogram bars represent mean ± SD values from at least 4 independent experiments (n=4). *Significant differences related to untreated control, P< 0.05.*

The exposure to hypertrophic stimuli lasted 48 h and was performed both in the absence and presence of serum. The q-PCR data showed a moderate level of induction of the genes NPPA and NPPB specifically encoding for ANP and BNP respectively, in the presence of aldosterone, phenylepherine and isoprenaline under serum deprivation, and a significant level of induction of the same genes in the presence of serum (Figure 2A). In contrast, angiotensin II which did not induce any change in either ANP or BNP expression in the absence of serum, and induced only a moderate (not significant) increase in ANP expression in the presence of serum, while the levels of BNP remained the same (Figure 2B).

2.3. Hypertrophic stimuli alter the expression profile of calcium channels

CMS that were treated with the different hypertrophic stimuli where analyzed for alterations in the Ca^{2+} channels expression. For this purpose their RNA was extracted, and cDNA was retro-transcribed and probed for the genes encoding $Ca_v3.1$, $Ca_v3.2$, $Ca_v3.3$ and $Ca_v1.2$ channels, in a series of q-PCR assays.

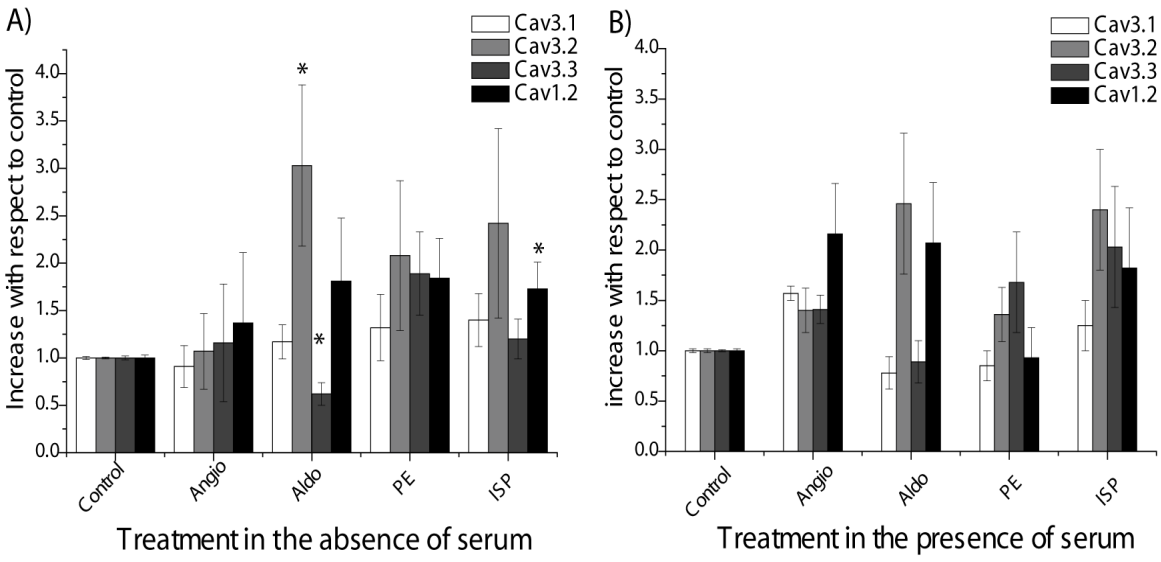

***Figure 3**: Changes in VGCCs expression upon induction of hypertrophy. A) Hypertrophic stimuli alter the expression of VGCCs in the absence of serum. Except for angiotensin II, all the other hypertrophic stimuli used in this study increased the expression of $Ca_v3.2$ and $Ca_v1.2$ channels. B) In the presence of serum, angiotensin II moderately increased*

*the expression of all T-type and Cav1.2 L-type channels, while the other hypertrophic stimuli induced a significant increase of $Ca_v3.2$ and $Ca_v1.2$. β- actin was used as a house-keeping control. Histogram bars represent mean ± SD values from at least 4 independent experiments *Significant differences related to untreated control, P< 0.05.*

Irrespective of the presence of serum, $Ca_v3.2$ mRNA in CMs was induced by 2.5-3-fold by aldosterone and 2.2-2.5-fold by isoprenaline. Isoprenaline also enhanced the expression of $Ca_v1.2$ channels, by nearly 2-fold, in either culturing condition. In comparison, phenylephrine increased moderately the levels of $Ca_v3.2$ and $Ca_v1.2$ mRNA in the absence of serum, and only the expression of $Ca_v3.2$ in the presence of serum. Finally, angiotensin II induced a moderate increase of $Ca_v3.1$, $Ca_v3.2$ and Cav1.2 only in the presence of serum (Figure. 3).

2.4. ER stress mediated by hypertrophic stimuli

Having shown that the hypertrophic stimuli remodel the expression of VGCCs which are relevant for Ca^{2+}-homeostasis mantainance, we next wondered if hypertrophy was linked to the development of ER stress.

Like in the previous experiments, CMs were treated with the hypertrophic stimuli in the presence and absence of serum. The effect of hypertrophic stimuli on the ER homeostasis was monitored by analyzing the levels of transcripts from the UPR genes XBP1, GRP78 and GADD153, with the q-PCR technique.

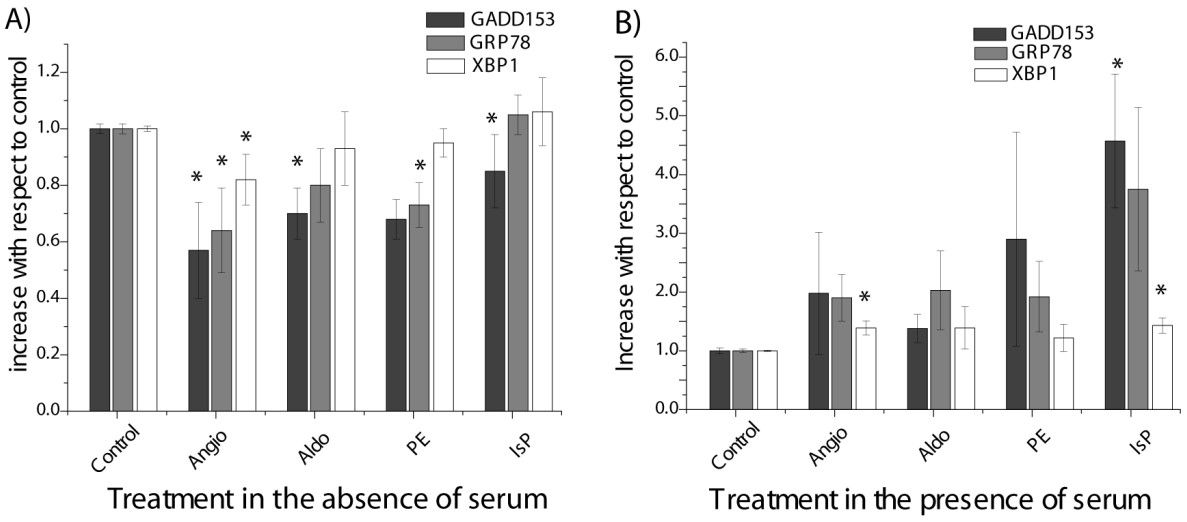

***Figure 4**: UPR regulation by hypertrophic stimuli. It can be seen that the presence of serum enabled the overexpression of UPR markers by hypertrophic stimuli. A) In the absence of serum, the hypertrophic stimuli did not induce an increase in any of the UPR gene expression, but in fact reduced the expression of GRP78 and GADD153. B) In the presence of serum the four hypertrophic stimuli induced the expression of the genes for UPR, with phenylephrine and isoprenaline exerting a stronger effect on GRP78 and GADD153. β-actin was used as a house-keeping control. Histogram bars represent mean ± SD values from at least 4 independent experiments *Significant differences related to untreated control, P< 0.05.*

When the cells were cultured in serum-free media, we observed that none of the hypertrophic stimuli induced a significant upregulation of UPR genes (Figure 4A). On the contrary, the treatment with all the hypertrophic stimuli except isoprenaline showed a down-regulation of the UPR genes GRP78 and GADD153. The presence of serum in the media proved to be determinant for hypertrophic stimuli-mediated ER stress; in this condition, angiotensin II, aldosterone and the adrenergic receptor agonists induced the expression of GRP78 and GADD153 to varying degrees.

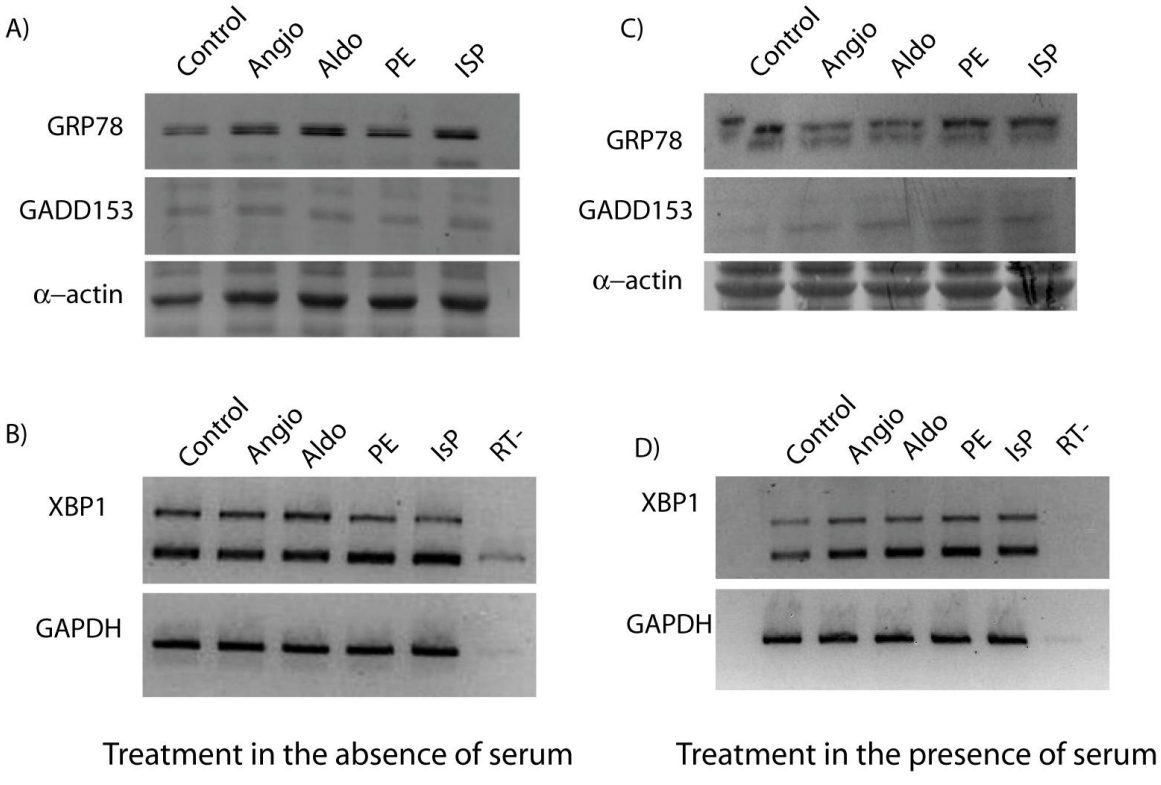

***Figure 5**: Protein expression of UPR markers and XBP1 splicing upon hypertrophic stimuli. A) GRP78 levels were increased by all four hypertrophic stimuli in serum free conditions, whereas GADD153 level was not altered. B) Under serum deprivation, there was no splicing of XBP1 due to any of the hypertrophic stimuli. C) In the presence of serum, angiotensin and aldosterone exerted a reduction of the GRP78 levels, whereas the expression of GADD153 was increased by all four hypertrophic stimuli. D) In the presence of serum all four hypertrophic stimuli induced splicing of XBP1.*

The results were paradoxically different when monitoring the protein levels. Western blot experiments for the UPR markers showed that, in the absence of serum, all four hypertrophic stimuli increased the intensity of the GRP78 band, while the expression of GADD153 remained the same (Figure 5A). On the other hand, the hypertrophic stimuli in the presence of serum increased the expression of GADD153, with angiotensin and aldosterone additionally downregulating GRP78 expression (Figure 5B).
The presence of serum also proved to be determinant for hypertrophy-induced XBP1 splicing: in the absence of serum there was none (Figure 5 B), whereas in the presence of serum the splicing of XBP1 was enhanced by the four hypertrophic stimuli (Figure. 5D).

2.5. The Expression of autophagy related genes is altered by hypertrophic stimuli

It is known that autophagy is activated during ventricular hypertrophy. It has also been reported that autophagy mediates regression of cardiac hypertrophy during unloading[109]. Considering that in CMs cultured in serum-containing medium, the hypertrophic stimuli induced ER stress and upregulated the UPR genes, we set out to examine a putative effect of the same stimuli on the expression of autophagy related genes.

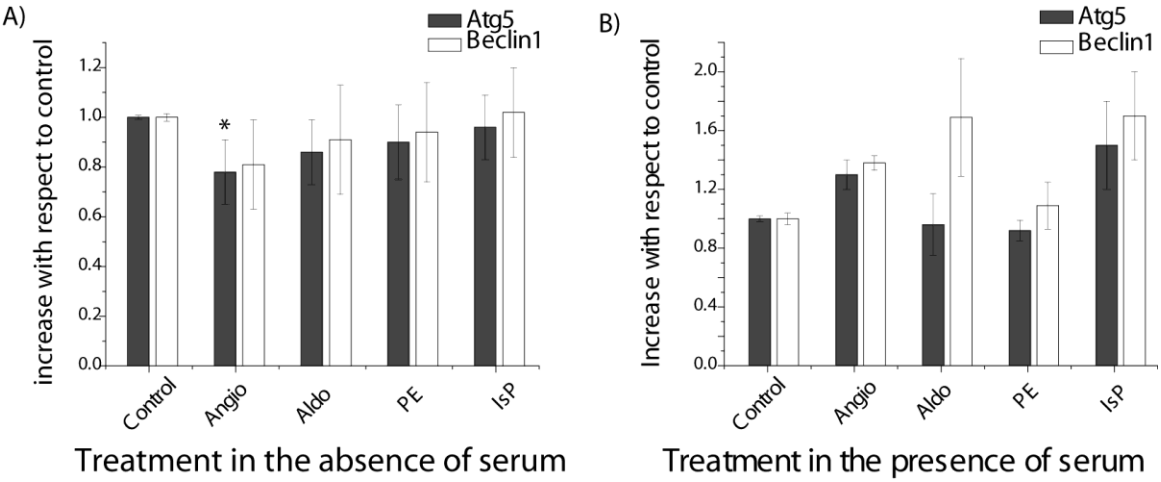

***Figure 6**: Regulation of ATG genes by hypertrophic stimuli. A) In the absence of serum, none of the treatments increased the expression of Beclin1 or Atg5; rather, a trend towards a reduced expression of both Atgs was observed. B) In the presence of serum, a moderate induction of Beclin1 was observed upon treatment with angiotensin II, aldosterone and isoprenaline, as well as a moderate induction of Atg5 by angiotensin II and isoprenaline. Neither Beclin1 nor Atg5 mRNA levels were changed by phenylephrine treatments. β- actin was used as a house-keeping control Histogram bars represent mean ±SD values from at least 4 independent experiments *Significant differences related to untreated control, P< 0.05.*

In the absence of serum, none of the hypertrophic stimuli increased the expression of either Beclin1 or Atg5 (Figure. 6A), but a trend towards a reduced expression could be observed. On the contrary, in the presence of serum (Figure. 6A), all the hypertrophic stimuli except phenylephrine induced a moderate upregulation of Beclin1, and angiotensin II and isoprenaline induced, additionally, a moderate upregulation of Atg5.
We also studied the expression of autophagy-related genes at the protein level. Western blot analysis reflects putative changes in gene induction but also any accompanying post-transcritptional and post-translational modifications.

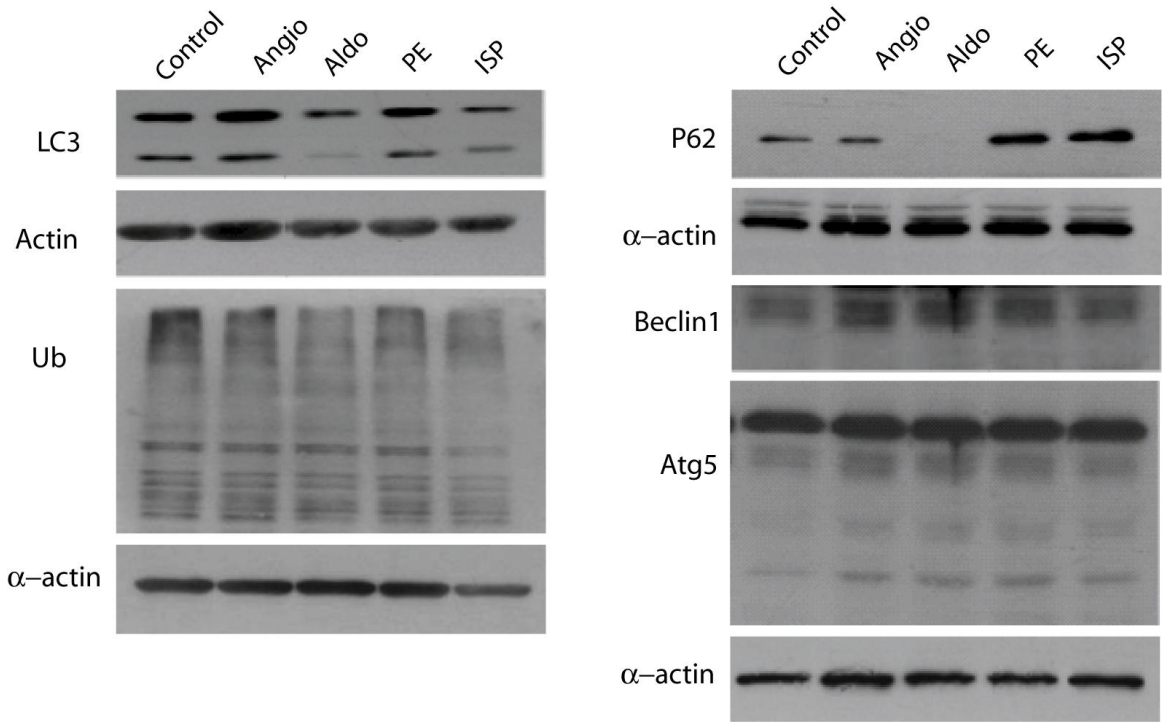

***Figure 7**: Protein expression of Atg-related genes upon hypertrophic stimuli under serum deprivation. The LC3-II ratio was not increased by any drug and, in fact, aldosterone reduced both LC3-I and LC3-II bands. All the stimuli promoted moderate increases of Beclin1, Atg5 and Atg5-Atg12. Aldosterone reduced to a minimum the p62/SQSTM1 band and limited the accumulation of poly-ubiquitinated aggregates. These western blots are representative of at least four independent experiments.*

CMs were treated with the four hypertrophic stimuli in the absence of serum. The western blot analysis revealed a moderate increase of Beclin1 and Atg5 upon treatment with all the hypertrophic stimuli. However, the ratio LC3-II/LC3-I did not increase with any treatment; rather it was reduced by aldosterone and ISP (Figure 7). Aldosterone induced a decrease of the p62/SQSTM1 band, a result that was in line with the reduction of the ubiquitinated protein aggregates. Angiotensin II did not alter the level of p62/SQSTM1, whereas phenylephrine and isoprenaline induced the increase of p62/SQSTM1. Irrespective of the p62/SQSTM1 levels, angiotensin II, phenylephrine, isoprenaline and aldosterone promoted a reduction in ubiquitin aggregates.

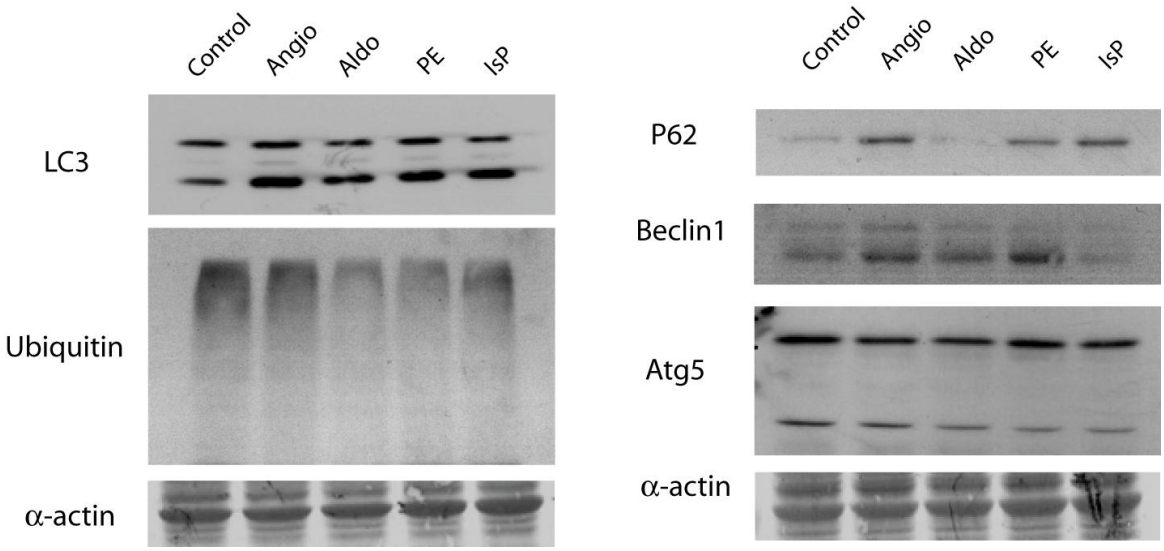

Figure 8*: Protein expression of ATG genes upon hypertrophic stimuli in CMs cultured in full-serum culture conditions. Similar to serum free conditions, aldosterone reduced the P62/SQSTM1 level which was followed by a reduction in ubiquitin aggregates. Beclin1 was increased by angiotensin II, aldosterone and phenylephrine, whereas isoprenaline promoted a decrease in Beclin1. The Atg5 protein level was reduced by aldosterone, phenylephrine and isoprenaline. These western blots are representative of at least four independent experiments.*

The experiments performed in the presence of serum showed a similar p62/SQSTM1 and ubiquitin expression pattern when compared to serum deprived experiments (Figure 8), except that angiotensin II increased the p62/SQSTM1 levels. In these conditions, western blotting using an antibody against Atg5 did not show significant alterations with Atg5-Atg12 complex by any of the treatments, whereas Atg5 was reduced by aldosterone, phenylephrine and isoprenaline. Nonetheless, angiotensin II and phenylephrine were found to increase the level of Beclin1 protein, which was however reduced by isoprenaline. In addition, all four treatments performed in the presence of serum increased the LC3 II/LC3 I ratio. Similar to the serum-deprived conditions, aldosterone in the presence of serum decreased the p62/SQSTM1 level, which was otherwise upregulated by angiotensin II, phenylephrine and isoprenaline. However, the ubiquitin results showed a decrease in the aggregation of high molecular weight proteins by aldosterone and phenyephrine, whereas the levels of these proteins were not altered by angiotensin II and isoprenaline.

2.6. Hypertrophic stimuli increases autophagic flux

In order to further assess the changes in the autophagic flux induced by the hypertrophic stimuli, we transfected the cells with tandem flagged LC3 contructs followed by a 24h treatment with the different hypertrophic stimuli.

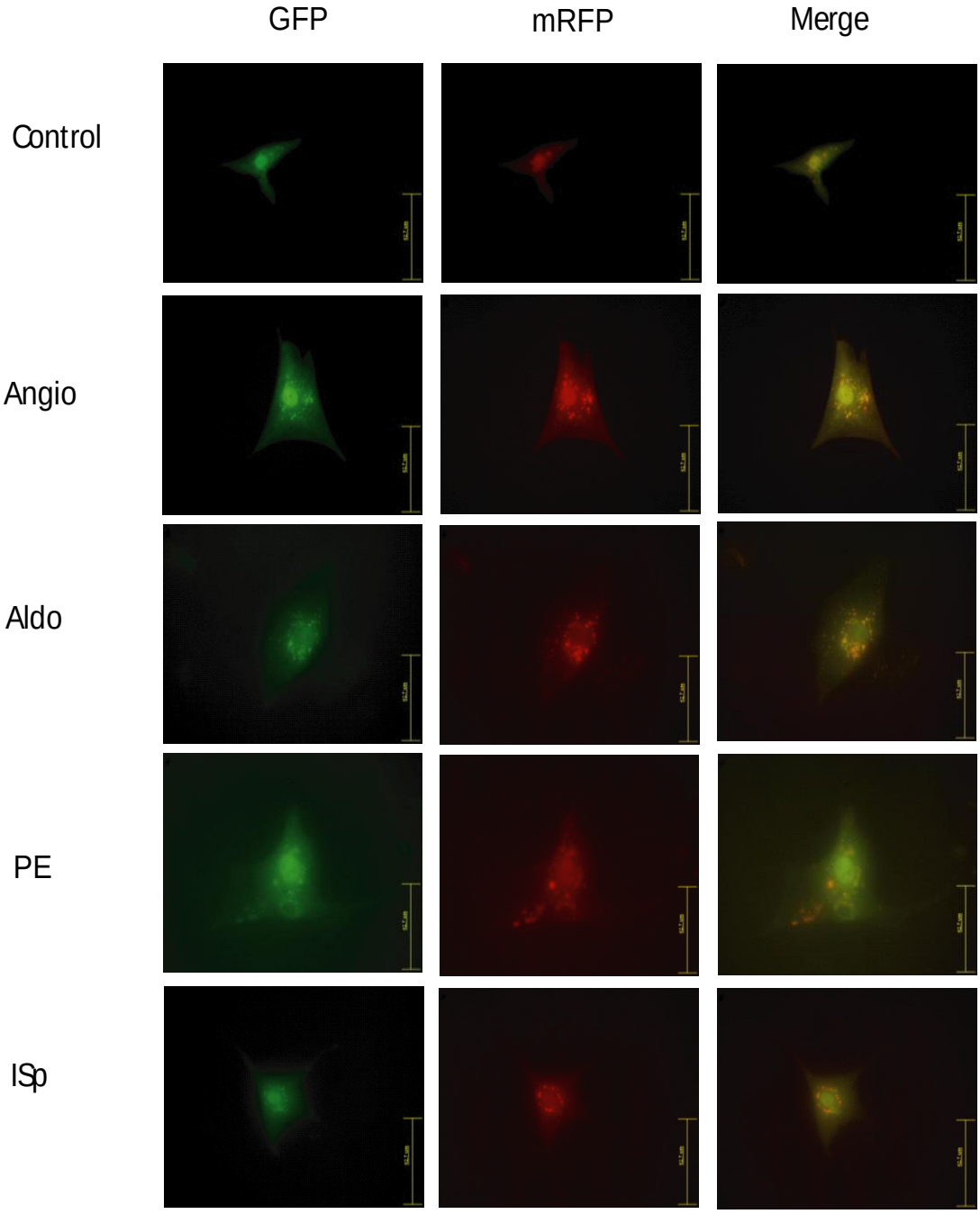

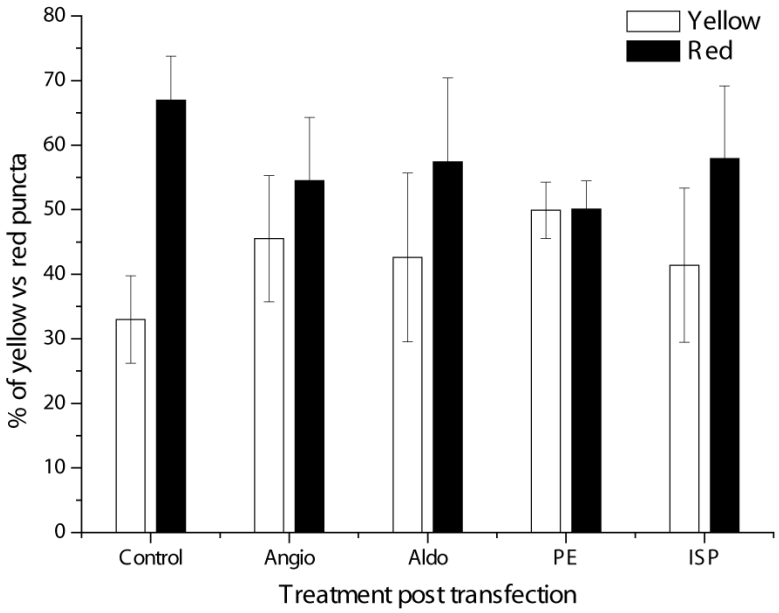

Figure 9*: Autophagic flux accessed by tandem flagged LC3. A) CMs challenged with hypertrophic stimuli displayed an increased ratio of yellow over red puncta. B) The graph shows the percentage of yellow punta over red puncta. Histogram bars represent mean ± SD values from at least 4 independent experiments *Significant differences related to untreated control, P< 0.05.*

We observed that angiotensin II, aldosterone and the adrenergic agonists, phenylephrine and isoprenaline slightly increased the ratio of yellow over red puncta (Figure 9).

3. Discussion

This chapter deals with the involvement of VGCCs in the induction of cardiac hypertrophy. It has long been reported that autophagy is induced during cardic hypertrophy, and we have earlier showed that both L-type and T-type channel blockers de-regulate autophagy in CMs. Thus, this study also intended to elucidate a putative involvement of VGCCs in the induction of autophagy upon hypertrophic stimuli.

Application of the four hypertrophic stimuli increased the cell beating frequency as reported earlier. Lalevee et al. reported that aldosterone accelerated spontaneous cell contractions by inducing the expression of $Ca_v3.2$[268]. They also reported that pharmacological blocking of T-type channels with mibefradil, after aldosterone stimulation, decreased the cell beating frequency. The other three hypertrophic stimuli,

namely angiotensin II, phenylephrine and isoprenaline were also known to increase the frequency of cell beating. An increase in cell beating is associated to an increase of the cytosolic Ca^{2+} oscillations, which can substantially activate calcineurin/NFAT pathway leading to hypertrophic signal[269].

We also found that the four drugs used on the CMs *in vitro* were effective in inducing hypertrophy, which was evident from the altered expression of atrial- and brain-natriuretic peptides. Both of these natriuretic peptides are synthesized in the heart and are essential for cardioprotection. Earlier studies have demonstrated that disruption of proANP gene in mice led to hypertension and hypertrophy[270], and that transgenic overexpression of ANP led to protection against hypertrophic stimuli[271]. However, ANP and BNP are induced upon progression of hypertrophy. Our results with the hypertrophic stimuli showed that three of the drugs namely aldosterone, phenylephrine and isoprenaline induced hypertrophic markers both in the presence or absence of serum, whereas angiotensin II was successful in inducing hypertrophic markers only in the presence of serum.

Taking into account that Ca^{2+} oscillations are responsible for changes in cell beating frequency, and that aldosterone and other stimuli contribute to ventricular arrhythmia, we examined the effect of these drugs in the alterations in gene expression of Ca^{2+} channels isoforms. Under both culture conditions (serum-containing and serum-free), aldosterone, phenylephrine and isoprenaline increased the expression of T-type $Ca_v3.2$ and L-type $Ca_v1.2$ Ca^{2+} channel isoforms. The expression of $Ca_v3.1$ was induced by phenylephrine and isoprenaline under serum free conditions, and by angiotensin and isoprenaline in the presence of serum. β-adrenergic stimulation has previously been reported to increase $Ca_v3.1$ activity in CMs through the activation of protein kinase A[272].

A disruption in Ca^{2+} homeostasis has been reported to be directly responsible for ER stress and cardiac remodeling leading to cardiac hypertrophy[273]. Under such conditions of ER stress, cytoplasmic Ca^{2+} levels increase leading to the regulation of store operated Ca^{2+} entry (SOCE). An increase of cytosolic Ca^{2+}, Ca^{2+} release from the ER and "rebound" SOCE have been suggested to play an important role in the progression of cardiac remodeling and hypertrophy[274].

While the hypertrophic stimuli, in the absence of serum, decreased the levels of UPR transcripts in spite of increasing the expression of GRP78 protein the hypertrophic stimuli, in the presence of serum, unequivocally upregulated the UPR genes, including the splicing of the XBP1 transcription factor. Because serum deprivation is a known

inducer of ER stress by itself, the effect of the hypertrophic stimuli on ER stress was probably masked in this culture condition. The presence of serum implied opposite effects on the regulation of Atg genes as well. Experiments on mouse model of cardiomyopathy by Schlossarek et al. had shown that protein levels of autophagosome markers can be induced without alterations in mRNA levels, indicative of defective autophagosome degradation. However, our western blot results pointed to an induction of autophagy by aldosterone, which was evident from the reduced levels of p62/SQSTM1 and subsequent clearance of ubiquitinated aggregates, irrespective of the presence or absence of serum.

On the other hand, angiotensin II, under serum deprivation, did not induce a change in the p62/SQSTM1 levels, but increased the clearance of poly-ubiquitinated protein aggregates. Similarly, in the presence of serum, although angiotensin II, phenylephrine and isoprenaline induced an increase in the p62/SQSTM1 levels, they also induced a clearance of poly-ubiquitinated aggregates. The linkage between p62/SQSTM1 and autophagic flux is not straightforward: proteotoxicity resulting from the increased expression of misfolded/damaged proteins lead to cardiac proteosome functional insufficiency, which in turn upregulated p62/SQSTM1 and triggered compensatory autophagy[275-276]. Also, pharmacological inhibition of proteosomal activity has been reported to increase the expression of p62/SQSTM1 [277-278]. In addition, Zheng et al have shown that p62/SQSTM1 and macroautophagy are concurrently upregulated in DRC mouse hearts[202]. Apart from that, p62/SQSTM1 has been reported to control its own expression by NRF2 activation regulation[279].

In addition to booster the removal of poly-ubiquitinated proteins, the hypertrophy-inducing drugs except phenylephrine increased the green/yellow over the red puncta in CMs transfected with ptf-LC3 constructs, a result which is compatible with inhibition of the autophagic flux, adding to confusion.

Although, as mentioned earlier, there are a few reports suggesting that autophagy is induced during cardiac hypertrophy, Nakai et al. reported that autophagy is not essential for cardiac hypertrophy induced by various stressors including angiotensin II [159]; they also reported that inhibition of autophagy led to the development of cardiac hypetrophy. Also, Oyabu et al. have recently reported, using a pressure-overload induced mice model, that autophagy is involved in the regression of pressure-overload induced cardiac hypertrophy[264]. Taking our own results and published (contradictory) data together, it is evident that the molecular mechanisms underlying autophagic regulation by cardiac hypertrophy have not been clearly elucidated.

In an attempt to reconcile discrepancies and, as a matter of speculation, we put forward the hypothesis that forms of protein degradation other than macroautophagy, i.e. chaperone-mediated autophagy, and/or the activation of the ubiquitin proteasome system, are involved in the adaptation of CMs to hypertrophic insults. Such compensatory mechanisms would be triggered in response to a decreased autophagic flux during the initial, anabolic phase of hypertrophy.

In conclusion, our data shows that hypertrophy involves the upregulation of both L-type and T-type Ca^{2+} channels, although different stimuli display qualitative and quantitative differences regarding the induction of channel isoforms; it also shows that ER stress is a consequence of all hypertrophic stimuli, although it is masked by culturing the cells under serum deprivation; finally, it is inconclusive regarding the autophagic status of the CMs exposed to hypertrophic insults, irrespective of the culture conditions, as mentioned a few lines above. Nonetheless, the fact that T-type channels, which are expressed during the embryonic stages and dissapear during the neonatal development, reappear under pathological cardiac hypertrophy, strongly encourages the screening of T-type channel blockers to tackle the late-phase remodeling that anticipates heart failure and that is unmistakenly associated with an exacerbated autophagy[280].

Conclusions

Conclusion

1. L-type, but not T-type calcium channel pharmacological blockers, induce the apoptotic death of *in vitro*-cultured neonatal CMs.

2. Both T-type and L-type calcium channel blockers promote a transitory cellular ER stress response, which can be monitored through the upregulation of 3 key actors of the unfolded protein response (UPR).

3. T-type channel, but not L-type channel blockers, induce the splicing of XBP1 into its transcriptionally active form.

4. L-type calcium channel blockers increase the basally strong autophagic flux in CMs, whereas T-type channel blockers exert the opposite effect and inhibit autophagy by preventing the formation of autophagolysosomes.

5. Gene knockdown of the T-type channel isoform $Ca_v3.2$ by the siRNA approach activates the UPR and inhibits the constitutive macroautophagy of CMs, thus mimicking the effects of T-type calcium channel blockers. However, the knockdown of the L-type channel isoform $Ca_v1.2$ mimicks the effects of T-type channel blockers too.

6. The expression of the different voltage-gated calcium channel isoforms is inter-related, such that the silencing of $Ca_v3.1$ is concomitant to the upregulation of $Ca_v3.2$, and the knockdown of both $Ca_v1.2$ and $Ca_v1.3$ channels is linked to the upregulation of both T-type channel isoforms (predominantly $Ca_v3.1$).

7. Serum and glucose deprivation induce ER sress and an Unfolded Protein Response characterized by induction of GRP78 and GADD153 genes. However, when deprived cells are subjected to chronic hypoxia (0.2% O_2 for 18-24h) as an *in vitro* paradigm of chronic ischemia, the expression of GRP78 and GADD153 is reduced, and the splicing of XBP1 is induced. Upon reoxygenation (an *in vitro* paradigm of ischemia/reperfusion) the levels of XB1s return to control values.

8. Serum and glucose deprivation for 24 h deregulate autophagy in CMs in a complex manner: increasing the transcripts for Atg5 and Beclin1 but reducing their protein levels. Chronic hypoxia and reoxygenation attenuate deprivation-induced changes in Atgs expression and, particularly reoxygenation, increase the level of Beclin1 protein above control. Putting together Atg expression and the analysis of the autophagic flux, we conclude that hypoxia increase moderately and reoxygenation increase drastically macroautophagy, which is reduced by deprivation.

9. Serum and glucose deprivation increase the percentage of tunel positive CMs, indicative of apoptosis. Hypoxia protect against deprivation-induced cell death to some extent, whereas reoxygenation increase cell death above deprivation.

10. Serum and glucose deprivation induce the transcription of all analyzed VGCC channel types in CMs, including the three T-type channel isoforms. Hypoxia normalizes the expression of VGCCs to great extent, and reoxygenation does not involve further changes compared to hypoxia.

11. Preconditioning with the T-type channel blocker mibefradil reduces the autophagic flux present in CMs subjected to hypoxia or reoxygenation.

12. Preconditioning with mibefradil increases the death of CMs by hypoxia, but decreases the death of CMs by reoxygenation.

13. Application of four functionally different hypertrophic stimuli enhances the contractility and increases the expression of two hypertrophic markers ANP and BNP in CMs cultured *in vitro*.

14. Specific isoforms of L-type and T-type calcium channel are upregulated in CMs by the four functionally different hypertrophic stimuli, to varying degrees.

15. In the absence of serum in the culture medium, the UPR markers in CMs are decreased by the four hypertrophic stimuli, as serum deprivation is a UPR inducer

by itself. In the presence of serum, the four hypertrophic stimuli upregulate UPR markers to some extent.

16. The different hypertrophic stimuli exert distinct effects on Atg transcripts and proteins, and on p62/SQSTM1 levels. Nevertheless, they all coincide in reducing the autophagic flux from the viewpoint of tandem-fluorescent LC3, while increasing the clearance of poly-ubiquitinated aggregates. We thus conclude that, in the initial stages of hypertrophic insults, the macroautophagy in CMs is reduced. In turn, this feature unleashes compensatory mechanisms in the shape of alternative forms of autophagy and/or augmented proteasomal degradation.

Conclusiones

1. Los bloqueantes farmacológicos de canales de tipo L, pero no los de tipo T, inducen la muerte apoptótica de los cardiomiocitos neonatales cultivados i*n vitro*

2. Los bloqueantes de canales de tipo L y T promueven un estrés de retículo transitorio, que monitorizamos a través de la sobre-regulación de 3 actores clave de la respuesta UPR: la chaperona molecular GRP78, el regulador transcripcional XBP1 y el factor de transcripción GADD153.

3. Los bloqueantes de canals de tipo T, pero no los de tipo L, inducen el procesamiento de XBP1 hasta una forma transcripcionalmente activa.

4. Los bloqueantes de canales de tipo L aumentan el flujo autofágico basal en los cardiomiocitos, mientras que los bloqueantes de de canales de tipo T ejercen el efecto contrario e inhiben la autofagia previniendo la formación de autofagolisosomas.

5. El silencimiento génico de la isoforma $Ca_v3.2$ mediante la aproximación del siRNA activa la UPR e inhibe la macroautofagia constitutiva de los cardiomiocitos, mimetizando así los efectos de los bloqueantes de canales de tipo T. No obstante, el silenciamiento de la isoforma $Ca_v1.2$ también mimetiza los efectos de los bloqueantes de canales de tipo T.

6. La expression de los distintos tipos de canals de calcio voltaje-dependientes está inter-relacionada, de modo que el silenciamiento de $Ca_v3.1$ es concomitante a la sobre-regulación de $Ca_v3.2$, y el silenciamiento de $Ca_v1.2$ y $Ca_v1.3$ se asocia con la sobre-regulación de ambas isoformas de canales de tipo T (aunque predominantemente de $Ca_v3.1$).

7. La deprivación de suero y glucose induce estrés de retículo y una respuesta UPR caracterizada por la inducción de GRP78 y GADD153. No obstante, cuando las células deprivadas se someten a hipoxia crónica (0.2% O_2 durante 18-24h) como paradigm *in vitro* de isquemia crónica, se reduce la expresión de GRP78 y GADD153 y aumenta el procesamiento postranscripcional de XBP1. Cuando los cardiomiocitos

son reoxigenados (un paradigm *in vitro* de la isquemia/reperfusión) los niveles de XBP1s se reducen hasta los valores control.

8. La deprivación de suero y glucosa durante 24 h desregula la autofagia en los cardiomiocitos de una forma compleja: incrementa el mARN para Atg5 y Beclin1 y, no obstante, reduce los respectivos niveles de proteína. La hypoxia crónica y la reoxigenación atenuan los cambios en la expresión de Atgs inducidos por la deprivación y, particularmente la reoxigenación, incrementó los niveles de Beclin1 proteína por encima de los niveles control. Al considerar la expression de Atg y el análisis del flujo autofágico, concluímos que la hypoxia incrementa moderadamente y la reoxigenación drásticamente la macroautofagia inhibida por la deprivación.

9. Serum and glucose deprivation increased the percentage of tunel positive cardiomyocytes, indicative of apoptosis. Hypoxia protected against deprivation-induced cell death to some extent, whereas reoxygenation increased cell death above deprivation.

10. La deprivación de suero y glucosa induce la transcripción de todos los tipos de canales de calcio voltaje-dependientes analizados, incluyendo las 3 isoformas de canales de tipo T. La hipoxia tiende a normalizar la expresión de los canales, y la reoxigenación no implica cambios respecto a la hipoxia.

11. El precondicionamiento con el bloqueante de canales de tipo T mibefradil reduce el flujo autofágico presente en cardiomiocitos sometidos a hipoxia o reoxigenación.

12. El precondicionamiento con mibefradil incrementa la muerte de los cardiomiocitos debida a la hipoxia, pero redúce la muerte de los cardiomiocitos debida a la reoxigenación.

13. La aplicación de 4 estímulos hipertróficos funcionalmente distintos aumenta la contractilidad e incrementa la expresión de los marcadores de hipertrofia ANP and BNP en cardiomiocitos.

14. Los 4 estímulos hipertróficos sobre-regulan la expresión de isoformas específicas de canales de tipo L y T *in vitro*, en grado variable.

15. En la ausencia de suero en el medio de cultivo los estímulos hipertróficos disminuyen los marcadores de UPR en los cardiomiocitos, debido a que la deprivación de suero es un inductor de UPR por si misma. En la presencia de suero los 4 estímulos hipertróficos sobreregularon los marcadores UPR en grado variable.

16. Los distintos estímulos hipertróficos ejercen efectos diferenciales sobre los tránscritos y las proteínas de Atg, y sobre los niveles de proteína p62, aunque todos ellos reducen el flujo autofágico medido a través de tf-LC3, mientras que aumentan la degradación de los agregados poli-ubicuitinizados. Por ello concluímos que, en los estadios iniciales del estímulo hipertrófico, en los que predominan las vías anabólicas, se reduce de forma concomitante la macroautofagia; no obstante, ello desencadena mecanismos compensatorios a través de la activación de formas alternativas de autofagia y/o de un aumento de la degradación proteasomal.

References

1 Roger VL, V. L. *et al.* Heart Disease and Stroke Statistics—2012 Update: A Report From the American Heart Association. *Circulation* **125**, e2-e220 (2012).

2 Seta, Y., Shan, K., Bozkurt, B., Oral, H. & Mann, D. L. Basic mechanisms in heart failure: the cytokine hypothesis. *Journal of cardiac failure* **2**, 243-249 (1996).

3 Ringer, S. A third contribution regarding the Influence of the Inorganic Constituents of the Blood on the Ventricular Contraction. *The Journal of Physiology* **4**, 222-225 (1883).

4 Lompré, A.-M. *et al.* Ca2+ Cycling and New Therapeutic Approaches for Heart Failure. *Circulation* **121**, 822-830 (2010).

5 Berridge, M. J. The endoplasmic reticulum : a multifunctional signaling organelle. **32**, 235-249, doi:10.1016/s0143-4160(02)00182-3 (2002).

6 Widmaier, E. P. & Strang, K. T. *H u m a n P h y s i o l o g y*. (2004).

7 Catterall, W. a. Voltage-gated calcium channels. *Cold Spring Harbor perspectives in biology* **3**, a003947-a003947, doi:10.1101/cshperspect.a003947 (2011).

8 Tanabe, T. *et al.* Primary structure of the receptor for calcium channel blockers from skeletal muscle. *Nature* **328**, 313-318 (1987).

9 Mikami, A. *et al.* Primary structure and functional expression of the cardiac dihydropyridine-sensitive calcium channel. *Nature* **340**, 230-233 (1989).

10 Mori, Y. *et al.* Primary structure and functional expression from complementary DNA of a brain calcium channel. *Nature* **350**, 398-402 (1991).

11 Williams, M. E. *et al.* Structure and functional expression of α1, α2, and β subunits of a novel human neuronal calcium channel subtype. *Neuron* **8**, 71-84, doi:http://dx.doi.org/10.1016/0896-6273(92)90109-Q (1992).

12 Perez-Reyes, E. *et al.* Molecular characterization of a neuronal low-voltage-activated T-type calcium channel. *Nature* **391**, 896-900 (1998).

13 Cribbs, L. L. *et al.* Cloning and Characterization of α1H From Human Heart, a Member of the T-Type Ca2+ Channel Gene Family. *Circulation Research* **83**, 103-109 (1998).

14 Lee, J.-H., Gomora, J. C., Cribbs, L. L. & Perez-Reyes, E. Nickel Block of Three Cloned T-Type Calcium Channels: Low Concentrations Selectively Block α1H. *Biophysical Journal* **77**, 3034-3042, doi:http://dx.doi.org/10.1016/S0006-3495(99)77134-1 (1999).

15 Karess, R. *et al.* Structure of a complex between a voltage-gated calcium channel b -subunit and an a -subunit domain. **429**, 671-675, doi:10.1038/nature02590.1. (2004).

16 Takahashi, M., Seagar, M. J., Jones, J. F., Reber, B. F. & Catterall, W. A. Subunit structure of dihydropyridine-sensitive calcium channels from skeletal muscle. *Proceedings of the National Academy of Sciences* **84**, 5478-5482 (1987).

17 Birnbaumer, L. *et al.* The naming of voltage-gated calcium channels. *Neuron* **13**, 505-506, doi:http://dx.doi.org/10.1016/0896-6273(94)90021-3 (1994).

18 Dolphin, A. C. The α(2)δ subunits of voltage-gated calcium channels. *Biochimica et biophysica acta*, doi:10.1016/j.bbamem.2012.11.019 (2012).

19 Bauer, C. S., Tran-Van-Minh, A., Kadurin, I. & Dolphin, A. C. A new look at calcium channel α2δ subunits. *Current Opinion in Neurobiology* **20**, 563-571, doi:10.1016/j.conb.2010.05.007 (2010).

20 Dolphin, A. C. Calcium channel diversity: multiple roles of calcium channel subunits. *Current Opinion in Neurobiology* **19**, 237-244, doi:10.1016/j.conb.2009.06.006 (2009).

21 Endo, M. *et al.* Classification and Function of Voltage-Gated Calcium Channels.

22 Bertolino, M. & Llinas, R. R. The Central Role of Voltage-Activated and Receptor-Operated Calcium Channels in Neuronal Cells. *Annual Review of Pharmacology and Toxicology* **32**, 399-421, doi:10.1146/annurev.pa.32.040192.002151 (1992).

23 Stock, L., Souza, C. & Treptow, W. Structural Basis for Activation of Voltage-Gated Cation Channels. *Biochemistry* **52**, 1501-1513, doi:10.1021/bi3013017 (2013).

24 Weiss, N. & Zamponi, G. in *Calcium Signaling* Vol. 740 *Advances in Experimental Medicine and Biology* (ed Md Shahidul Islam) Ch. 33, 759-775 (Springer Netherlands, 2012).

25 Catterall, W. A., Perez-reyes, E., Snutch, T. P. & Striessnig, J. International Union of Pharmacology . XLVIII . Nomenclature and Structure-Function Relationships of Voltage-Gated Calcium Channels. **57**, 411-425, doi:10.1124/pr.57.4.5.units (2005).

26 Miljanich, G. P. & Ramachandran, J. Antagonists of Neuronal Calcium Channels: Structure, Function, and Therapeutic Implications. *Annual Review of Pharmacology and Toxicology* **35**, 707-734, doi:10.1146/annurev.pa.35.040195.003423 (1995).

27 Chuang, R. S. I., Jaffe, H., Cribbs, L., Perez-Reyes, E. & Swartz, K. J. Inhibition of T-type voltage-gated calcium channels by a new scorpion toxin. *Nat Neurosci* **1**, 668-674 (1998).

28 Sidach, S. S. & Mintz, I. M. Kurtoxin, A Gating Modifier of Neuronal High- and Low-Threshold Ca Channels. *The Journal of Neuroscience* **22**, 2023-2034 (2002).

29 Perez-Reyes, E. Molecular Physiology of Low-Voltage-Activated T-type Calcium Channels. *Physiological reviews* **83**, 117-161 (2003).

30 Bénitah, J. P. *et al.* Voltage-gated Ca2+ currents in the human pathophysiologic heart: a review. *Basic research in cardiology* **97 Suppl 1**, I11-18 (2002).

31 Bers, D. M. coupling. **415** (2002).

32 Bodi, I., Mikala, G., Koch, S. E., Akhter, S. A. & Schwartz, A. The L-type calcium channel in the heart : the beat goes on. **115**, doi:10.1172/jci27167.3306 (2005).

33 Seisenberger, C. *et al.* Functional Embryonic Cardiomyocytes after Disruption of the L-type α1C (Ca v 1.2) Calcium Channel Gene in the Mouse. *Journal of Biological Chemistry* **275**, 39193-39199 (2000).

34 Schroder, E., Byse, M. & Satin, J. L-Type Calcium Channel C Terminus Autoregulates Transcription. *Circulation Research* **104**, 1373-1381 (2009).

35 Benitah, J.-P., Alvarez, J. L. & Gómez, A. M. L-type Ca(2+) current in ventricular cardiomyocytes. *Journal of molecular and cellular cardiology* **48**, 26-36, doi:10.1016/j.yjmcc.2009.07.026 (2010).

36 Lipscombe, D., Helton, T. D. & Xu, W. L-Type Calcium Channels: The Low Down. *Journal of Neurophysiology* **92**, 2633-2641 (2004).

37 Xu, X. P. & Best, P. M. Increase in T-type calcium current in atrial myocytes from adult rats with growth hormone-secreting tumors. *Proceedings of the National Academy of Sciences* **87**, 4655-4659 (1990).

38 Yeoman, M. S., Brezden, B. L. & Benjamin, P. R. LVA and HVA Ca2+ Currents in Ventricular Muscle Cells of the Lymnaea Heart. *Journal of Neurophysiology* **82**, 2428-2440 (1999).

39 Hirano, Y., Fozzard, H. A. & January, C. T. Characteristics of L- and T-type Ca2+ currents in canine cardiac Purkinje cells. *American Journal of Physiology - Heart and Circulatory Physiology* **256**, H1478-H1492 (1989).

40 Bogdanov, K. Y., Ziman, B. D., Spurgeon, H. A. & Lakatta, E. G. L- andT-type Calcium Currents Differ in Finch and Rat Ventricular Cardiomyocytes. *Journal of Molecular and Cellular Cardiology* **27**, 2581-2593, doi:http://dx.doi.org/10.1006/jmcc.1995.0045 (1995).

41 Ono, K. & Iijima, T. Cardiac T-type Ca2+ channels in the heart. *Journal of Molecular and Cellular Cardiology* **48**, 65-70, doi:http://dx.doi.org/10.1016/j.yjmcc.2009.08.021 (2010).

42 Jurado, L. A., Chockalingam, P. S. & Jarrett, H. W. Apocalmodulin. *Physiological reviews* **79**, 661-682 (1999).

43 Erickson, J. R., He, B. J., Grumbach, I. M. & Anderson, M. E. CaMKII in the cardiovascular system: sensing redox states. *Physiological reviews* **91**, 889-915, doi:10.1152/physrev.00018.2010 (2011).

44 Swulius, M. T. & Waxham, M. N. Ca2+/Calmodulin-dependent Protein Kinases. *Cell. Mol. Life Sci.* **65**, 2637-2657, doi:10.1007/s00018-008-8086-2 (2008).

45 Barry, S. P. & Townsend, P. a. What causes a broken heart--molecular insights into heart failure. *International review of cell and molecular biology* **284**, 113-179, doi:10.1016/s1937-6448(10)84003-1 (2010).

46 Hudmon, A. *et al.* CaMKII tethers to L-type Ca2+ channels, establishing a local and dedicated integrator of Ca2+ signals for facilitation. *The Journal of cell biology* **171**, 537-547 (2005).

47 Pitt, G. S. Calmodulin and CaMKII as molecular switches for cardiac ion channels. *Cardiovascular research* **73**, 641-647, doi:10.1016/j.cardiores.2006.10.019 (2007).

48 Wu, Y. *et al.* Calmodulin Kinase II and Arrhythmias in a Mouse Model of Cardiac Hypertrophy. *Circulation* **106**, 1288-1293 (2002).

49 Cribbs, L. L. *et al.* Identification of the T-Type Calcium Channel (CaV3.1d) in Developing Mouse Heart. *Circulation Research* **88**, 403-407 (2001).

50 Izumi, T. *et al.* Reinduction of T-Type Calcium Channels by Endothelin-1 in Failing Hearts In Vivo and in Adult Rat Ventricular Myocytes In Vitro. *Circulation* **108**, 2530-2535 (2003).

51 Welsby, P. J. *et al.* A Mechanism for the Direct Regulation of T-Type Calcium Channels by Ca2+/Calmodulin-Dependent Kinase II. *The Journal of Neuroscience* **23**, 10116-10121 (2003).

52 Bers, D. M. & Grandi, E. Calcium/Calmodulin-dependent Kinase II Regulation of Cardiac Ion Channels. *Journal of cardiovascular pharmacology* **54** (2009).

53 Kirchhefer, U., Schmitz, W., Scholz, H. & Neumann, J. Activity of cAMP-dependent protein kinase and Ca2+/calmodulin-dependent protein kinase in failing and nonfailing human hearts. *Cardiovascular Research* **42**, 254-261 (1999).

54 MacDonnell, S. M. *et al.* CaMKII Negatively Regulates Calcineurin–NFAT Signaling in Cardiac Myocytes. *Circulation Research* **105**, 316-325 (2009).

55 Netticadan, T., Temsah, R. M., Kawabata, K. & Dhalla, N. S. Sarcoplasmic Reticulum Ca2+/Calmodulin-Dependent Protein Kinase Is Altered in Heart Failure. *Circulation Research* **86**, 596-605 (2000).

56 Passier, R. *et al.* CaM kinase signaling induces cardiac hypertrophy and activates the MEF2 transcription factor in vivo. *The Journal of Clinical Investigation* **105**, 1395-1406, doi:10.1172/jci8551 (2000).

57 Katz, a. M. Calcium channel diversity in the cardiovascular system. *Journal of the American College of Cardiology* **28**, 522-529, doi:10.1016/0735-1097(96)00170-2 (1996).

58 Meyer, T., Hanson, P. I., Stryer, L. & Schulman, H. Calmodulin Trapping by Calcium-Calmodulin-Dependent Protein Kinase. *Science* **256**, 1199-1202 (1992).

59 Wehrens, X. H. T., Lehnart, S. E., Reiken, S. R. & Marks, A. R. Ca2+/Calmodulin-Dependent Protein Kinase II Phosphorylation Regulates the Cardiac Ryanodine Receptor. *Circulation Research* **94**, e61-e70 (2004).

60 Wehrens, X. H. T. & Marks, A. R. Novel therapeutic approaches for heart failure by normalizing calcium cycling. *Nat Rev Drug Discov* **3**, 565-574 (2004).

61 De Koninck, P. & Schulman, H. Sensitivity of CaM Kinase II to the Frequency of Ca2+ Oscillations. *Science* **279**, 227-230 (1998).

62 Li, N. *et al.* Inhibition of CaMKII Phosphorylation of RyR2 Prevents Induction of Atrial Fibrillation in FKBP12.6 Knockout Mice. *Circulation Research* **110**, 465-470 (2012).

63 Kushnir, A. & Marks, A. R. in *Advances in Pharmacology* Vol. Volume 59 (ed M. Vanhoutte Paul) 1-30 (Academic Press, 2010).

64 Rumi-Masante, J. *et al.* Structural Basis for Activation of Calcineurin by Calmodulin. *Journal of Molecular Biology* **415**, 307-317, doi:http://dx.doi.org/10.1016/j.jmb.2011.11.008 (2012).

65 Rusnak, F. & Mertz, P. Calcineurin: form and function. *Physiological reviews* **80**, 1483-1521 (2000).

66 Molkentin, J. D. *et al.* A Calcineurin-Dependent Transcriptional Pathway for Cardiac Hypertrophy. *Cell* **93**, 215-228, doi:http://dx.doi.org/10.1016/S0092-8674(00)81573-1 (1998).

67 Diedrichs, H., Chi, M., Boelck, B., Mehlhorm, U. & Schwinger, R. H. G. Increased regulatory activity of the calcineurin/NFAT pathway in human heart failure. *European Journal of Heart Failure* **6**, 3-9 (2004).

68 Dolmetsch, R. E., Lewis, R. S., Goodnow, C. C. & Healy, J. I. Differential activation of transcription factors induced by Ca2+ response amplitude and duration. *Nature* **386**, 855-858 (1997).

69 Graef, I. A. *et al.* L-type calcium channels and GSK-3 regulate the activity of NF-ATc4 in hippocampal neurons. *Nature* **401**, 703-708 (1999).

70 Tandan, S. *et al.* Physical and Functional Interaction Between Calcineurin and the Cardiac L-Type Ca2+ Channel. *Circulation Research* **105**, 51-60 (2009).

71 Wang, Z., Kutschke, W., Richardson, K. E., Karimi, M. & Hill, J. A. Electrical Remodeling in Pressure-Overload Cardiac Hypertrophy: Role of Calcineurin. *Circulation* **104**, 1657-1663 (2001).

72 Muth, J. N., Bodi, I., Lewis, W., Varadi, G. & Schwartz, A. A Ca2+-Dependent Transgenic Model of Cardiac Hypertrophy : A Role for Protein Kinase Cα. *Circulation* **103**, 140-147 (2001).

73 Semsarian, C. *et al.* The L-type calcium channel inhibitor diltiazem prevents cardiomyopathy in a mouse model. *The Journal of Clinical Investigation* **109**, 1013-1020, doi:10.1172/jci14677 (2002).

74 Klingbeil, A. U., Schneider, M., Martus, P., Messerli, F. H. & Schmieder, R. E. A meta-analysis of the effects of treatment on left ventricular mass in essential hypertension. *The American Journal of Medicine* **115**, 41-46, doi:http://dx.doi.org/10.1016/S0002-9343(03)00158-X (2003).

75 Zou, Y. *et al.* <B>Continuous Blockade of L-Type Ca²⁺ Channels Suppresses Activation of Calcineurin and Development of Cardiac Hypertrophy in Spontaneously Hypertensive Rats</B>. *Hypertension Research* **25**, 117-124 (2002).

76 Jaleel, N. *et al.* Ca2+ Influx Through T- and L-Type Ca2+ Channels Have Different Effects on Myocyte Contractility and Induce Unique Cardiac Phenotypes. *Circulation Research* **103**, 1109-1119 (2008).

77 Markandeya, Y. S., Fahey, J. M., Pluteanu, F., Cribbs, L. L. & Balijepalli, R. C. Caveolin-3 Regulates Protein Kinase A Modulation of the CaV3.2 (α1H) T-type Ca2+ Channels. *Journal of Biological Chemistry* **286**, 2433-2444 (2011).

78 Chiang, C.-S. *et al.* The Ca(v)3.2 T-type Ca(2+) channel is required for pressure overload-induced cardiac hypertrophy in mice. *Circulation research* **104**, 522-530, doi:10.1161/circresaha.108.184051 (2009).

79 Nakayama, H. *et al.* α1G-dependent T-type Ca2+ current antagonizes cardiac hypertrophy through a NOS3-dependent mechanism in mice. *The Journal of Clinical Investigation* **119**, 3787-3796, doi:10.1172/jci39724 (2009).

80 Heineke, J. & Ritter, O. Cardiomyocyte calcineurin signaling in subcellular domains: from the sarcolemma to the nucleus and beyond. *Journal of molecular and cellular cardiology* **52**, 62-73, doi:10.1016/j.yjmcc.2011.10.018 (2012).

81 Bravo, R. *et al.* in *International review of cell and molecular biology* Vol. Volume 301 (ed W. Jeon Kwang) 215-290 (Academic Press, 2013).

82 Coe, H. & Michalak, M. Calcium binding chaperones of the endoplasmic reticulum. *General physiology and biophysics* **28 Spec No Focus**, F96-F103 (2009).

83 Marks, A. R. Ryanodine Receptors/Calcium Release channels in Heart Failure and Sudden Cardiac Death. *Journal of Molecular and Cellular Cardiology* **33**, 615-624, doi:http://dx.doi.org/10.1006/jmcc.2000.1343 (2001).

84 Zalk, R., Lehnart, S. E. & Marks, A. R. Modulation of the Ryanodine Receptor and Intracellular Calcium. *Annual Review of Biochemistry* **76**, 367-385, doi:10.1146/annurev.biochem.76.053105.094237 (2007).

85 Tovey, S. C. *et al.* Regulation of Inositol 1,4,5-Trisphosphate Receptors by cAMP Independent of cAMP-dependent Protein Kinase. *Journal of Biological Chemistry* **285**, 12979-12989 (2010).

86 Liu, C. Y., Wong, H. N., Schauerte, J. A. & Kaufman, R. J. The Protein Kinase/Endoribonuclease IRE1α That Signals the Unfolded Protein Response Has a Luminal N-terminal Ligand-independent Dimerization Domain. *Journal of Biological Chemistry* **277**, 18346-18356 (2002).

87 Toth, A. *et al.* Endoplasmic reticulum stress as a novel therapeutic target in heart diseases. *Cardiovascular & hematological disorders drug targets* **7**, 205-218 (2007).

88 Bertolotti, A., Zhang, Y., Hendershot, L. M., Harding, H. P. & Ron, D. Dynamic interaction of BiP and ER stress transducers in the unfolded-protein response. *Nat Cell Biol* **2**, 326-332 (2000).

89 Harding, H. P., Zhang, Y. & Ron, D. Protein translation and folding are coupled by an endoplasmic-reticulum-resident kinase. *Nature* **397**, 271-274 (1999).

90 Harding, H. P. *et al.* An Integrated Stress Response Regulates Amino Acid Metabolism and Resistance to Oxidative Stress. *Molecular cell* **11**, 619-633, doi:http://dx.doi.org/10.1016/S1097-2765(03)00105-9 (2003).

91 Yoshida, H., Matsui, T., Yamamoto, A., Okada, T. & Mori, K. XBP1 mRNA Is Induced by ATF6 and Spliced by IRE1 in Response to ER Stress to Produce a Highly Active Transcription Factor. *Cell* **107**, 881-891, doi:http://dx.doi.org/10.1016/S0092-8674(01)00611-0 (2001).

92 Shen, J., Chen, X., Hendershot, L. & Prywes, R. ER Stress Regulation of ATF6 Localization by Dissociation of BiP/GRP78 Binding and Unmasking of Golgi

Localization Signals. *Developmental Cell* **3**, 99-111, doi:http://dx.doi.org/10.1016/S1534-5807(02)00203-4 (2002).

93 Lee, A.-H., Iwakoshi, N. N. & Glimcher, L. H. XBP-1 Regulates a Subset of Endoplasmic Reticulum Resident Chaperone Genes in the Unfolded Protein Response. *Molecular and cellular biology* **23**, 7448-7459 (2003).

94 Nadanaka, S., Okada, T., Yoshida, H. & Mori, K. Role of Disulfide Bridges Formed in the Luminal Domain of ATF6 in Sensing Endoplasmic Reticulum Stress. *Molecular and cellular biology* **27**, 1027-1043 (2007).

95 Nickson, P., Toth, A. & Erhardt, P. PUMA is critical for neonatal cardiomyocyte apoptosis induced by endoplasmic reticulum stress. *Cardiovascular Research* **73**, 48-56 (2007).

96 Toth, A. *et al.* Targeted deletion of Puma attenuates cardiomyocyte death and improves cardiac function during ischemia-reperfusion. *American Journal of Physiology - Heart and Circulatory Physiology* **291**, H52-H60 (2006).

97 Okada, K.-i. *et al.* Prolonged Endoplasmic Reticulum Stress in Hypertrophic and Failing Heart After Aortic Constriction: Possible Contribution of Endoplasmic Reticulum Stress to Cardiac Myocyte Apoptosis. *Circulation* **110**, 705-712 (2004).

98 Jill A. Barnes. Vol. 4 (ed Ida W. Smoak) 250-258 (Cell stress & Chaperones, 1999).

99 Mao, C., Tai, W.-C., Bai, Y., Poizat, C. & Lee, A. S. In Vivo Regulation of Grp78/BiP Transcription in the Embryonic Heart: ROLE OF THE ENDOPLASMIC RETICULUM STRESS RESPONSE ELEMENT AND GATA-4. *Journal of Biological Chemistry* **281**, 8877-8887 (2006).

100 Masaki, T., Yoshida, M. & Noguchi, S. Targeted Disruption of CRE-Binding Factor TREB5 Gene Leads to Cellular Necrosis in Cardiac Myocytes at the Embryonic Stage. *Biochemical and biophysical research communications* **261**, 350-356, doi:http://dx.doi.org/10.1006/bbrc.1999.0972 (1999).

101 Harpster, M. *et al.* Earliest changes in the left ventricular transcriptome post-myocardial infarction. *Mamm Genome* **17**, 701-715, doi:10.1007/s00335-005-0120-1 (2006).

102 Martindale, J. J. *et al.* Endoplasmic Reticulum Stress Gene Induction and Protection From Ischemia/Reperfusion Injury in the Hearts of Transgenic Mice With a Tamoxifen-Regulated Form of ATF6. *Circulation Research* **98**, 1186-1193 (2006).

103 Glembotski, C. C. Endoplasmic Reticulum Stress in the Heart. *Circulation Research* **101**, 975-984 (2007).

104 Xie, Z. & Klionsky, D. J. Autophagosome formation: core machinery and adaptations. *Nat Cell Biol* **9**, 1102-1109 (2007).

105 Mizushima, N., Levine, B., Cuervo, A. M. & Klionsky, D. J. Autophagy fights disease through cellular self-digestion. *Nature* **451**, 1069-1075 (2008).

106 Hardie, D. G. AMP-activated protein kinase—an energy sensor that regulates all aspects of cell function. *Genes & development* **25**, 1895-1908 (2011).

107 Yang, Z. & Klionsky, D. J. Mammalian autophagy: core molecular machinery and signaling regulation. *Current opinion in cell biology* **22**, 124-131, doi:http://dx.doi.org/10.1016/j.ceb.2009.11.014 (2010).

108 Mizushima, N. & Komatsu, M. Autophagy: Renovation of Cells and Tissues. *Cell* **147**, 728-741, doi:http://dx.doi.org/10.1016/j.cell.2011.10.026 (2011).

109 Hariharan, N. *et al.* Autophagy plays an essential role in mediating regression of hypertrophy during unloading of the heart. *PLoS ONE* **8**, e51632-e51632, doi:10.1371/journal.pone.0051632 (2013).

110 He, C. & Klionsky, D. J. Regulation Mechanisms and Signaling Pathways of Autophagy. *Annual Review of Genetics* **43**, 67-93, doi:10.1146/annurev-genet-102808-114910 (2009).

111 Johansen, T. L. a. T. Aggrephagy: Selective Disposal of Protein Aggregates by Macroautophagy. *International Journal of Cell Biology* **2012**, 21 doi: doi:10.1155/2012/736905 (2012).

112 Shen, H.-M. & Codogno, P. Autophagic cell death: Loch Ness monster or endangered species? *Autophagy* **7**, 457-465 (2011).

113 Burman, C. & Ktistakis, N. T. Regulation of autophagy by phosphatidylinositol 3-phosphate. *FEBS letters* **584**, 1302-1312, doi:http://dx.doi.org/10.1016/j.febslet.2010.01.011 (2010).

114 Shintani, T. *et al.* Apg10p, a novel protein-conjugating enzyme essential for autophagy in yeast. *EMBO J* **18**, 5234-5241 (1999).

115 Mizushima, N. *et al.* Dissection of Autophagosome Formation Using Apg5-Deficient Mouse Embryonic Stem Cells. *The Journal of cell biology* **152**, 657-668 (2001).

116 Rotter, D. & Rothermel, B. a. Targets, trafficking, and timing of cardiac autophagy. *Pharmacological research : the official journal of the Italian Pharmacological Society* **66**, 494-504, doi:10.1016/j.phrs.2012.10.001 (2012).

117 Gustafsson, A. B. & Gottlieb, R. a. Recycle or die: the role of autophagy in cardioprotection. *Journal of molecular and cellular cardiology* **44**, 654-661, doi:10.1016/j.yjmcc.2008.01.010 (2008).

118 Jung, C. H. *et al.* ULK-Atg13-FIP200 Complexes Mediate mTOR Signaling to the Autophagy Machinery. *Molecular Biology of the Cell* **20**, 1992-2003 (2009).

119 Han, Jung M. *et al.* Leucyl-tRNA Synthetase Is an Intracellular Leucine Sensor for the mTORC1-Signaling Pathway. *Cell* **149**, 410-424, doi:http://dx.doi.org/10.1016/j.cell.2012.02.044 (2012).

120 Fayard, E., Xue, G., Parcellier, A., Bozulic, L. & Hemmings, B. in *Phosphoinositide 3-kinase in Health and Disease* Vol. 346 *Current Topics in Microbiology and Immunology* eds Christian Rommel, Bart Vanhaesebroeck, & Peter K. Vogt) Ch. 58, 31-56 (Springer Berlin Heidelberg, 2011).

121 Johansen, T. & Lamark, T. Selective autophagy mediated by autophagic adapter proteins. *Autophagy* **7**, 279-296 (2011).

122 Jackson, K. A., Snyder, D. S. & Goodell, M. A. Skeletal Muscle Fiber-Specific Green Autofluorescence: Potential for Stem Cell Engraftment Artifacts. *STEM CELLS* **22**, 180-187, doi:10.1634/stemcells.22-2-180 (2004).

123 Høyer-Hansen, M. & Jäättelä, M. AMP-Activated Protein Kinase: A Universal Regulator of Autophagy? *Autophagy* **3**, 381-383 (2007).

124 Gao, W. induction of mactroautophagy by exogenously introduced calcium. **4**, 754-761 (2008).

125 Harr, M. W. & Distelhorst, C. W. Apoptosis and autophagy: decoding calcium signals that mediate life or death. *Cold Spring Harbor perspectives in biology* **2**, a005579-a005579, doi:10.1101/cshperspect.a005579 (2010).

126 Foskett, J. K., White, C., Cheung, K.-H. & Mak, D.-O. D. Inositol Trisphosphate Receptor Ca2+ Release Channels. *Physiological reviews* **87**, 593-658 (2007).

127 Ionescu, L. *et al.* Graded recruitment and inactivation of single InsP3 receptor Ca2+-release channels: implications for quartal Ca2+release. *The Journal of Physiology* **573**, 645-662 (2006).

128 Taylor, C. W. & Laude, A. J. IP3 receptors and their regulation by calmodulin and cytosolic Ca2+. *Cell calcium* **32**, 321-334, doi:http://dx.doi.org/10.1016/S0143416002001859 (2002).

129 Parys, J., Decuypere, J.-P. & Bultynck, G. Role of the inositol 1,4,5-trisphosphate receptor/Ca2+-release channel in autophagy. *Cell Communication and Signaling* **10**, 17 (2012).

130 Khan, M. T. & Joseph, S. K. Role of inositol trisphosphate receptors in autophagy in DT40 cells. *J Biol Chem* **285**, 16912-16920 (2010).

131 Vicencio, J. M. *et al.* The inositol 1,4,5-trisphosphate receptor regulates autophagy through its interaction with Beclin 1. *Cell Death Differ* **16**, 1006-1017, doi:http://www.nature.com/cdd/journal/v16/n7/suppinfo/cdd200934s1.html (2009).

132 Rizzuto, R., Brini, M., Murgia, M. & Pozzan, T. Microdomains with high Ca2+ close to IP3-sensitive channels that are sensed by neighboring mitochondria. *Science* **262**, 744-747 (1993).

133 Rizzuto, R. *et al.* Ca2+ transfer from the ER to mitochondria: when, how and why. *Biochim Biophys Acta* **1787**, 1342-1351 (2009).

134 Decuypere, J. P. *et al.* The IP3 receptor-mitochondria connection in apoptosis and autophagy. *Biochim Biophys Acta* **1813**, 1003-1013 (2011).

135 Williams, A. *et al.* Novel targets for Huntington's disease in an mTOR-independent autophagy pathway. *Nat Chem Biol* **4**, 295-305, doi:http://www.nature.com/nchembio/journal/v4/n5/suppinfo/nchembio.79_S1.html (2008).

136 Decuypere, J.-P., Bultynck, G. & Parys, J. B. A dual role for Ca(2+) in autophagy regulation. *Cell calcium* **50**, 242-250, doi:10.1016/j.ceca.2011.04.001 (2011).

137 Taneike, M. *et al.* Inhibition of autophagy in the heart induces age-related cardiomyopathy. *Autophagy* **6**, 600-606 (2010).

138 Demontis, F. & Perrimon, N. FOXO/4E-BP Signaling in Drosophila Muscles Regulates Organism-wide Proteostasis during Aging. *Cell* **143**, 813-825, doi:http://dx.doi.org/10.1016/j.cell.2010.10.007 (2010).

139 Boluyt, M. O., Converso, K., Hwang, H. S., Mikkor, A. & Russell, M. W. Echocardiographic assessment of age-associated changes in systolic and diastolic function of the female F344 rat heart. *Journal of Applied Physiology* **96**, 822-828 (2004).

140 Klionsky, D. J. & Emr, S. D. Autophagy as a Regulated Pathway of Cellular Degradation. *Science* **290**, 1717-1721 (2000).

141 Kuma, A. *et al.* The role of autophagy during the early neonatal starvation period. *Nature* **432**, 1032-1036 (2004).

142 Wang, Z. V., Rothermel, B. A. & Hill, J. A. Autophagy in Hypertensive Heart Disease. *Journal of Biological Chemistry* **285**, 8509-8514 (2010).

143 Matsui, Y. *et al.* Distinct Roles of Autophagy in the Heart During Ischemia and Reperfusion: Roles of AMP-Activated Protein Kinase and Beclin 1 in Mediating Autophagy. *Circulation Research* **100**, 914-922 (2007).

144 Sinha, S. & Levine, B. The autophagy effector Beclin 1: a novel BH3-only protein. *Oncogene* **27**, S137-S148 (0000).

145 Zhu, H. *et al.* Cardiac autophagy is a maladaptive response to hemodynamic stress. **117**, doi:10.1172/jci27523ds1 (2007).

146 Tannous, P. *et al.* Autophagy is an adaptive response in desmin-related cardiomyopathy. *Proceedings of the National Academy of Sciences* **105**, 9745-9750 (2008).
147 Mazure, N. M. & Pouysségur, J. Hypoxia-induced autophagy: cell death or cell survival? *Current opinion in cell biology* **22**, 177-180, doi:10.1016/j.ceb.2009.11.015 (2010).
148 Matsui, Y. *et al.* Molecular mechanisms and physiological significance of autophagy during myocardial ischemia and reperfusion. *Autophagy* **4**, 409-415 (2008).
149 Qian, J. *et al.* Blockade of Hsp20 Phosphorylation Exacerbates Cardiac Ischemia/Reperfusion Injury by Suppressed Autophagy and Increased Cell Death. *Circulation Research* **105**, 1223-1231 (2009).
150 Valentim, L. *et al.* Urocortin inhibits Beclin1-mediated autophagic cell death in cardiac myocytes exposed to ischaemia/reperfusion injury. *Journal of molecular and cellular cardiology* **40**, 846-852, doi:10.1016/j.yjmcc.2006.03.428 (2006).
151 Rothermel, B. A. & Hill, J. A. Myocyte Autophagy in Heart Disease: Friend or Foe? *Autophagy* **3**, 632-634 (2007).
152 Oudit, G. Y. *et al.* The role of phosphoinositide-3 kinase and PTEN in cardiovascular physiology and disease. *Journal of Molecular and Cellular Cardiology* **37**, 449-471, doi:http://dx.doi.org/10.1016/j.yjmcc.2004.05.015 (2004).
153 Lupu, F., Terwilliger, J. D., Lee, K., Segre, G. V. & Efstratiadis, A. Roles of Growth Hormone and Insulin-like Growth Factor 1 in Mouse Postnatal Growth. *Developmental Biology* **229**, 141-162, doi:http://dx.doi.org/10.1006/dbio.2000.9975 (2001).
154 Molkentin, J. D. & Dorn Ii, G. W. CYTOPLASMIC SIGNALING PATHWAYS THAT REGULATE CARDIAC HYPERTROPHY. *Annual review of physiology* **63**, 391-426, doi:10.1146/annurev.physiol.63.1.391 (2001).
155 Dorn, G. W. Adrenergic pathways and left ventricular remodeling. *Journal of cardiac failure* **8**, S370-373, doi:10.1054/jcaf.2002.129267 (2002).
156 Takeda, Y., Yoneda, T., Demura, M., Usukura, M. & Mabuchi, H. Calcineurin Inhibition Attenuates Mineralocorticoid-Induced Cardiac Hypertrophy. *Circulation* **105**, 677-679 (2002).
157 Young, M., Head, G. & Funder, J. Determinants of cardiac fibrosis in experimental hypermineralocorticoid states. *American Journal of Physiology - Endocrinology and Metabolism* **269**, E657-E662 (1995).
158 Robert, V. *et al.* Angiotensin AT1 Receptor Subtype as a Cardiac Target of Aldosterone : Role in Aldosterone-Salt–Induced Fibrosis. *Hypertension* **33**, 981-986 (1999).
159 Nakai, A. *et al.* The role of autophagy in cardiomyocytes in the basal state and in response to hemodynamic stress. *Nature medicine* **13**, 619-624, doi:10.1038/nm1574 (2007).
160 Kuzman, J. A., O'Connell, T. D. & Gerdes, A. M. Rapamycin Prevents Thyroid Hormone-Induced Cardiac Hypertrophy. *Endocrinology* **148**, 3477-3484 (2007).
161 Zhu, H. *et al.* Cardiac autophagy is a maladaptive response to hemodynamic stress. *The Journal of Clinical Investigation* **117**, 1782-1793, doi:10.1172/jci27523 (2007).
162 Hill, J. A. & Olson, E. N. Cardiac Plasticity. *New England Journal of Medicine* **358**, 1370-1380, doi:10.1056/NEJMra072139 (2008).

163 Ravikumar, B. *et al.* Regulation of Mammalian Autophagy in Physiology and Pathophysiology. *Physiological reviews* **90**, 1383-1435 (2010).

164 Nemchenko, A., Chiong, M., Turer, A., Lavandero, S. & Hill, J. a. Autophagy as a therapeutic target in cardiovascular disease. *Journal of molecular and cellular cardiology* **51**, 584-593, doi:10.1016/j.yjmcc.2011.06.010 (2011).

165 Bernales, S., Papa, F. R. & Walter, P. Intracellular Signaling by the Unfolded Protein Response. *Annual Review of Cell and Developmental Biology* **22**, 487-508, doi:10.1146/annurev.cellbio.21.122303.120200 (2006).

166 Parmar, V. & Schröder, M. in *Self and Nonself* Vol. 738 *Advances in Experimental Medicine and Biology* (ed Carlos López-Larrea) Ch. 10, 153-168 (Springer US, 2012).

167 Hetz, C. The unfolded protein response: controlling cell fate decisions under ER stress and beyond. *Nat Rev Mol Cell Biol* **13**, 89-102 (2012).

168 Meusser, B., Hirsch, C., Jarosch, E. & Sommer, T. ERAD: the long road to destruction. *Nat Cell Biol* **7**, 766-772 (2005).

169 Ogata, M. *et al.* Autophagy is activated for cell survival after endoplasmic reticulum stress. *Molecular and cellular biology* **26**, 9220-9231, doi:10.1128/mcb.01453-06 (2006).

170 J, L. NIH Public Access. **15**, 1460-1471, doi:10.1038/cdd.2008.81.The (2009).

171 Lee, A.-H., Chu, G. C., Iwakoshi, N. N. & Glimcher, L. H. XBP-1 is required for biogenesis of cellular secretory machinery of exocrine glands. *EMBO J* **24**, 4368-4380, doi:http://www.nature.com/emboj/journal/v24/n24/suppinfo/7600903a_S1.html (2005).

172 Kouroku, Y. *et al.* ER stress (PERK//eIF2[alpha] phosphorylation) mediates the polyglutamine-induced LC3 conversion, an essential step for autophagy formation. *Cell Death Differ* **14**, 230-239, doi:http://www.nature.com/cdd/journal/v14/n2/suppinfo/4401984s1.html (2006).

173 Tallóczy, Z. *et al.* Regulation of starvation- and virus-induced autophagy by the eIF2α kinase signaling pathway. *Proceedings of the National Academy of Sciences* **99**, 190-195 (2002).

174 Zhu, K., Dunner, K., Jr. & McConkey, D. J. Proteasome inhibitors activate autophagy as a cytoprotective response in human prostate cancer cells. *Oncogene* **29**, 451-462, doi:http://www.nature.com/onc/journal/v29/n3/suppinfo/onc2009343s1.html (2009).

175 Ding, W.-X. *et al.* Linking of Autophagy to Ubiquitin-Proteasome System Is Important for the Regulation of Endoplasmic Reticulum Stress and Cell Viability. *The American Journal of Pathology* **171**, 513-524, doi:http://dx.doi.org/10.2353/ajpath.2007.070188 (2007).

176 Lépine, S., Allegood, J. C., Edmonds, Y., Milstien, S. & Spiegel, S. Autophagy Induced by Deficiency of Sphingosine-1-phosphate Phosphohydrolase 1 Is Switched to Apoptosis by Calpain-mediated Autophagy-related Gene 5 (Atg5) Cleavage. *Journal of Biological Chemistry* **286**, 44380-44390 (2011).

177 Pellieux, C. *et al.* Neuropeptide Y (NPY) potentiates phenylephrine-induced mitogen-activated protein kinase activation in primary cardiomyocytes via NPY Y5 receptors. *Proceedings of the National Academy of Sciences* **97**, 1595-1600 (2000).

178 Iwawaki, T. & Akai, R. Analysis of the XBP1 splicing mechanism using endoplasmic reticulum stress-indicators. *Biochemical and biophysical research communications* **350**, 709-715, doi:10.1016/j.bbrc.2006.09.100 (2006).
179 Nakamura, M. *et al.* Activation of the endoplasmic reticulum stress pathway is associated with survival of myeloma cells. *Leukemia & Lymphoma* **47**, 531-539, doi:10.1080/10428190500312196 (2006).
180 Leuranguer, V., Mangoni, M. E., Nargeot, J. & Richard, S. Inhibition of T-Type and L-Type Calcium Channels by Mibefradil: Physiologic and Pharmacologic Bases of Cardiovascular Effects. *Journal of cardiovascular pharmacology* **37** (2001).
181 Mehrke, G., Zong, X. G., Flockerzi, V. & Hofmann, F. The Ca(++)-channel blocker Ro 40-5967 blocks differently T-type and L-type Ca++ channels. *Journal of Pharmacology and Experimental Therapeutics* **271**, 1483-1488 (1994).
182 Bezprozvanny, I. & Tsien, R. W. Voltage-dependent blockade of diverse types of voltage-gated Ca2+ channels expressed in Xenopus oocytes by the Ca2+ channel antagonist mibefradil (Ro 40-5967). *Molecular pharmacology* **48**, 540-549 (1995).
183 Gill, C., Mestril, R. & Samali, A. Losing heart: the role of apoptosis in heart disease—a novel therapeutic target? *The FASEB Journal* **16**, 135-146 (2002).
184 Ylä-Anttila, P., Vihinen, H., Jokitalo, E. & Eskelinen, E. L. in *Methods in Enzymology* Vol. Volume 452 (ed J. Klionsky Daniel) 143-164 (Academic Press, 2009).
185 Chen, R. *et al.* Reticulon 3 attenuates the clearance of cytosolic prion aggregates via inhibiting autophagy. *Autophagy* **7**, 205-216 (2011).
186 Kabeya, Y. *et al.* LC3, a mammalian homologue of yeast Apg8p, is localized in autophagosome membranes after processing. *The EMBO Journal* **19**, 5720-5728 (2000).
187 Mizushima, N. & Yoshimori, T. How to Interpret LC3 Immunoblotting ND RIB ND ES SC RIB. 4-7 (2007).
188 Barth, S., Glick, D. & Macleod, K. F. Autophagy: assays and artifacts. *The Journal of Pathology* **221**, 117-124, doi:10.1002/path.2694 (2010).
189 Kimura, S., Noda, T. & Yoshimori, T. Dissection of the Autophagosome Maturation Process by a Novel Reporter Protein, Tandem Fluorescent-Tagged LC3. *Autophagy* **3**, 452-460 (2007).
190 Kimura, S., Fujita, N., Noda, T. & Yoshimori, T. in *Methods in Enzymology* Vol. Volume 452 (ed J. Klionsky Daniel) 1-12 (Academic Press, 2009).
191 Zhou, C. *et al.* impairs autophagic flux in cancer cells. **3**, 1215-1226 (2012).
192 Klionsky, D. J. *et al.* Guidelines for the use and interpretation of assays for monitoring autophagy in higher eukaryotes. *Autophagy* **4**, 151-175 (2008).
193 Mizushima, N., Yoshimori, T. & Levine, B. Methods in Mammalian Autophagy Research. *Cell* **140**, 313-326 (2010).
194 Gülow, K., Bienert, D. & Haas, I. G. BiP is feed-back regulated by control of protein translation efficiency. *Journal of Cell Science* **115**, 2443-2452 (2002).
195 Yoshida, H., Oku, M., Suzuki, M. & Mori, K. pXBP1(U) encoded in XBP1 pre-mRNA negatively regulates unfolded protein response activator pXBP1(S) in mammalian ER stress response. *The Journal of cell biology* **172**, 565-575, doi:10.1083/jcb.200508145 (2006).
196 Sengupta, A., Molkentin, J. D. & Yutzey, K. E. FoxO Transcription Factors Promote Autophagy in Cardiomyocytes. *Journal of Biological Chemistry* **284**, 28319-28331, doi:10.1074/jbc.M109.024406 (2009).

197 Zhao, Y. *et al.* The axis of MAPK1/3-XBP1u-FOXO1 controls autophagic dynamics in cancer cells. *Autophagy* **9**, 794-796, doi:10.4161/auto.23918 (2013).
198 Vidal, R. L. & Hetz, C. Unspliced XBP1 controls autophagy through FoxO1. *Cell Res* **23**, 463-464 (2013).
199 Kubli, D. A. & Gustafsson, Å. B. Cardiomyocyte health: adapting to metabolic changes through autophagy. *Trends in Endocrinology & Metabolism*, doi:http://dx.doi.org/10.1016/j.tem.2013.11.004.
200 Kanamori, H. *et al.* Resveratrol Reverses Remodeling in Hearts with Large, Old Myocardial Infarctions through Enhanced Autophagy-Activating AMP Kinase Pathway. *The American Journal of Pathology* **182**, 701-713, doi:http://dx.doi.org/10.1016/j.ajpath.2012.11.009 (2013).
201 Klionsky, D. J. *et al.* Guidelines for the use and interpretation of assays for monitoring autophagy. *Autophagy* **8**, 445-544 (2012).
202 Zheng, Q., Su, H., Ranek, M. J. & Wang, X. Autophagy and p62 in cardiac proteinopathy. *Circulation research* **109**, 296-308, doi:10.1161/circresaha.111.244707 (2011).
203 Bjørkøy, G. *et al.* p62/SQSTM1 forms protein aggregates degraded by autophagy and has a protective effect on huntingtin-induced cell death. *The Journal of cell biology* **171**, 603-614, doi:10.1083/jcb.200507002 (2005).
204 Ganley, I. G., Wong, P.-M., Gammoh, N. & Jiang, X. Distinct autophagosomal-lysosomal fusion mechanism revealed by thapsigargin-induced autophagy arrest. *Molecular cell* **42**, 731-743, doi:10.1016/j.molcel.2011.04.024 (2011).
205 Ganley, Ian G., Wong, P.-M., Gammoh, N. & Jiang, X. Distinct Autophagosomal-Lysosomal Fusion Mechanism Revealed by Thapsigargin-Induced Autophagy Arrest. *Molecular cell* **42**, 731-743, doi:http://dx.doi.org/10.1016/j.molcel.2011.04.024 (2011).
206 Ramírez-Peinado, S. *et al.* Glucose-starved Cells Do Not Engage in Prosurvival Autophagy. *The Journal of biological chemistry* **288**, 30387-30398, doi:10.1074/jbc.M113.490581 (2013).
207 Klionsky, D. J. & Nemchenko, A. There is more to autophagy than induction: Regulating the roller coaster. *Autophagy* **7**, 801-802 (2011).
208 Komatsu, M. *et al.* Homeostatic Levels of p62 Control Cytoplasmic Inclusion Body Formation in Autophagy-Deficient Mice. *Cell* **131**, 1149-1163, doi:http://dx.doi.org/10.1016/j.cell.2007.10.035 (2007).
209 Dehay, B. *et al.* Pathogenic Lysosomal Depletion in Parkinson's Disease. *The Journal of Neuroscience* **30**, 12535-12544, doi:10.1523/jneurosci.1920-10.2010 (2010).
210 Høyer-Hansen, M. & Jäättelä, M. Connecting endoplasmic reticulum stress to autophagy by unfolded protein response and calcium. *Cell death and differentiation* **14**, 1576-1582, doi:10.1038/sj.cdd.4402200 (2007).
211 Gottlieb, R. a. & Mentzer, R. M. Autophagy: an affair of the heart. *Heart failure reviews* **18**, 575-584, doi:10.1007/s10741-012-9367-2 (2013).
212 Kanamori, H. *et al.* The role of autophagy emerging in postinfarction cardiac remodelling. *Cardiovascular Research* **91**, 330-339, doi:10.1093/cvr/cvr073 (2011).
213 Kanamori, H. *et al.* Autophagy limits acute myocardial infarction induced by permanent coronary artery occlusion. *American Journal of Physiology - Heart and Circulatory Physiology* **300**, H2261-H2271 (2011).

214 Gottlieb, R. a. & Mentzer, R. M. Autophagy during cardiac stress: joys and frustrations of autophagy. *Annual review of physiology* **72**, 45-59, doi:10.1146/annurev-physiol-021909-135757 (2010).

215 Miyata, S. *et al.* Autophagic Cardiomyocyte Death in Cardiomyopathic Hamsters and Its Prevention by Granulocyte Colony-Stimulating Factor. *The American Journal of Pathology* **168**, 386-397, doi:http://dx.doi.org/10.2353/ajpath.2006.050137 (2006).

216 Kinoshita, H. *et al.* T-type Ca2+ channel blockade prevents sudden death in mice with heart failure. *Circulation* **120**, 743-752, doi:10.1161/circulationaha.109.857011 (2009).

217 Rossier, M. F. T channels and steroid biosynthesis: in search of a link with mitochondria. *Cell calcium* **40**, 155-164, doi:10.1016/j.ceca.2006.04.020 (2006).

218 Ono, K. & Iijima, T. Cardiac T-type Ca(2+) channels in the heart. *Journal of molecular and cellular cardiology* **48**, 65-70, doi:10.1016/j.yjmcc.2009.08.021 (2010).

219 Yasui, K. *et al.* Pathophysiological Significance of T-type Ca²⁺ Channels:
Expression of T-type Ca²⁺ Channels in Fetal and Diseased Heart. *Journal of Pharmacological Sciences* **99**, 205-210 (2005).

220 Niwa, N. *et al.* Cav3.2 subunit underlies the functional T-type Ca2+ channel in murine hearts during the embryonic period. *American Journal of Physiology - Heart and Circulatory Physiology* **286**, H2257-H2263 (2004).

221 Vassort, G., Talavera, K. & Alvarez, J. L. Role of T-type Ca2+ channels in the heart. *Cell calcium* **40**, 205-220, doi:10.1016/j.ceca.2006.04.025 (2006).

222 Ferron, L., Ruchon, Y., Renaud, J.-F. & Capuano, V. T-type Ca^{2+} signalling regulates aldosterone-induced CREB activation and cell death through PP2A activation in neonatal cardiomyocytes. *Cardiovascular research* **90**, 105-112, doi:10.1093/cvr/cvq379 (2011).

223 Horiba, M. *et al.* T-type Ca2+ channel blockers prevent cardiac cell hypertrophy through an inhibition of calcineurin-NFAT3 activation as well as L-type Ca2+ channel blockers. *Life sciences* **82**, 554-560, doi:10.1016/j.lfs.2007.11.010 (2008).

224 Sandmann, S., Spormann, J., Prenzel, F., Shaw, L. & Unger, T. Calcium channel blockade limits transcriptional, translational and functional up-regulation of the cardiac calpain system after myocardial infarction. *European journal of pharmacology* **453**, 99-109, doi:http://dx.doi.org/10.1016/S0014-2999(02)02384-1 (2002).

225 Min, J.-Y., Meissner, A., Wang, J. & Morgan, J. P. Mibefradil Improves β-Adrenergic Responsiveness and Intracellular Ca2+ Handling in Hypertrophied Rat Myocardium. *Experimental Biology and Medicine* **227**, 336-344 (2002).

226 Hong, T.-T. *et al.* BIN1 is reduced and Cav1.2 trafficking is impaired in human failing cardiomyocytes. *Heart rhythm : the official journal of the Heart Rhythm Society* **9**, 812-820, doi:10.1016/j.hrthm.2011.11.055 (2012).

227 Yan, L. *et al.* Autophagy in chronically ischemic myocardium. *Proceedings of the National Academy of Sciences of the United States of America* **102**, 13807-13812 (2005).

228 Elsässer, A. *et al.* Human hibernating myocardium is jeopardized by apoptotic and autophagic cell death. *Journal of the American College of Cardiology* **43**, 2191-2199, doi:http://dx.doi.org/10.1016/j.jacc.2004.02.053 (2004).

229 Marciniak, S. J. & Ron, D. Endoplasmic Reticulum Stress Signaling in Disease. *Physiological reviews* **86**, 1133-1149 (2006).

230 Glembotski, C. C. Endoplasmic reticulum stress in the heart. *Circulation research* **101**, 975-984, doi:10.1161/circresaha.107.161273 (2007).
231 Nishida, K., Kyoi, S., Yamaguchi, O., Sadoshima, J. & Otsu, K. The role of autophagy in the heart. *Cell Death Differ* **16**, 31-38 (2008).
232 Opie, L. H. & du Toit, E. F. Postischemic Stunning: The Two-Phase Model for the Role of Calcium as Pathogen. *Journal of cardiovascular pharmacology* **20** (1992).
233 Pluteanu, F. & Cribbs, L. L. T-type calcium channels are regulated by hypoxia/reoxygenation in ventricular myocytes. *American journal of physiology. Heart and circulatory physiology* **297**, H1304-1313, doi:10.1152/ajpheart.00528.2009 (2009).
234 Pastukh, V. *et al.* Effect of hypernatremia on injury caused by energy deficiency: Role of T-type Ca2+ channel. *American Journal of Physiology - Cell Physiology* **299**, C289-C297 (2010).
235 du Toit, E. F. & Opie, L. H. Modulation of severity of reperfusion stunning in the isolated rat heart by agents altering calcium flux at onset of reperfusion. *Circulation Research* **70**, 960-967 (1992).
236 Bersohn, M. M., Morey, A. K. & Weiss, R. S. Sarcolemmal Calcium Transporters in Myocardial Ischemia. *Journal of Molecular and Cellular Cardiology* **29**, 2525-2532, doi:http://dx.doi.org/10.1006/jmcc.1997.0487 (1997).
237 Zucchi, R. *et al.* Are dihydropyridine receptors downregulated in the ischemic myocardium? *Cardiovascular Research* **30**, 769-774 (1995).
238 Théroux, P. *et al.* Intravenous diltiazem in acute myocardial infarction: Diltiazem as adjunctive therapy to activase (DATA) trial. *Journal of the American College of Cardiology* **32**, 620-628, doi:http://dx.doi.org/10.1016/S0735-1097(98)00281-2 (1998).
239 Muller, C. A. *et al.* Effects of mibefradil, a novel calcium channel blocking agent with T-type activity, in acute experimental myocardial ischemia: maintenance of ventricular fibrillation threshold without inotropic compromise. *Journal of the American College of Cardiology* **32**, 268-274, doi:http://dx.doi.org/10.1016/S0735-1097(98)00182-X (1998).
240 Mozaffari, M. S., Patel, C. & Schaffer, S. W. Mechanisms Underlying Afterload-Induced Exacerbation of Myocardial Infarct Size: Role of T-Type Ca2+ Channel. *Hypertension* **47**, 912-919 (2006).
241 Sandmann, S. *et al.* Effects of the calcium channel antagonist mibefradil on haemodynamic and morphological parameters in myocardial infarction-induced cardiac failure in rats. *Cardiovascular Research* **39**, 339-350 (1998).
242 Arh, M. & Budihna, M. V. Comparison of effects of nitrendipine, lacidipine and mibefradil on postischaemic myocardial damage in isolated rat hearts. *Pflügers Arch* **440**, r149-r150, doi:10.1007/s004240000042 (2000).
243 Del Toro, R., Levitsky, K. L., López-Barneo, J. & Chiara, M. D. Induction of T-type calcium channel gene expression by chronic hypoxia. *The Journal of biological chemistry* **278**, 22316-22324, doi:10.1074/jbc.M212576200 (2003).
244 Carabelli, V. *et al.* Chronic hypoxia up-regulates α1H T-type channels and low-threshold catecholamine secretion in rat chromaffin cells. *The Journal of Physiology* **584**, 149-165 (2007).
245 Das, a. *et al.* Functional expression of voltage-gated calcium channels in human melanoma. *Pigment cell & melanoma research* **25**, 200-212, doi:10.1111/j.1755-148X.2012.00978.x (2012).

246 Hariharan, N., Zhai, P. & Sadoshima, J. Oxidative stress stimulates autophagic flux during ischemia/reperfusion. *Antioxidants & redox signaling* **14**, 2179-2190, doi:10.1089/ars.2010.3488 (2011).

247 Levitsky, K. L. & López-Barneo, J. Developmental change of T-type Ca2+ channel expression and its role in rat chromaffin cell responsiveness to acute hypoxia. *The Journal of Physiology* **587**, 1917-1929 (2009).

248 Carbone, E. & Carabelli, V. O2 sensing in chromaffin cells: new duties for T-type channels. *The Journal of Physiology* **587**, 1859-1860 (2009).

249 Heaps, C. L., Sturek, M., Price, E. M., Laughlin, M. H. & Parker, J. L. Sarcoplasmic reticulum Ca2+ uptake is impaired in coronary smooth muscle distal to coronary occlusion. *American Journal of Physiology - Heart and Circulatory Physiology* **281**, H223-H231 (2001).

250 Shintani-Ishida, K., Nakajima, M., Uemura, K. & Yoshida, K.-i. Ischemic preconditioning protects cardiomyocytes against ischemic injury by inducing GRP78. *Biochemical and biophysical research communications* **345**, 1600-1605, doi:http://dx.doi.org/10.1016/j.bbrc.2006.05.077 (2006).

251 Doroudgar, S., Thuerauf, D. J., Marcinko, M. C., Belmont, P. J. & Glembotski, C. C. Ischemia Activates the ATF6 Branch of the Endoplasmic Reticulum Stress Response. *Journal of Biological Chemistry* **284**, 29735-29745 (2009).

252 Russell, R. R., III *et al.* AMP-activated protein kinase mediates ischemic glucose uptake and prevents postischemic cardiac dysfunction, apoptosis, and injury. *The Journal of Clinical Investigation* **114**, 495-503, doi:10.1172/jci19297 (2004).

253 Terai, K. *et al.* AMP-Activated Protein Kinase Protects Cardiomyocytes against Hypoxic Injury through Attenuation of Endoplasmic Reticulum Stress. *Molecular and cellular biology* **25**, 9554-9575 (2005).

254 Takagi, H. *et al.* AMPK Mediates Autophagy during Myocardial Ischemia In Vivo. *Autophagy* **3**, 405-407 (2007).

255 Komatsu, M. & Ichimura, Y. Physiological significance of selective degradation of p62 by autophagy. *FEBS letters* **584**, 1374-1378, doi:10.1016/j.febslet.2010.02.017 (2010).

256 Aley, P. *et al.* Hypoxic remodelling of Ca2+ signalling in proliferating human arterial smooth muscle. *Molecular and cellular biochemistry* **318**, 101-108, doi:10.1007/s11010-008-9861-y (2008).

257 Ozturk, H., Ozturk, H., Duran, H. & Uzunlar, A. Mibefradil, a T-Type Ca2+ Channel Blocker, Protects Against Mesenteric Ischemia-Reperfusion-Induced Oxidative Injury and Histologic Alterations in Intestinal Mucosa in Rats. *Dig Dis Sci* **51**, 1454-1460, doi:10.1007/s10620-005-9060-6 (2006).

258 Nakayama, H. *et al.* Ca2+- and mitochondrial-dependent cardiomyocyte necrosis as a primary mediator of heart failure. *The Journal of Clinical Investigation* **117**, 2431-2444, doi:10.1172/jci31060 (2007).

259 Lips, D. J., deWindt, L. J., van Kraaij, D. J. W. & Doevendans, P. A. Molecular determinants of myocardial hypertrophy and failure: alternative pathways for beneficial and maladaptive hypertrophy. *European Heart Journal* **24**, 883-896 (2003).

260 Berenji, K., Drazner, M. H., Rothermel, B. A. & Hill, J. A. Does load-induced ventricular hypertrophy progress to systolic heart failure? *American Journal of Physiology - Heart and Circulatory Physiology* **289**, H8-H16 (2005).

261 Haider, A. W., Larson, M. G., Benjamin, E. J. & Levy, D. Increased left ventricular mass and hypertrophy are associated with increased risk for sudden

death. *Journal of the American College of Cardiology* **32**, 1454-1459, doi:http://dx.doi.org/10.1016/S0735-1097(98)00407-0 (1998).

262 Burchfield, J. S., Xie, M. & Hill, J. A. Pathological Ventricular Remodeling: Mechanisms: Part 1 of 2. *Circulation* **128**, 388-400 (2013).

263 Nakai, A. *et al.* The role of autophagy in cardiomyocytes in the basal state and in response to hemodynamic stress. *Nat Med* **13**, 619-624, doi:http://www.nature.com/nm/journal/v13/n5/suppinfo/nm1574_S1.html (2007).

264 Oyabu, J. *et al.* Autophagy-mediated degradation is necessary for regression of cardiac hypertrophy during ventricular unloading. *Biochemical and biophysical research communications* **441**, 787-792, doi:http://dx.doi.org/10.1016/j.bbrc.2013.10.135 (2013).

265 Hsu, S.-C., Chang, Y.-T. & Chen, C.-C. Early growth response 1 is an early signal inducing Cav3.2 T-type calcium channels during cardiac hypertrophy. *Cardiovascular Research* **100**, 222-230, doi:10.1093/cvr/cvt190 (2013).

266 Gao, H. *et al.* Ca(2+) influx through L-type Ca(2+) channels and transient receptor potential channels activates pathological hypertrophy signaling. *Journal of molecular and cellular cardiology* **53**, 657-667, doi:10.1016/j.yjmcc.2012.08.005 (2012).

267 Chen, X. *et al.* Calcium influx through Cav1.2 is a proximal signal for pathological cardiomyocyte hypertrophy. *Journal of Molecular and Cellular Cardiology* **50**, 460-470, doi:http://dx.doi.org/10.1016/j.yjmcc.2010.11.012 (2011).

268 Lalevée, N. *et al.* Aldosterone increases T-type calcium channel expression and in vitro beating frequency in neonatal rat cardiomyocytes. *Cardiovascular research* **67**, 216-224, doi:10.1016/j.cardiores.2005.05.009 (2005).

269 Colella, M. *et al.* Ca2+ oscillation frequency decoding in cardiac cell hypertrophy: Role of calcineurin/NFAT as Ca2+ signal integrators. *Proceedings of the National Academy of Sciences* **105**, 2859-2864 (2008).

270 John, S. W. *et al.* Genetic decreases in atrial natriuretic peptide and salt-sensitive hypertension. *Science* **267**, 679-681 (1995).

271 Klinger, J. R. *et al.* Cardiopulmonary responses to chronic hypoxia in transgenic mice that overexpress ANP. *Journal of Applied Physiology* **75**, 198-205 (1993).

272 Li, Y. *et al.* β-Adrenergic stimulation increases Cav3.1 activity in cardiac myocytes through protein kinase A. *PLoS ONE* **7**, e39965-e39965, doi:10.1371/journal.pone.0039965 (2012).

273 Frey, N., Katus, H. a., Olson, E. N. & Hill, J. a. Hypertrophy of the heart: a new therapeutic target? *Circulation* **109**, 1580-1589, doi:10.1161/01.cir.0000120390.68287.bb (2004).

274 Luo, X. *et al.* STIM1-dependent store-operated Ca2+ entry is required for pathological cardiac hypertrophy. *Journal of Molecular and Cellular Cardiology* **52**, 136-147, doi:http://dx.doi.org/10.1016/j.yjmcc.2011.11.003 (2012).

275 Sanbe, A. *et al.* Reversal of amyloid-induced heart disease in desmin-related cardiomyopathy. *Proceedings of the National Academy of Sciences of the United States of America* **102**, 13592-13597 (2005).

276 Weekes, J. *et al.* Hyperubiquitination of proteins in dilated cardiomyopathy. *PROTEOMICS* **3**, 208-216, doi:10.1002/pmic.200390029 (2003).

277 Nakaso, K. *et al.* Transcriptional activation of p62/A170/ZIP during the formation of the aggregates: possible mechanisms and the role in Lewy body formation in Parkinson's disease. *Brain Research* **1012**, 42-51, doi:http://dx.doi.org/10.1016/j.brainres.2004.03.029 (2004).

278 Kuusisto, E., Suuronen, T. & Salminen, A. Ubiquitin-Binding Protein p62 Expression Is Induced during Apoptosis and Proteasomal Inhibition in Neuronal Cells. *Biochemical and biophysical research communications* **280**, 223-228, doi:http://dx.doi.org/10.1006/bbrc.2000.4107 (2001).

279 Jain, A. *et al.* p62/SQSTM1 Is a Target Gene for Transcription Factor NRF2 and Creates a Positive Feedback Loop by Inducing Antioxidant Response Element-driven Gene Transcription. *Journal of Biological Chemistry* **285**, 22576-22591 (2010).

280 Heusch, G. *et al.* Cardiovascular remodelling in coronary artery disease and heart failure. *The Lancet* **383**, 1933-1943, doi:http://dx.doi.org/10.1016/S0140-6736(14)60107-0.